The effects of alcohol exposure on the development of the rat superior colliculus
by Tiffany Hardin Selong

A thesis submitted in partial fulfillment of the requirements for the degree of Master of Science in Biological Sciences
Montana State University

Abstract:
Victims of Fetal Alcohol Syndrome (FAS) are known to have visual system dysfunctions; however, with the exception of studies demonstrating damage to the rat optic nerve, experimental studies have not characterized the effects of developmental alcohol exposure on central nervous system (CNS) structures that may be involved. Because the main target of the rat optic nerve is the stratum griseum superficiale (SGS) of the superior colliculus, this study examined the effects of developmental alcohol exposure on cell populations in the SGS using light microscopic stereology.

In the first experiment offspring were exposed to alcohol throughout gestation by maternal consumption of alcohol and were analyzed on postnatal days 15 and 35. In the second experiment artificially reared rat pups were exposed to alcohol via gastrostomy in a high dose "binge" exposure on postnatal days 5 and 6, and were analyzed on postnatal days 15 and 90. In animals exposed throughout gestation alcohol caused a 30% loss of neurons and a 25% reduction in the volume of the SGS at 15 days of age, but there was no longer a loss of neurons at 35 days. However, there was an 83% increase in the volume density of glia and an 85% increase in the total number of glia in the 35 day animals. In the postnatal "binge" exposed animals alcohol caused a 16% reduction in the volume of the SGS and a marginally significant 18% loss of glia ($p=0.06$) at 15 days. In the same experiment at 90 days of age alcohol caused a 16% reduction in the volume of the SGS and a marginally significant 17% increase in the volume density of neurons ($p=0.06$). It appears that gestational alcohol exposure delayed neuronal proliferation and migration; this delay was followed by gliosis. Binge postnatal alcohol exposure apparently delayed glial maturation and decreased volume and thus possibly the complexity of the neuropil. These findings correlate with alcohol-induced effects on the developing optic nerve and together with more detailed future studies may help clarify the mechanisms by which alcohol affects developing CNS structures in the visual system.

THE EFFECTS OF ALCOHOL EXPOSURE ON THE DEVELOPMENT OF THE RAT SUPERIOR COLLICULUS

by

Tiffany Hardin Selong

A thesis submitted in partial fulfillment
of the requirements for the degree

of

Master of Science

in

Biological Sciences

MONTANA STATE UNIVERSITY-BOZEMAN
Bozeman, Montana

July 1999

APPROVAL

of a thesis submitted by

Tiffany Hardin Selong

This thesis has been read by each member of the thesis committee and has been found to be satisfactory regarding content, English usage, format, citations, bibliographic style, and consistency, and is ready for submission to the College of Graduate Studies.

Dwight E. Phillips, Ph.D. Dwight E. Phillips (Signature) 08/02/99 Date

Approved for the Department of Biology

Ernest R. Vyse, Ph.D. E R Vyse (Signature) 8/2/99 Date

Approved for the College of Graduate Studies

Bruce R. McLeod, Ph.D. Bruce R. McLeod (Signature) 8-3-99 Date

STATEMENT OF PERMISSION TO USE

In presenting this thesis in partial fulfillment of the requirements for a master's degree at Montana State University-Bozeman, I agree that the Library shall make it available to borrowers under rules of the Library.

If I have indicated my intention to copyright this thesis by including a copyright notice page, copying is allowable only for scholarly purposes, consistent with "fair use" as prescribed in the U.S. Copyright Law. Requests for permission for extended quotation from or reproduction of this thesis in whole or in parts may be granted only by the copyright holder.

Signature Tillie H. Selz

Date August 3, 1999

ACKNOWLEDGMENTS

I would like to thank Dr. Dwight Phillips for his kind advice, direction, and support. I would like to thank Susan Gibson, M.S. for her teaching and friendship. I would like to express my gratitude to Dr. Anne Rusoff and Dr. Charles Paden for serving on my graduate committee. I would especially like to acknowledge Dr. Rusoff for teaching me about technical writing and Dr. Paden for his kind encouragement to pursue an advanced degree.

I would like to thank Jason Selong, my husband, for his patience and encouragement. I would like to thank my parents, Gail and Michael Hardin, for their support and guidance. I would especially like to thank my mother for her expertise in word processing and for technical support in preparing this manuscript.

TABLE OF CONTENTS

TABLE OF CONTENTS--Continued

LIST OF TABLES

Table Page

LIST OF TABLES--Continued

LIST OF FIGURES

LIST OF FIGURES--Continued

ABSTRACT

Victims of Fetal Alcohol Syndrome (FAS) are known to have visual system dysfunctions; however, with the exception of studies demonstrating damage to the rat optic nerve, experimental studies have not characterized the effects of developmental alcohol exposure on central nervous system (CNS) structures that may be involved. Because the main target of the rat optic nerve is the stratum griseum superficiale (SGS) of the superior colliculus, this study examined the effects of developmental alcohol exposure on cell populations in the SGS using light microscopic stereology. In the first experiment offspring were exposed to alcohol throughout gestation by maternal consumption of alcohol and were analyzed on postnatal days 15 and 35. In the second experiment artificially reared rat pups were exposed to alcohol via gastrostomy in a high dose "binge" exposure on postnatal days 5 and 6, and were analyzed on postnatal days 15 and 90. In animals exposed throughout gestation alcohol caused a 30% loss of neurons and a 25% reduction in the volume of the SGS at 15 days of age, but there was no longer a loss of neurons at 35 days. However, there was an 83% increase in the volume density of glia and an 85% increase in the total number of glia in the 35 day animals. In the postnatal "binge" exposed animals alcohol caused a 16% reduction in the volume of the SGS and a marginally significant 18% loss of glia ($p=0.06$) at 15 days. In the same experiment at 90 days of age alcohol caused a 16% reduction in the volume of the SGS and a marginally significant 17% increase in the volume density of neurons ($p=0.06$). It appears that gestational alcohol exposure delayed neuronal proliferation and migration; this delay was followed by gliosis. Binge postnatal alcohol exposure apparently delayed glial maturation and decreased volume and thus possibly the complexity of the neuropil. These findings correlate with alcohol-induced effects on the developing optic nerve and together with more detailed future studies may help clarify the mechanisms by which alcohol affects developing CNS structures in the visual system.

INTRODUCTION

Fetal alcohol syndrome (FAS) was first classified as a syndrome in 1973 in a classic article by Jones and Smith (1973), in which they described the distinctive pattern of birth defects found in children born to chronic alcoholic women. FAS is characterized by growth deficiency, characteristic facial anomalies, and central nervous system (CNS) dysfunction (Sokol and Clarren,'89; Streissguth et al.,'91). The most serious consequences of FAS are the CNS dysfunctions and anomalies including microencephaly, mental retardation, behavioral deficits, visual and auditory system dysfunction, fine motor deficits, and cerebellar dysfunction (Clarren et al.,'78; Clarren,'81; Streissguth,'86; Driscoll et al.,'90). FAS is the most common cause of mental retardation in the Western world (Abel and Sokol,'87).

Animal research has been essential in characterizing specific CNS effects and the mechanisms of alcohol teratogenicity in the development of the mammalian CNS (Becker et al.,'94). Animal models allow researchers to control such variables as nutritional requirements for pregnant females and their offspring, dosage of alcohol and blood alcohol concentration, and specific timing of alcohol exposures to identify vulnerable periods of CNS development. Many specific regions in the rat CNS have been shown to be vulnerable to developmental alcohol exposure, including the cerebral cortex (Miller,'97), cerebellum (Goodlett et al.,'97), the hippocampal formation (Bellinger et al.,'99), and the olfactory bulb (Bonthius et al.,'92; Maier et al.,'99). The types of alcohol-induced changes that have been demonstrated include neuron cell loss (Bonthius and West,'90), defects in neurogenesis and neuronal migration (Miller,'86; Miller,'95), and astrogliosis (Shetty and Phillips,'92; Goodlett et al.,'97). Most studies have focused on areas of the CNS with well-defined

layers or borders and well-studied developmental histories, while other less well-defined areas have generally been neglected including structures in the visual pathway that are likely affected by alcohol.

Visual anomalies are frequently encountered in human victims of FAS and include optic nerve (ON) hypoplasia, poor vision, and strabismus (Stromland,'90; Stromland et al.,'91; Stromland and Pinazo-Duran,'94; Stromland and Hellstrom,'96). Animal studies investigating the effects of alcohol on the development of the visual system have demonstrated ON hypoplasia and decreased myelination of ON fibers in the mouse (Ashwell and Zhang,'94), reduced myelin thickness and delayed myelination in the rat ON (Phillips,'89; Phillips et al.,'91), loss of ON fibers in the rat (Phillips et al.,'98), delayed migration and maturation of neurons in the rat oculomotor nucleus (Burrows et al.,'95), and altered maturation of neurons in both the kitten lateral geniculate nucleus (Magloczky et al.,'90) and in the rat and mouse superior colliculus (SC) (Zajac,'87; Wall and Phillips,'93; Ashwell and Zhang,'94). It is known that for proper connections to be made during CNS development, including the development of the visual system, adequate input stimuli must exist (Galli-Resta et al.,'93). If alcohol-induced changes alter visual system input, developing target structures of the CNS might also be affected (Simon et al.,'94). Such effects on target structures in the visual system could contribute to some of the neurological problems frequently associated with FAS such as poor vision, strabismus, poor eye-hand coordination, and mental retardation (Jones and Smith,'75; Streissguth et al.,'91; Rosenberg,'96).

The SC, an integrative nucleus in the visual pathway, is one of the main targets of the ON fibers from the retina in the rat (Sefton and Dreher,'95). Because developmental alcohol exposures have been shown to produce significant changes in the rat ON in terms of both nerve fiber numbers and myelination (Phillips,'89; Phillips et al.,'91; Phillips et al.,'96; Phillips et al.,'98), it is reasonable to hypothesize that significant effects will be seen in the SC, particularly since activity-dependent input has been shown to be essential to the normal development of the SC or optic tectum of several

species, including rats (O'Leary et al.,'86; Williams et al.,'94; Cramer and Sur,'96; Rajan and Cline,'98).

The specific goals of this project were to complete analyses of previously collected SC tissues taken from rats exposed to alcohol in two different experimental models. One model is a gestational exposure in which pregnant dams were fed alcohol throughout gestation and is the equivalent of alcohol exposure during the first two trimesters of human gestation (Wall and Phillips,'93). The other model is a 5-6 day (d) postnatal binge exposure which used artificially reared postnatal rats fed dietary alcohol via gastrostomy and is the equivalent of acute alcohol exposure during the third trimester of human gestation (Phillips et al.,'98). Light microscopic stereology and immunocytochemistry were used to analyze the effects of these alcohol exposures on the neuronal populations that receive retinal input and their associated glial cell populations in the superficial (visual) layers of the SC.

The light microscopic methods utilized in this study were based on principles of modern stereology. Stereology, as applied to quantitative neurohistology, is a collection of methods that estimate the volume density of cells in a structure, the total number of cells in a structure, and the volume of defined regions of the brain. Stereological methods use three dimensional (3-D) probes called "disectors" to deal with cells as 3-D structures. These methods are considered "unbiased" because assumptions do not have to be made about cell size, shape, or orientation, and are called "design-based" because the precision with which one can estimate the true value of cell density or total number of cells in a defined region is related to the actual stereological sampling design one employs to obtain the estimate of cell density, total volume, and total cell number.

LITERATURE REVIEW

Fetal Alcohol Syndrome

Fetal alcohol syndrome (FAS), first described as a syndrome in 1973, is characterized by a distinctive pattern of birth defects found in children born to chronic alcoholic women (Jones and Smith,'73). Characteristics of FAS commonly include growth deficiency, characteristic facial anomalies, and central nervous system (CNS) dysfunction (Sokol and Clarren,'89; Streissguth et al.,'91). The most serious consequence of FAS is the CNS dysfunction (physically characterized by microencephaly) that is manifested as lifelong disabilities including mental retardation, hyperactivity, poor fine-motor function, and auditory and visual dysfunction (Clarren,'81). In 1987, FAS was reported as the most common cause of mental retardation in the Western world, creating a substantial economic impact on our society (Abel and Sokol,'87; Abel and Sokol,'91) Results of longitudinal clinical studies indicate that the intellectual, behavioral, and neurological handicaps attributed to FAS do not improve over time, even with good care given by parents, doctors, and educators (Streissguth et al.,'91; Stromland and Hellstrom,'96).

Clinical studies have shown that the development of the human visual system is affected by alcohol exposure in utero (Aronson et al.,'85; Stromland,'90; Stromland and Hellstrom,'96). The ocular and visual anomalies frequently associated with FAS include optic nerve hypoplasia, poor vision, ptosis, strabismus, and tortuous retinal arteries (Holzman et al.,'90; Stromland,'90; Chan et al.,'91; Stromland et al.,'91; Stromland and Pinazo-Duran,'94; Stromland and Hellstrom,'96). FAS has also been correlated with severe delays in development of visual perception and with poor eye-hand coordination (Aronson et al.,'85; Aronson et al.,'97). Thus, the insult of developmental alcohol

exposure on the human visual system reaches from the physical development of the eyes to the development of visual perception. Since "visual perception" is a higher order CNS function, this suggests that alcohol affects some part of the visual pathway, from the eye to higher levels in the CNS. "Perception" is usually thought of as a function of the cerebral cortex, but a complex behavior such as eye-hand coordination certainly involves additional CNS structures in the visual pathway such as the superior colliculus, which in the human helps coordinate head and eye movement with visual stimuli (Nolte,'99).

For proper connections to be made during CNS development, including development of the visual system, adequate input stimuli must exist (Williams et al.,'94; Cramer and Sur,'96; Rajan and Cline,'98). If visual input is altered by ocular or optic nerve (ON) manipulations or deformities, the developing target structures of the CNS are also affected (Galli-Resta et al.,'93; Simon et al.,'94). Such effects on target structures may contribute to neurological problems such as poor vision, mental retardation, and poor eye-hand coordination (Jones and Smith,'75; Streissguth et al.,'91; Rosenberg,'96).

Studies in human victims of FAS are limited mainly to clinical characterizations that, except for magnetic resonance imaging (MRI) (Mattson et al.,'94, Roebuck et al.,'98) and autopsy (Clarren et al.,'78; Peiffer et al.,'79; Wisniewski et al.,'83; Clarren,'86), rarely include tissue examination. MRI studies have shown microencephaly with substantial reduction in volume of particular structures in the CNS including the cerebellum, basal ganglia, diencephalon, and corpus callosum (Mattson et al.,'94). Autopsy studies have shown fairly consistent alcohol-induced anomalies in CNS development including microencephaly, malformations of the corpus callosum and cerebellum, and glial heterotopias (Clarren et al.,'78; Peiffer et al.,'79; Wisniewski et al.,'83; Clarren,'86). Variables that are impossible to control in human studies such as nutrition, multiple drug use, and environmental influence, often confound results (Becker et al.,'94). Thus, various animal models

have been implemented to investigate how alcohol affects the development of the brain and other organs. The experimental design of such models controls for nutrition and environment, the manipulation of dosage, and the timing of exposure to pinpoint specific developmental events. Nutrition is an important variable since it is possible for nutritional deficits alone to cause some of the same effects seen in FAS (Weinberg,'84; Wiggins,'86; Phillips,'92) and because FAS children are borne of alcoholic women who are often malnourished.

Animal Models: Methods of Developmental Alcohol Exposure

Animal models of developmental alcohol exposure, and particularly the rat animal model, have evolved and become quite sophisticated in recent years allowing for proper nutritional controls (Lieber and Decarli,'94), and allowing specific developmental events to be targeted (West,'93). The rat model using both gestational and early postnatal exposures has been used extensively in this laboratory to investigate the effects of alcohol on brain development (Phillips,'89; Phillips et al.,'91; Shetty and Phillips,'92; Phillips,'94; Burrows et al.,'95; Phillips et al.,'97). In terms of relative brain development, the full three trimesters of human gestation is equivalent to the 21-22 day gestation of a rat plus the first 10 postnatal days (Dobbing and Sands,'79; Dobbing,'81). Therefore, a rat gestational exposure is approximately equivalent to an exposure occurring during the first two trimesters of human gestation, and exposure during the first 10 postnatal days is approximately equivalent to an exposure occurring during the third trimester of human gestation.

Several different methods have been used to expose fetal rats to alcohol during gestation, including exposing the mother via intubation, injection, and either dietary or drinking water inclusion (Weinberg,'84). Though dose can be strictly controlled by both intubation and injection, these methods and the intoxication from the alcohol are stressful to the dams causing them to decrease diet intake and introduce concerns about adequate nutrition (Weinberg,'84). Alcohol inclusion in

drinking water provided as the only source of fluid causes experimental dams to decrease both fluid and diet intake, leading to malnutrition (Testar et al.,'88). Including alcohol in liquid diet provided as the only source of fluid and diet is generally acknowledged as the best method for gestational alcohol exposure (Rao et al.,'88; Lieber and Decarli,'94). The liquid diets are formulated to minimize any effects of decreased food intake because of alcohol content (Lieber and Decarli,'94). The pair-fed method of the present study involves feeding pregnant dams liquid diet as the only source of water and food, and feeding a calorically equivalent equal volume to weight-matched control dams. This ensures that nutrition is controlled for and that the dose can be monitored. It has been shown that the offspring of pair-fed animals do not differ significantly from the offspring of chow-fed controls in terms of litter size, offspring size, and brain weight of offspring, or in terms of developmental markers such as righting reflex, dental eruption, startle response, and eye opening (Gottesfeld et al.,'89).

Several different methods have been used to expose neonatal rat pups to alcohol, including lactational exposure, gavage, inhalation, injection, and artificial rearing (Swiatek et al.,'86; Phillips,'94). Lactational exposure presents the risk of malnutrition due to the altered nursing behavior of the pups and decreased milk production by lactating dams (Swiatek et al.,'86). Gavage, inhalation, and injection also present the risk of altered nursing behavior in the intoxicated rat pups. The postnatal rat exposure used in the present study involves an artificial rearing technique, similar to the method developed in the lab of James West (West et al.,'84; West,'93). This technique controls for nutrition, while leaving the dose and timing of alcohol administration available for manipulation (West, J.R., Goodlett, C.R., and Kelly, S.J. (1987)). To my knowledge the present study is the first to use a postnatal artificial rearing technique to examine the effects of alcohol exposure on the development of the rat superior colliculus.

The Superior Colliculus

The superior colliculus of the rat midbrain is equivalent to the optic tectum of submammalian vertebrates such as the chick and the frog, and is an important relay nucleus of the rat visual pathway (Sefton and Dreher,'95). Most of the retinal ganglion cells (RGCs), whose axons comprise the optic nerve (ON), project to the SC in the rat while others (fewer in number) project to the lateral geniculate nucleus of the thalamus (LGN) (Linden and Perry,'83; Sefton and Dreher,'95). In the human, the main target of the ON is the LGN with a smaller projection directly to the SC. Thus the human SC is a lesser part of the direct visual system but remains a relay point in the pathway for coordinating head and eye movement responses to visual input (Nolte,'99).

The rat SC is an integrative nucleus that projects to the substantia nigra, pons, medulla, cervical spinal cord, and other visual nuclei such as the oculomotor nucleus (Sefton and Dreher,'95; Nolte,'99). Similarly, the human SC projects to the cervical spinal cord, mesencephalic reticular formation, and the lateral and medial geniculate nuclei (Nolte,'99). The SC coordinates eye and neck movements in response to visual and other sensory stimuli (Sefton and Dreher,'95) and thus functions in helping an organism respond to where an object is in space. It has also been implicated in a variety of other visual activities including coordinating avoidance reactions and saccadic eye movements (Sefton and Dreher,'95).

Organization of the Superior Colliculus

The adult rat SC appears in histologic section as a well-laminated structure with seven horizontal layers of alternating grey and white matter. The laminae can be divided into two functional regions, the superficial (visual) laminae and the deep (projection) laminae. The visual laminae are the focus of the present study and from superficial to deep consist of: stratum zonale (SZ); stratum griseum superficiale (SGS); and stratum opticum (SO) (Figure 1). The SO consists

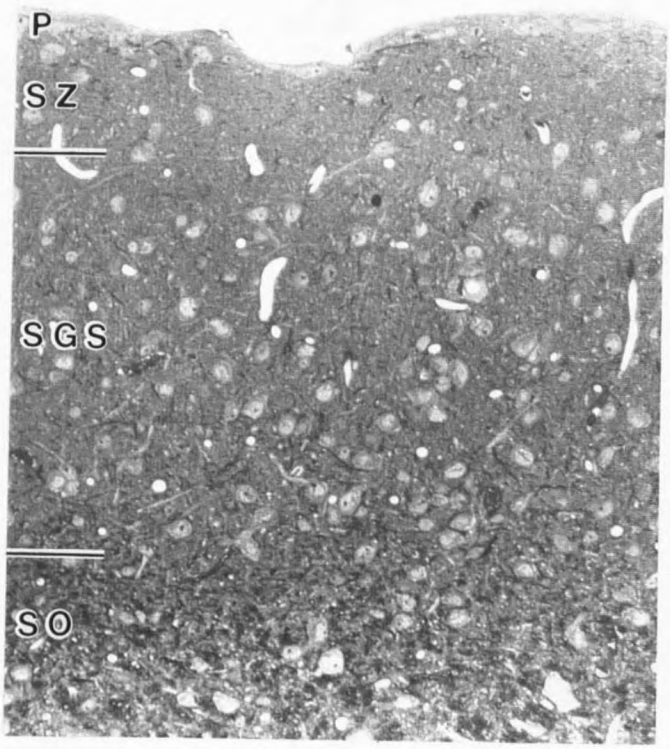

Figure 1. Light micrograph of a 1 μm coronal section through the superficial (visual) laminae of the left superior colliculus of a 90 day old rat, stained with toluidine blue. The pial surface (P) is at the top. Note: the transversely sectioned myelinated fibers in the stratum opticum (SO); the high density of cells in the stratum griseum superficiale (SGS); and the relative lack of cells in the stratum zonale (SZ). Magnification is 175X.

mainly of rostrocaudally oriented myelinated nerve fibers from the ON and afferents from other parts of the visual system such as the visual cortex. The nerve fibers from the ON enter the nucleus in the SO, then after a longitudinal course, turn superficially to synapse in the SZ and outer SGS on neurons whose cell bodies are found in the SGS (Lund,'72). The SZ is a molecular layer consisting mainly of neuronal processes and synapses. Neurons in the SGS project axons to the deep laminae where visual information is integrated with input from other sources, such as from the somatosensory cortex (sensory modalities) and the inferior colliculus (auditory input) (Sefton and Dreher,'95).

Golgi techniques have been used to classify six neuron types in the superficial laminae of the mature rat SC, all of which are assumed to receive input from the ON (Langer and Lund,'74; Labriola and Laemle,'77; Warton and Jones,'85), and include marginal cells, horizontal cells, piriform cells, stellate cells, narrow field vertical cells, and wide field vertical cells. The piriform cells, narrow field vertical cells, and wide field vertical cells are projection neurons that are primarily found in the SGS and that project axons to the deep integrative laminae of the SC. Piriform cells are located in the outer SGS and have cup-shaped somata with dendrites projecting superficially and axons originating from the base. Narrow field vertical cells are located in the SGS and have fusiform shaped somata oriented perpendicular to the pial surface. Wide field vertical cells are located in the deep SGS near the border of the SO and have shapes similar to that of the more superficial piriform cells. The horizontal cells, marginal cells, and stellate cells are fewer in number and are considered local interneurons in the superficial SC. Horizontal cells are located along the zone between SZ and outer SGS and their processes are arranged tangential to the pial surface. Marginal cells are located in the SZ and their processes project deeper within the superficial laminae of the SC. Stellate cells are randomly oriented multipolar neurons found throughout the superficial layers but which are most numerous in the SO and the SGS.

Development of the Rat Superior Colliculus

Neurogenesis, Histogenesis, and Synaptogenesis

Neurogenesis in the rat SC has been studied using autoradiographic techniques (Labriola and Laemle,'77; Altman and Bayer,'81). In these studies, animals were given an intraperitoneal or amniotic sac injection of systemic tritiated thymidine (thymidine labeled with ^{3}H) that was incorporated into DNA during replication (Angevine and Sidman,'61). Initially, cells incorporating ^{3}H-thymidine were heavily labeled, but after pulse labeling the signal became more dilute as the cells continued to divide. Experiments of this type can identify cells that were "born" during the period of time ^{3}H-thymidine was available for incorporation into DNA. By tracing when cells were born and to where these cells migrate, it has been possible to demonstrate the time course of origin of specific cells in the SC and their migration routes to form definitive layers (Labriola and Laemle,'77; Altman and Bayer,'81).

As the neuroepithelial cells that form the wall of the neural tube become layered, several zones can be distinguished (Boulder Committee,'70). The ventricular zone surrounds the lumen of the neural tube and eventually becomes the ependymal lining of the ventricles of the brain and central canal of the spinal cord. The ventricular zone is initially characterized by a high mitotic rate. As the wall of the tube thickens, a subventricular zone can be distinguished and becomes the main site of cell proliferation. Cells migrate out of the proliferative zones and eventually differentiate into the neurons and glia of the CNS. The intermediate zone extends from the subventricular zone to the marginal zone and the marginal zone extends to the pial surface (Boulder Committee,'70). The intermediate zone is composed of postmitotic migrating neurons and the marginal zone is formed by their processes. Neuronal cell bodies from the intermediate zone organize into the gray matter of the CNS in the spinal cord and brain stem, and their myelinated axons become the white matter.

Neurons are thought to migrate along radial glia from the ventricular and subventricular zones to their respective locations in cerebral cortex (Rakic,'81). In the chick diencephalon early migration does occur radially, but tangential migration of neurons along axonal tracks accounts for a significant part of later neuronal migration (Golden et al.,'97). Similarly, radial migration is followed by tangential migration of neurons in the chick brain stem (Hemond and Glover,'93). Studies in the rat SC have verified that its development is similar to other parts of the CNS, where neurons are derived from the ventricular and subventricular zones of the embryonic mesencephalic tectum and are thought to be guided during neuronal migration by the processes of radial glia (Mustari et al.,'79; Ganzler-Odenthal and Redies,'98), but to my knowledge tangential migration has not been studied in the rat brain stem.

Neurogenesis in the rat SC takes place on gestational days (G) 12 - 18 with both a rostrocaudal and an inside-out gradient of development (Bruckner et al.,'76; Mustari et al.,'79; Altman and Bayer,'81; Raedler et al.,'81). Thus, the oldest neurons are located rostral in the SC and in the deepest layer. One group suggests a more complicated gradient where the deep layers have an inside-out sequence of development but the superficial layers have a complex outside-in gradient of development (Altman and Bayer,'81). Neurogenesis specific to the superficial laminae occurs in a more restricted temporal window than that of the entire SC, from G15 - 18 (Mustari et al.,'79; Altman and Bayer,'81) (see Figure 16 in the Discussion).

The postnatal development of neurons in the superficial layers of the SC has been studied by Golgi-Cox impregnation methods (Labriola and Laemle,'77; Warton and Jones,'85). At 3d, neurons have immature morphology with few branched dendrites that develop further through elongation and branching. Adult neuron types can be identified by 9-15d. Dendritic spines can be seen as early as 9d, but most develop between 23-31d. The larger neurons, such as the vertical-type neurons, develop

earlier than the smaller neurons, such as the marginal and stellate cells (Labriola and Laemle,'77; Warton and Jones,'85).

Neuron development in the superficial SC can also be characterized by the expression of specific neurotransmitters. In the cat SC γ-aminobutyric acid (GABA), an inhibitory neurotransmitter, is expressed early in neuronal development during neuronal migration (Mize et al.,'96). GABA is found mainly in the superficial SC and even though immunoreactivity can be seen early on, it seems that GABAergic inhibition develops postnatally. Glutamate, which is involved in most retinotectal synapses, is expressed during synaptogenesis and fiber refinement which occur from birth through 31d (Warton and McCart,'89; Sakurai and Okada,'92).

Nervous system development generally involves an initial overproduction of neurons and subsequent elimination by apoptosis or programmed (or naturally occurring) cell death (Cowan et al.,'84). Cell death during the normal development of the rat SC occurs from G20 to 11d with the peak rate of cell death on the day of birth (Arees and Astrom,'77), which is coincident with neuronal migration and differentiation in the rat SC (Labriola and Laemle,'77; Warton and Jones,'85). Cell death is thought to occur normally for two reasons: (1) to match the size of the afferent RGC population with the size of the target SC neuronal population, and (2) to eliminate neurons that are connected improperly in the formation of the retinotopic map (Bunt et al.,'83; Jeffery,'84). Developing RGCs also go through a period of naturally occurring cell death that occurs over the first 10 postnatal days in the rat (Cunningham et al.,'82), during which the cell population drops from ~200,000 to ~117,000 and ON fibers drop from ~250,000 to ~120,000 (close to adult numbers) (Perry et al.,'83). The period of cell death in the superficial layers of the SC and the ganglion cell layer of the retina overlap, and the days at which neuronal cell death appears maximal in both populations coincide at 6-7d (Cunningham et al.,'82). Afferent input is necessary to mediate naturally occurring cell death in the SC (Cunningham et al.,'79; Galli-Resta et al.,'93). If the

spontaneous firing of the retina is silenced on 6d by the application of tetrodotoxin (TTX), cell death in the rat SC is increased (Galli-Resta et al.,'93). A similar increase in cell death occurs in the rat SC if enucleation is performed at birth (Giordano and Cunningham,'82). At least two possibilities exist to explain these effects on cell death: (1) electrical stimulation of ON fibers releases a trophic factor that sustains neurons in the SC, or (2) activity of the ON fibers is directly trophic to the target neurons in the SC. These studies indicate that cell death is a normal part of SC development and that the process of cell death is modified by afferent input from the ON. The SC has also been implicated in modulating RGC cell death (Huxlin et al.,'95). The SC has been shown to produce proteoglycan which was hypothesized to act as a trophic factor for RGCs, and when this proteoglycan was injected into the early postnatal rat retina, it rescued a significant number of RGCs from apoptosis (Huxlin et al.,'95).

The development of the retinocollicular pathway results in a precise retinotopic map (Lund,'72; Diao et al.,'83; Simon and O'Leary,'91) in which greater than 90% of the afferent axons from each retina project to the contralateral SC (Linden and Perry,'83). Rat optic tract axons enter the SC in the SO and run in a rostrocaudal direction, and then turn superficially to synapse in the superficial laminae of the SC (Langer and Lund,'74). These axons have en passant synapses in the zone of vertical cells in the SGS but the greatest density of terminal synapses occurs in the SZ. Most retinal axons synapse with the dendrites of wide and narrow field vertical cells of the SGS although it is assumed that all neurons in the SGS receive ON input (Warton and Jones,'85; Boyes and Veronesi,'88). Nasal retina projects to the caudal SC, temporal retina projects to the rostral SC, dorsal retina projects to the lateral SC, and ventral retina projects to the medial SC (Diao et al.,'83). To achieve this precise pattern, normally developing RGC axons must grow out from the retina to form the optic nerves; decussate at the optic chiasm to form the optic tracts; select a target (primarily SC in the rat); form initial diffuse synaptic contacts within the SC; and refine synaptic connections to

form a precise retinotopic map on the SC. The current paradigm classifies mechanisms involved in the development of the retinocollicular projection as either activity-independent or activity-dependent (Goodman and Shatz,'93). The activity-independent mechanisms are predominantly responsible for early development of the retinocollicular projection including neurite outgrowth and axonal guidance and are based on molecular guidance cues and trophic factors (Goodman and Shatz,'93). Activity-dependent mechanisms are predominantly responsible for later development of the retinocollicular projection including synaptogenesis and refinement of the retinotopic map. Activity-dependent mechanisms include both spontaneous afferent electrical activity from the retina up until eye opening at around 12-14d (Lund and Lund,'72; Galli-Resta et al.,'93), and patterned visual activity from the retina after eye opening (Lund and Lund,'72; Simon et al.,'94).

Activity-independent processes are guided by the molecular interactions of cell adhesion molecules in both cell-cell and cell-substrate interactions, and by diffusible chemical gradients (Hankin and Lund,'91; Goodman and Shatz,'93). In the rat, target extract from the developing SC has been shown to stimulate neurite outgrowth from RGCs in vitro (Bosco et al.,'93). Nerve growth factor (NGF) has also been shown to stimulate the outgrowth of neurites but in a nonspecific manner, causing growth of processes from many types of retinal cells (Bosco et al.,'93). Since SC extract has been shown to be type-specific for RGCs, it appears that RGC development is differentially regulated by soluble signals from the target tissue. In the mouse, evidence supports the hypothesis that pioneer RGC axons lead the way out of the retina forming a pathway for the next axons to follow in the formation of the ONs (Silver and Sidman,'80). RGC axons must choose whether to cross or not to cross at the optic chiasm, where more than 90% decussate to innervate the contralateral SC (Linden and Perry,'83). From the optic chiasm the nerve fibers form the optic tracts and must find the appropriate target in the SC. The first afferents from the retina arrive at the rat SC on G16 (Bunt et al.,'83).

Retinal afferents are prevented from crossing the tectal midline by glial cells that function as part of the substrate that helps compartmentalize axons during retinal afferent innervation (Wu et al.,'98). On G13 the median ventricular formation (MVF) appears in the dorsal mesencephalic wall (Raedler et al.,'81). As the MVF develops, it appears to contain many parallel fibers of astrocytes projecting towards the pial surface and likely contributes to the formation of the midline glial septum. In hamsters, it has been found that the midline glial septum plays a role in compartmentalizing the optic input to the SC (Wu et al.,'98). If the glial processes of the midline septum are lesioned, axons can be induced to aberrantly cross the midline indicating that these glia have a barrier function. The midline glial septum in the rat also functions to compartmentalize the retinal input to the SC (Snow et al.,'90).

The development of a precise retinotopic map from an initially diffuse retinal projection to the SC depends on competitive interactions between axons with the correct topographic target and axons projecting to an aberrant location (Simon et al.,'94). The ipsilateral retinocollicular projection is larger in the neonate than in the adult (Laemle and Labriola,'82). This projection increases in density from birth to 6d but then gradually recedes until the adult projection is attained by about 10d (Perry et al.,'83). Many of the axons that initially reach the SC have collaterals that branch to connect to a wider area of the SC. When contralateral innervation is removed by enucleation in the newborn rat, the ipsilateral projection does not recede and instead forms functional synapses (Laemle and Labriola,'82). The period of synaptic proliferation in the SGS extends through 30d and is followed by a period of synaptic elimination until the adult synaptic density is attained by about 85d (Warton and McCart,'89). Neural activity accounts for the strengthening of some synapses and the elimination of others. There is a 'critical period' during which normal vision (activity) is necessary for development of the precise retinocollicular map that occurs from eye opening to 30-35d (Lund and Lund,'72).

Activity-dependent mechanisms account for the refinement of neural connections, including the refinement of the retinotopic map in the SC and are thought to involve glutamate activation of N-methyl-D-aspartate (NMDA) receptors on the postsynaptic neurons (Shatz,'90; Chen and Tonegawa,'97). One hypothesis is that NMDA receptor activation on the postsynaptic neuron causes an influx of Ca^{2+}, which is required for calmodulin to stimulate the enzymatic synthesis of nitric oxide (NO) by nitric oxide synthase (NOS) (Garthwaite,'91). NO can then diffuse across the cell membrane, and is thought to be a retrograde messenger which can stimulate guanylate cyclase in the presynaptic cell and raise intracellular levels of the second messenger, cyclic guanosine monophosphate (cGMP) (Garthwaite,'91). Although the specific role of cGMP is still unclear, it has been shown to act directly on ionic channels of neuronal cell membranes, neurotransmitter production and release, and growth cone motility (Garthwaite,'91), and through these actions may be involved in the refinement of the retinotopic map.

Several lines of evidence implicate the NMDA-NO mechanism in the activity-dependent development of the retinocollicular (or retinotectal, depending on the species) projection. In the development of the chick retinotectal projection, which at maturity is completely contralateral, a transient ipsilateral projection is present which persists if NOS in the tectum is inhibited (Wu et al.,'94). Since NO is normally expressed in chick tectal cells and inhibiting its synthesis affects the refinement of the retinotopic map, NO is likely a messenger from tectal cells for feedback to the retinal cells during development (Wu et al.,'94). The transient chick ipsilateral retinotectal projection will also persist if the NMDA receptor itself is blocked, which directly implicates NMDA receptor activation in the refinement of the retinotopic map (Ernst et al.,'99). This particular activity-dependent mechanism is not universal for connections involving other neurotransmitters such as acetylcholine, as the cholinergic fiber patches that develop in the rat SC are not affected by inhibiting NOS (Mize et al.,'97). Further, NOS expression by tectal cells in the chick optic tectum is dependent

upon the presence of ON fibers (Williams et al.,'94). Thus, if the eyes are removed during early development, NOS expression significantly decreases, which further implicates NO as a retrograde messenger. The specific role of NO in refinement is not understood, but there is evidence that NO stops axonal elongation when an appropriate target is contacted by causing the collapse of RGC growth cones, and it is suggested to be an important messenger in stabilizing synapses (Gally et al.,'90; Hofer and Constantine-Paton,'94).

NOS, the enzyme that produces NO, is expressed during the time period corresponding to the refinement of synapses (Mize et al.,'96). In the chick optic tectum, NOS expression has been correlated with the period of optic nerve innervation but then peaks before hatching during the initial period of synaptogenesis (Williams et al.,'94). There appears to be a different temporal expression of NOS-positive staining in the rat (Tenorio et al.,'95). NOS-positive cells are first seen on 7d, with peak expression on 15d. Thus, NOS expression correlates with RGC cell and axon death and synaptic refinement (Perry et al.,'83).

Since there is good evidence that NMDA receptor activation and NO feedback are involved in the development of the retinocollicular projection, studies examining the effects of alcohol on the development of neurons expressing NOS in the SC have been started in this laboratory (Phillips et al.,'99). Gestational alcohol exposure decreased the areal cell density of NOS-containing neurons in the SGS indicating either a cell loss or a loss of NOS expression. The implication of these findings is that gestational alcohol exposure could alter the developing connectivity of the neurons in the SGS and, therefore, could have further ramifications on cell death and neuronal maturation.

Gliogenesis

Macroglia (astrocytes and oligodendrocytes) of the SC are distributed in a pattern and express molecules similar to elsewhere in the CNS (Harvey et al.,'93). During CNS development

astrocytes form limiting membranes (Snow et al.,'90), induce and maintain the blood-brain barrier formed by the endothelial cells of CNS blood vessels (Janzer and Raff,'87; Janzer,'93), secrete growth factors (Martin,'92), play a role in axonal guidance (Silver and Sidman,'80), enhance neuronal survival (O'Malley et al.,'94), and stimulate neuronal morphogenesis (Chamak et al.,'87). In the mature CNS, astrocytes play such roles as enhancing the efficacy of synapses (Pfrieger and Barres,'97), transporting substances between blood and neurons (Abbott,'87), and cycling glutamate (Rothstein et al.,'96). Oligodendrocytes are the myelinating cells of the CNS (Compston et al.,'97) but can also play an inhibitory role in axon growth (Schwab and Caroni,'88). Microglia are macrophage-derived immunocompetent cells in the CNS (Davis et al.,'94; Compston et al.,'97). These cells migrate into CNS tissue from the periphery during embryogenesis and are thought to form the mature resident population (Davis et al.,'94). Microglia perform phagocytic functions to remove cellular debris resulting from natural cell death during development and in response to injury and disease (Davis et al.,'94). Microglia were not specifically analyzed in the present study.

There are few references in the literature that directly investigate ghogenesis in the rat SC although inferences can be made from experiments examining glial development in other regions of the CNS. Tissue transplant studies in rats have shown that macroglial precursor cells are present by G15 in the SC (Harvey et al.,'93). In a qualitative study of the development of the rat visual system, gliogenesis in the SC was found to be similar to that of the visual cortex (Raedler and Sievers,'75) and, therefore, studies of glial development in the rat visual cortex can provide clues to similar events in the SC. Autoradiography of the postnatal formation of macroglia in the rat visual cortex showed that gliogenesis occurs in two peaks (Mares and Bruckner,'78). The first peak from 3-7d is due primarily to astrocyte proliferation and occurs during the period of growth and maturation of neurons. The second peak on 16d is due primarily to oligodendrocyte proliferation and occurs at the onset of myelination (Mares and Bruckner,'78). This same pattern of macroglial proliferation, in

which astrocytes are generated before oligodendrocytes, should occur in the development of the SC. A postnatal assay for two enzymes used as specific glial markers in the rat CNS [glutamine synthetase - astrocytes; 2',3' cyclic nucleotide phosphohydrolase (CNPase) - oligodendrocytes and myelin], suggests large differences in the functional maturation of these two glial cell populations: metabolic activity increases only modestly in astrocytes after birth; CNPase has a steep increase between 8-14d in oligodendrocytes (Virgili et al.,'90). This supports the idea that astrocytes are already present and functional in the rat CNS at birth, whereas oligodendrocytes generally mature postnatally. In the hamster, oligodendrocytes mature and myelination occurs along the proximo-distal axis of the ON fibers in the visual pathway, such that even myelination of the SO occurs in a rostrocaudal direction (Jhaveri et al.,'92). Therefore, the timing of myelination for different components of the rat visual system is expected to be different depending upon where the structure lies physically along the CNS visual pathway. Myelination of the SO begins on 12d (Warton and Jones,'85) and occurs relatively late in comparison to myelination of the ON, which begins on 6d (Tennekoon et al.,'77). In the present study the development of myelin was not studied; however, immunocytochemical staining was used to characterize the effects of alcohol on the development of the astrocytes in the SC.

Antibodies to glial fibrillary acidic protein (GFAP) and S-100 were used as markers to study astrocytes (Schmidt-Kastner and Szymas,'90). GFAP is an intermediate filament located in the cytoplasm of astrocytes (Schmidt-Kastner and Szymas,'90). It is important to recognize that in the study of GFAP+ cells, GFAP expression in astrocytes is being characterized rather than a direct study of astrocyte numbers or process size (Hawrylak and Greenough,'95). S-100 is a calcium-binding protein that is specific to astrocyte soma and cell processes in the CNS (Ghandour et al.,'81; Wijsman and Shivers,'93). In the normal mature SC, heavy GFAP staining is localized to the external limiting membrane, to the area surrounding blood vessels, and to the midline of the tectum,

but more diffuse staining is found throughout the SGS (Harvey et al.,'93). Anti-GFAP has been used to stain CNS tissues from rats developmentally exposed to alcohol, and alcohol has been shown to cause transient astrogliosis in the cerebrum and cerebellum as judged by the increased number of reactive astrocytes which stain GFAP+ (Shetty and Phillips,'92; Goodlett et al.,'93).

Previous Work with Alcohol on the Development of the Visual System

Humans with FAS have ocular anomalies and visual dysfunctions (Stromland,'90; Stromland et al.,'91; Stromland and Pinazo-Duran,'94; Stromland and Hellstrom,'96). Animal studies have helped clarify which structures in the mammalian visual pathway are vulnerable to developmental alcohol exposure, and to some extent have helped to define the temporal windows of vulnerability of these structures. Damage to the retina and the eye caused by developmental alcohol exposure would obviously affect normal vision. Electroretinography was used to examine the functioning of photoreceptors in dark-adapted rats after developmental alcohol exposure and showed increased threshold and latency with decreased response amplitude (Katz and Fox,'91). Developmental alcohol exposure in rats has been shown to cause the improper migration of RGCs and 25% reduction in the thickness of the neural retina during early development (G16-4d) (Ferriero et al.,'92), and in the mouse has been shown to cause micropthalmia (Cook et al.,'87), and increased cell cycle time and cell loss during ocular ontogeny (Kennedy and Elliot,'86). Alcohol-induced cell loss and/or changes in the electrophysiology of photoreceptors in the retina may alter the activity of the RGCs, and so could help explain any changes in the activity-dependent developmental processes that occur in the development of the SC

The development of the alcohol-exposed ON has been examined extensively using animal models of FAS in this and other laboratories. Both a full three trimester human equivalent alcohol exposure and a third trimester human equivalent alcohol exposure caused a delay in myelin

acquisition, a permanent reduction in the myelin thickness (Phillips,'89; Phillips et al.,'91), and a delay in oligodendrocyte maturation (Phillips and Krueger,'90; Phillips and Krueger,'92). Postnatal "binge-like" alcohol exposures given at either 5-6d or 9-10d both caused significant developmental alterations at 15d, including reductions in the cross-sectional area of the ON and thinner myelin on ON axons (Phillips et al.,'96). Particularly relevant to the present study, the 5-6d binge exposure caused a significant reduction (-40%) in the number of nerve fibers in the ON at both 15 and 90d (Phillips et al.,'98). In the present study, SC tissues from the same 5-6d binge-exposed animals were analyzed at both 15d and 90d. Using a gestational alcohol exposure, Stromland and Pinazo-Duran ('94) reported a significant decrease in both ON glial cell density and the number of ON fibers, and delayed myelination in rat ON on 4d and 7d. In a very different exposure model whereby mice were exposed to ethanol in utero via intraperitoneal injection on G8, 15d ON was found to have a significantly reduced cross sectional area, a reduced number of ON axons, and a reduced percentage of myelinated axons (Ashwell and Zhang,'94). Because alcohol caused significant developmental changes in the ON in several alcohol exposure experiments, it may also alter the development of the connectivity of the neurons in the superficial laminae of the SC.

The rat oculomotor nucleus innervates extraocular eye muscles and receives some input from the SC, and is also vulnerable to developmental alcohol exposure (Burrows et al.,'95). After gestational alcohol exposure, there was a reduction in the cross-sectional area of the oculomotor nucleus, a decrease in the density of neurons, and an increase in the number of astrocytes in the nucleus. Neurons normally clustered in the center of the nucleus were more diffusely arranged at 15d, indicating that alcohol can either delay maturation of or permanently alter the structure of the oculomotor nucleus.

Studies of other regions of the visual pathway after alcohol exposures are limited. Gestational alcohol exposure has been shown to cause significant delay in the maturation of neurons

in the kitten LGN, as indicated by the extent of dendritic arbor in Golgi-Cox stained neurons (Magloczky et al.,'90). To my knowledge there have been no studies in the visual cortex in animal models of FAS.

Though the normal development of the SC has been well-studied in the rat, little research has focused on its development during or after alcohol exposure. G18 mice exposed to ethanol in utero were reported to have an increase in the neuronal areal density in the superficial SC, accompanied by a reduced total area of the midbrain, and a reduction in the ratio of midbrain cross sectional area to that of the cerebral aqueduct (Zajac et al.,'88). This study is hard to interpret because only G18 mice were analyzed and although the experimental dams were fed a commercially obtained alcohol-inclusive liquid diet, a pair-fed paradigm was not used so it is likely that the control group was not a proper control for nutrition. Ashwell and Zhang ('94) looked at the mouse 15d ON and SGS after an acute exposure to ethanol by intraperitoneal injection on G8. While they found significant differences in the cross-sectional areas of ON, a reduction in the number of ON axons, and deficient myelination, no significant differences were reported in the total size of the neuronal population in the superficial SC. However, alcohol caused an increase in the areal density of SGS neurons and a decrease in the total volume of the SC, which led the authors to conclude that the estimated total number of neurons was unaltered. This experiment suggests alcohol-induced changes to the neuronal population of the SC in the absence of changes in absolute neuronal number, even under the limited exposure to ethanol the mice received.

Studies in this lab have provided some evidence of significant alcohol-induced effects on the development of the superficial lamina of the rat SC (Wall and Phillips,'93; Phillips et al.,'99). In a pilot study, pregnant dams ingested alcohol throughout gestation via liquid diet, and male offspring were examined at 15 and 35d (Wall and Phillips,'93). Tissues were processed for either plastic embedding or Golgi impregnation. Alcohol caused a decrease in the complexity of the dendritic

arbors of one class of Golgi-stained neurons in the SGS (Wall and Phillips,'93). Light microscopic analysis of toluidine blue-stained plastic sections at 15d found no statistically significant differences in either neuronal or glial areal densities. That experiment was repeated in part using more consistent tissue sampling to produce the tissues of the present study. One set of SC tissues from the present exposure was stained for nitric oxide (NO) producing cells by the use of histochemical staining for nitric oxide synthase (NOS) (Phillips et al.,'99). Analysis at 15d found that alcohol caused a significant reduction (-24%) in the number of NOS+ neurons in the SGS of the SC (Phillips et al.,'99). NO is a neural messenger molecule that has been implicated in many roles in the CNS including as a messenger transiently expressed in the tectum during the development of synaptic connections (Wu et al.,'94). Since NOS+ neurons appear to be important for the acquisition of proper circuitry during SC development and NOS+ neurons are affected in the SC by gestational alcohol exposure, it is important to further characterize the development of the SC in alcohol-exposed animals.

Principles of Stereology

Neural Counting Methods

There are a variety of neural counting methods that have been used to quantify either the areal or volume density, or total number of cells in defined regions of the nervous system. Such methods include serial reconstruction, profile counts, assumption-based methods, and stereology (3-D) (Oorschot,'94; Coggeshall and Lekan,'96). Each of these methods has appropriate uses and distinct advantages and disadvantages. Currently, the issue of which methods are most appropriate for analysis of individual CNS regions is hotly debated in the literature (Geinisman et al.,'97; Hagg et al.,'97; Peterson et al.,'97; Schmitz,'97).

Counts derived from serial section reconstruction of an entire defined region or nucleus determine the actual number of cells within a defined region (Coggeshall and Lekan,'96). This is the most absolute neural counting method available. Briefly, the region of interest is exhaustively sectioned and the histological sections are analyzed in sequence to reconstruct the entire structure. Profiles of cells are followed from section to section such that each cell is counted once. The advantage to this method is that the number of cells counted is the true number, not an estimation that may be biased. The disadvantage is that this method is inefficient and extremely labor intensive, and can be limited by technical inconsistencies such as missing sections.

Less accurate but most commonly used methods of cell counting are 2-D profile counts whereby profiles of cells are sampled and counted on histologic sections to estimate areal densities or total numbers of cells (Oorschot,'94; Coggeshall and Lekan,'96; Morrison et al.,'98). The assumption is that changes in the areal density or number of profiles are representative of changes in the true volume density or total number of cells. Intuitively, one can imagine that larger cells will create more profiles than smaller cells. Another way to view this concept is that the profile of a larger cell has a higher probability of being on any section than does the profile of a smaller cell. Therefore, one disadvantage of these methods is that if profiles of different size cells are being counted, then total profile numbers may not be equal to total cell numbers. In addition, if an experimental manipulation changes cell volume, then comparing profile areal densities or total profile numbers between experimental and control groups would lead to difficulties in interpretation. These methods are considered biased because profiles of larger cells have a higher probability of being counted. The advantage of these methods is that they are relatively quick and simple. If it can be shown that cell volume is not affected by experimental manipulation, then relative changes in profile number/density are probably similar to real changes in cell number/density. However, since

the true number/density of cells is not estimated, interpretations of changes resulting from profile counts are still open to criticism.

Cell counting methods designed to correct for the overestimation of cell numbers in simple profile counts are the model-based methods that convert profile numbers to cell numbers using correction factors (Abercrombie,'46; Coggeshall and Lekan,'96). These methods have also been called assumption-based because they make geometric assumptions about cells in order to create the correction factors. For instance, the assumption is that all nuclei are spherical. A correction factor based on this assumption is entirely dependent on how well the cell nuclei fit the assumption. The most commonly used model-based method is the method of Abercrombie (Abercrombie,'46). The advantages to these methods are that they are efficient and accurate as long as the assumptions are met. The disadvantage is that there is no way to know if the estimations are biased unless the chosen method is calibrated for the cell type and region of interest using serial section reconstruction.

Stereological cell counting methods utilize sampling designs based on modified serial section reconstructions and are considered more accurate than simple profile counts and model-based counts (Sterio,'84; Gundersen,'86; Coggeshall and Lekan,'96; Mayhew and Gundersen,'96). These methods make no assumptions about size, shape, or orientation of cells, and are therefore considered unbiased. The assumptions which must be met are that every object has an equal probability of being counted and that profiles of cells can be followed from one section to the next. The simplest form of modern stereology is the physical disector consisting of two parallel sections of tissue separated by some distance defining a volume. All cells are counted which appear in the first section (reference section) but not in the second section (look-up section) (Sterio,'84). The distance between the two sections can be no greater than the height of the smallest object being counted; this insures each cell has an equal probability of being counted. Profiles of cells are analyzed on both sections, and cells are counted when a profile appears on one section but is not found in the next. Because

cells are counted in three dimensions, the physical disector yields an estimate of cell density (cells per unit volume, Nv). The volume of the brain region or structure (reference volume, Vref) can be determined by Cavalieri's method of volume estimation (Gundersen and Jensen,'87). In Cavalieri's method of volume estimation, a systematic (equally spaced along one axis of the structure) sample of sections through the structure is used to measure the area of the structure on each section. The sum of the areas is multiplied by the section separation to yield an estimation of volume, the reference volume. The cell density estimate can then be multiplied by the reference volume, to obtain an estimate of the total number of cells (N) in a structure. The advantage of stereological methods is that they yield unbiased estimates of cell counts and are efficient compared to serial reconstructions. The disadvantages are that they require more work than simple profile counts or assumption-based methods, and can be difficult to apply to structures with poorly defined margins.

As described above, the cell counting method has unique advantages and disadvantages. When determining which method to employ, there are certainly many factors to consider. The estimates of neuron number as determined by profile counts, the method of Abercrombie, and the physical disector have been compared to a serial section reconstruction of 965 neurons in a DRG (Coggeshall et al.,'94). The profile counting method overestimated the true number of neurons counted in the serial section reconstruction by 204% (1979±68 neurons) . The Abercrombie method underestimated the total number of neurons by 46% (527±86 neurons). Only the physical disector provided a precise estimation of cell numbers (969±136 neurons).

The Importance of Calculating N

Many proponents of stereology strongly suggest that the definitive data to be compared should be absolute number of cells, or N, rather than cell density, or Nv (cells per unit volume) (Oorschot,'94). An example of why this is so is apparent in a study in which developmental alcohol

or nicotine exposure was shown to cause a loss of mitral cells in the olfactory bulb, in the absence of any change in mitral cell density (Chen et al.,'99). The reason for this was that the reference volume of the olfactory bulb was reduced without any change in the volume density of mitral cells, so that when reference volume x volume density was applied, N was dramatically reduced. This demonstrates the potential lack of reliability in using changes in cell density alone for estimating changes in cell numbers. One could also imagine other possibilities where the density of cells could be affected, but the total number of cells in a structure is unchanged. For example, the cell density could be increased by experimental manipulation, while the reference volume could be decreased, such that there is no actual change in the total cell number in the structure. The interpretation in this scenario might be that the complexity of the neuropil has been altered, in the absence of cell loss. Due to the wide variety of possible outcomes when dealing with cell densities and numbers, interpretation is facilitated when as many parameters (such as cell density, cell number, and reference volume of the structure) as possible are measured, including N.

Coefficient of Error

The efficiency and the appropriateness of the sampling design of unbiased stereological methods that use systematic random sampling, such as the physical disector analysis, is commonly evaluated by calculating the coefficient of error (CE) of individual estimates for each parameter measured (Gundersen and Jensen,'87; West and Gundersen,'90; Geinisman et al.,'96; Miller et al.,'97). A physical disector analysis was used to evaluate the parameters examined in this study; CEs were calculated and their relevance to the data will be discussed in the Discussion. The CE is basically a measure of the intra-animal variation of each parameter measured, as a result of sampling. Several formulae have been developed that lead to the estimation of this statistical value based on the accepted sampling design (see Appendix) (Gundersen and Jensen,'87).

The sampling design of unbiased stereological methods is considered a systematic random sampling design. For example, if cell counts are to be performed for a region of interest (reference volume) using five physical disector pairs, then these physical disector pairs are equally spaced along one axis of the reference volume. This is the systematic application of the sampling design. The randomness of the sampling design comes from the random placement of the first physical disector pair within the first interval of length, and insures that each part of the reference volume has an equal probability of being sampled.

The systematic random sampling design contributes to the complexity of the formulae involved in the estimation of CE (see Appendix) (Gundersen and Jensen,'87). The following equation can be used to evaluate the sampling design for any given parameter:

Equation 1: $OCV^2 = CV^2 + OCE^2$ (Gundersen,'86),

where OCV is the observed coefficient of variation (standard deviation/mean) and is the computable or "observed" variance of a group of animals for the parameter (such as N), CV is the true biological variation between individual animals of the group (calculated from the other two variables), and OCE is the mean of the computable or "observed" intra-animal variations or coefficients of error for individual animals. In evaluating the stereological sampling design, the contribution of the OCE^2 should be roughly half or less than half of the OCV^2, indicating that variation among animals is due mainly to true biological variation among animals. In simpler terms, for stereological measurements for some parameter (such as N) from a group of animals there is a mean value and a standard deviation. The variance for the group (OCV) is calculated as the standard deviation/mean. The question is: to what extent is the observed variance for the group (for N) due to the true biological variability in neuron numbers among animals, and to what extent is it due to the intra-animal variation of neurons counted in each physical disector?

METHODS

Experimental Design

These experiments investigated the effects of alcohol on the development of the superior colliculus and were designed as an extension of previous studies in this laboratory showing that alcohol can cause significant alterations in the development of the rat optic nerve (ON). The aim of these studies was to develop appropriate quantitative stereological methods for tissue analyses and to analyze rat SC tissues obtained previously from both a gestational alcohol exposure experiment and a postnatal binge alcohol exposure experiment (Table 1).

Table 1. Experimental Groups for Physical Disector Analyses at Each Sacrifice Day

	Gestational Exposure		Postnatal Day 5 and 6 Binge Exposure	
Day of Sacrifice	EtOH-exposed	Control	EtOH-exposed	Control
15d	6	6	7	9
35d	6	6		
90d			9	8

In the gestational exposure, pregnant dams were fed an ethanol-containing diet throughout gestation. The gestational exposure occurs over the time of early neural tube development, neurogenesis, and much of the gliogenesis of astrocytes (Altman and Bayer,'81; Giulian et al.,'86; Harvey et al.,'93) (see Figure 16 in the Discussion). Tissues from rats sacrificed at 15 and 35 days postnatally were analyzed. At 15 days of age maturation of postmitotic neurons and their synapses is occurring in the SC, the majority of glia should already be present, and myelination of nerve fibers is

already underway. At around 15 days of age lamination in the SC is well-developed; this facilitated tissue analyses because the borders of the relevant laminae were visible (Labriola and Laemle,'77). Between 15 and 35 days of age further maturation of neurons, including dendritic and synaptic maturation, occurs in all visual layers of the SC, and myelination is being completed in the stratum opticum (SO) (Labriola and Laemle,'77; Warton and Jones,'85). By 35 days of age the overall morphology of the SC resembles that of the adult although some synapses are still being refined. Comparisons at these two sacrifice ages should provide information as to how gestational alcohol exposure affects development of the SC, and if changes do occur, whether alterations are likely to be permanent (see Figure 16 in Discussion).

In the postnatal binge exposure experiment, artificially-reared rat pups were fed an ethanol-containing diet via gastrostomy on postnatal days 5 and 6. This paradigm produced two bursts of high concentrations of blood alcohol, mimicking "binge" exposures that correspond to acute alcohol insult early in the third trimester of human pregnancy (Dobbing and Sands,'79; Dobbing,'81). The postnatal binge exposure occurs during the rat brain growth spurt. The brain growth spurt occurs around 5-10 days of age in the rat (Dobbing,'81; Thomson et al.,'88; Goodlett and West,'92; Coles,'94) and involves a period of rapid growth and dramatic increase in brain mass caused by neuronal growth and maturation and by glial cell proliferation, particularly of oligodendrocytes, followed by a period of rapid myelination (Lund and Lund,'72; Labriola and Laemle,'77; Warton and McCart,'89). An advantage of using temporally limited binge exposures is that they provide a means to compare temporal vulnerabilities with known developmental events. In postnatal binge exposure experiments, tissues from rats sacrificed at 15 and 90 days of age were analyzed. Postnatal day 15 was used for reasons similar to the gestational exposure. Postnatal day 90 was used because at this age rats are fully mature adults and have achieved maturation of all elements of the visual pathways, including optic nerve myelination, synapses in the SC, etc.

All tissue analyses targeted the retinorecipient superficial layers of the superior colliculus, the stratum griseum superficiale (SGS) and its accompanying molecular layer, the stratum zonale (SZ). For both alcohol exposure regimes toluidine blue stained plastic sections were used to measure the reference volume of the sampled regions of the superficial SC. Neuronal and glial cell volume densities were determined using a stereological physical disector probe, then total cell numbers for tissue slabs of known dimensions were estimated. Additionally, for the gestational alcohol exposure tissues, vibratome sections were immunocytochemically stained for glial fibrillary acidic protein (GFAP) and S-100 (a calcium binding protein) to characterize the maturation of astrocytes of the developing SC.

Methods

Gestational Alcohol Exposure

The animals in this series of experiments were exposed to alcohol and the tissues prepared as part of a study started by Ken Wall in the early 1990s. Animals were from a Sprague-Dawley colony maintained at the MSU Animal Resource Center. The colony was maintained under controlled conditions of constant temperature and humidity at 72 °F and 12 hour light/dark cycles, with the dark cycle beginning at 4PM. 3-4 month old nulliparous females (200-300g) were staged for the estrous cycle, placed with males overnight, and checked for vaginal plugs the next morning (gestational day 1 - G1). These dams were used as either the ethanol-exposed group or as chow-fed foster dams, while two days later, the same procedure was followed for the weight-matched control group. All pregnant dams were housed in individual nesting cages for the duration of gestation.

Alcohol-exposed dams were fed an ethanol-containing liquid diet ad libitum as their only source of food and fluids. The commercially-obtained diet (Bio-Serv #F1265SP) contained 37.5% of the calories from ethanol (6.7%v/v) and produced mean maternal blood alcohol concentrations

(BAC) of approximately 140 mg/dl (Shetty et al.,'93; Burrows et al.,'95). Mean BACs were determined following the same procedure as described in previous studies in this lab which used the same diet (Shetty et al.,'93; Burrows et al.,'95). Briefly, at 10:00 PM on the evening of G16 (2-4 hours after maximum feeding by dams), a tail vein blood sample was drawn from unanesthetized pregnant dams. The blood was separated in a centrifuge, and BAC was determined from the serum sample using a Sigma diagnostic kit #330-1. Pair-fed control dams were fed isocaloric diet (Bio-Serv Liquid Diet #F1264SP) of a volume equal to that of their weight-matched alcohol-exposed counterparts. This pair-fed paradigm was used to control for nutritional deficits that could occur in the alcohol ingesting dams. Chow-fed dams were reared in parallel to the experimental group, to be used as surrogate dams, with ad libitum access to standard rat chow. Chow-fed control pups were not included in this analysis because a pilot study in this lab and previous studies by other labs (Miller,'88; Miller and Potempa,'90), all of which used the same liquid diet, showed no significant differences between chow-fed and pair-fed dams in terms of weight gain during gestation and litter size. Their pups did not differ in terms of body and brain weights or other outwardly visible features of development such as day of eye-opening. On the day of birth (counted as day 0), pups from the alcohol-exposed and control groups were removed from their dams, and litters pooled. Pups from 3 or 4 dams were used in each group. Pups were culled by first selecting either all males or all females, and then by selecting those closest to the mean weight of these animals, to form rearing litters of eight pups. These litters were fostered to surrogate chow-fed dams. The foster rearing procedure controls for the possibility that experimental dams could have altered nursing behavior and/or lactational deficits that could result in malnutrition of offspring (Swiatek et al.,'86; Derr et al.,'87).

Offspring Used for Stereological Counts

Offspring used for stereological counts were male rats at 15 and 35 days of age. For each experimental group in the physical disector analysis, either control or alcohol-exposed, three male pups from each of two original litters (n=6) were used at 15 days of age, and two male pups from each of three original litters (n=6) were used at 35 days of age (Table 1).

Body weights were obtained at the time of sacrifice, then the animals were anesthetized with ether and perfused with 4% paraformaldehyde/ 2% glutaraldehyde in 0.1M cacodylate buffer (pH=7.4). Skulls and vertebral columns were opened immediately after perfusion and the brains and spinal cords were exposed to primary fixative in situ for three hours. Brains were then removed from the skull, trimmed (the olfactory bulbs were cut even with the frontal cortex, the cerebellar flocculus was removed, and the brainstem was cut transversely at the caudal end of the medullary pyramids), blotted dry, and then weighed. A midbrain block was removed from each whole brain using two coronal cuts made with a razor blade. The first cut was made through the cerebral cortex and diencephalon, just rostral to the midbrain. The second cut was made between the inferior colliculus and the cerebellum. The midbrain block was then embedded in a formaldehyde-fixed egg yolk-gelatin medium. Midbrain blocks were mounted on a chuck at the inferior collicular surface, and cut on a vibratome. The rostral end of the midbrain was sectioned until the SC was visible in a cut section and aligned by visualizing landmarks with reference to brain atlas plates (Paxinos and Watson, '82). Landmarks and section thicknesses were used to insure sections through the midbrain were from a uniform place along the rostrocaudal axis of the SC. This is important to note because the rat SC matures rostrocaudally (Altman and Bayer,'81). All SC sections for use in this study were taken from a location in the midbrain where the medial geniculate body and the cerebral peduncles were clearly visible while the interpeduncular nucleus was not. For 15 day old animals, three 100 μm sections were cut away and discarded. Then, two 200 μm sections were cut to obtain ventral

tegmental area tissue for use in another study. Next, two consecutive 200 μm sections of the midbrain were cut for this analysis. Thus the first section collected from the midbrain to be used for analysis at 15 days of age was approximately 700 μm into the SC from the rostral end. For 35 day old animals, five 100 μm sections were cut away and discarded. Then, eight 40 μm sections were cut to obtain tissue for use in another study. Next, two consecutive 200 μm sections of the midbrain were cut for this analysis. Thus the first section collected from the midbrain to be used for analysis at 35 days of age was approximately 820 μm into the SC from the rostral end. Each midbrain section was cut transversely by razor blade just dorsal to the cerebral aqueduct in order to separate the tectum from the tegmentum, then cut vertically such that the SC hemispheres were separated just to the right of the midline, to insure that the left hemisphere was fully intact.

All four SC hemisphere tissue slabs (2 right, 2 left) were prepared for plastic section study by either light or electron microscopy. Trimmed sections were placed back in primary fixative overnight and post-fixed the next day in 1% osmium tetroxide/1.5% potassium ferricyanide in 0.1M cacodylate buffer for 2.5 hours. Tissues were then dehydrated in a graded series of ethanol solutions (50%→70%→90%→100%) to propylene oxide, and flat embedded in Beem capsules using Embed 812 resin (Electron Microscopy Services, Ft. Washington, PA).

Offspring Used for ICC Analysis

The following sections regarding immunocytochemistry describe the tissue preparation and staining protocols used by Ken Wall to prepare the GFAP and S-100 stained tissues analyzed in the present study. Animals used in the immunocytochemistry (ICC) analysis (Table 2) were exposed to alcohol and reared in the same manner as those prepared for physical disector analysis, but were perfused and tissues prepared using procedures appropriate for ICC. Animals 15 and 35 days old were anesthetized with ether and transcardially perfused for 5 minutes with 4% paraformaldehyde in

0.1M phosphate buffered saline (PBS, pH=7.4). Immediately after perfusion, the brains were removed from the skull and immersed overnight in cold fixative (4°C). The next day brains were trimmed and weighed, and a midbrain block was removed as previously described. The midbrain block was egg-gel embedded and mounted on a vibratome chuck at the inferior collicular surface for sectioning from the rostral end of the SC.

Table 2. Stains and Groups Used for the Immunocytochemical Analysis of Astrocytes

Antibody to-	Age of Sacrifice	EtOH-exposed (n)	Control (n)
GFAP	15d	4	6
	35d	3	3
S-100	15d	7	7
	35d	7	8

GFAP Staining

Female animals were sacrificed at 15 and 35 days of age for GFAP studies. At 15 days of age 2 randomly selected females from each of two alcohol-exposed litters were used (n=4), and 3 randomly selected females from each of two control litters were used (n=6). At 35 days of age 2 randomly selected females from one litter and 1 female from one litter were used for the alcohol-exposed and control groups (n=3 for each group). The rostral end of the midbrain was sectioned until the SC was visible in a cut section and aligned by visualizing landmarks with reference to brain atlas plates (Paxinos and Watson, '82). All SC sections for use in this study were taken from a location in the midbrain where the medial geniculate body and the cerebral peduncles were clearly visible while the interpeduncular nucleus was not. For 15 day old animals, three 100 μm sections were cut away and discarded. First, a total of ten 30 μm sections were cut for CNPase and MBP ICC (5 alternating sections for CNP staining, and 5 sections for MBP staining). Then five 30 μm sections were cut for GFAP staining. For 35 day old animals, six 100 μm were cut away and

discarded. First, a total of ten 30 μm sections were cut for CNP and MBP ICC. Then five 30 μm sections were cut for GFAP staining. Free-floating sections were pretreated with 0.3% H_2O_2 in methanol for 25 minutes to eliminate endogenous peroxidase activity, and rinsed eight times in 0.01 PBS. Sections were then treated with sodium borohydride solution (1 mg/mL PBS) for 20 minutes and rinsed eight times in 0.01 PBS. Preincubation with sodium borohydride reduces free aldehydes, which result from the presence of fixative and can cause non-specific binding of antibodies, to alcohols (Kosaka et al.,'86).

Sections were incubated in blocking serum of 5% normal goat serum (NGS) and 0.3% Triton-X in 0.01M PBS for 2.5 hours at room temperature. Sections were then incubated in rabbit anti-GFAP antibody (Dako, Carpinteria, CA) at a 1:500 dilution in 5% NGS and 0.3% Triton-X in 0.01M PBS for 20 hours at room temperature and rinsed six times in 0.01M PBS. Incubation with secondary antibody (goat anti-rabbit with peroxidase conjugate; Dako) was done at 1:300 dilution in 0.01M PBS for 2 hours at room temperature, rinsing twice in 0.01M PBS and then three times in 0.05M Tris buffer. Sections were then incubated in a 0.05% DAB (3,3 diaminobenzidine tetrachloride) solution in 0.5M Tris buffer for 10 minutes, followed by a 5 minute incubation in 0.05% DAB and 0.01% H_2O_2 in 0.5M Tris buffer. Sections were rinsed twice in 0.05M Tris and then three times in 0.1M PBS. Sections were stored in PBS overnight and mounted on gelatin-coated slides, dehydrated, and coverslipped with Permount.

S-100 Staining

Male animals were sacrificed at 15 and 35 days of age for S-100 labeling. At 15 days of age 2 males from each of three litters and 1 male from one litter were used for both the alcohol-exposed and control groups (n=7 for each group). At 35 days of age 2 males from each of three litters and 1 male from one litter were used as alcohol-exposed animals (n=7), and 2 males from each of four

litters were used for the control group (n=8). Four consecutive 40 μm sections were cut from a uniform position in the SC. For 15 day old animals four 40 μm sections were cut for S-100 staining immediately after collection of the 200 μm sections collected for quantitative stereological analysis. For 35 day old animals six 100 μm sections were cut away and discarded. Then a total of 340 μm were cut for use in other studies. Then the sections were collected for S-100 staining. Free-floating sections were pretreated as described above to remove endogenous peroxidase activity.

Sections were incubated in blocking serum of 5% normal goat serum (NGS) and 0.3% Triton-X in 0.01M PBS for 2.5 hours at room temperature. Sections were then incubated in rabbit anti-S-100 antibody (Accurate, Westbury, NY) at a 1:1500 dilution in 5% NGS and 0.3% Triton-X in 0.01M PBS for 2 hours at room temperature with gentle agitation on a shaker and then left overnight in a 4°C refrigerator, then rinsed four times in 0.01M PBS. Next, sections were incubated with biotinylated goat anti-rabbit secondary antibody (Vector ABC kit) in a 1:200 dilution in 5% NGS and 0.3% Triton-X in 0.01M PBS, for 2 hours with gentle agitation at room temperature, and then rinsed three times in 0.1M PBS. Sections were then incubated with Vector ABC Reagent overnight at 4°C, and rinsed three times in 0.1M PBS. Sections were then incubated in DAB/glucose oxidase solution for 20 minutes in subdued light, and rinsed three times in 0.1M PBS. Sections were stored in 0.1M PBS with trimerosol until mounted on gelatin-coated slides, dehydrated and coverslipped with Permount.

5-6d Postnatal Binge Exposure

The animals in this series of experiments were exposed to alcohol and the tissues prepared by Susan Krueger and Lisa Shubloom as part of a study by Dr. Dwight Phillips investigating the effects of acute, high-dose alcohol exposures on CNS development. These exposures were designed to mimic binge drinking in the early third trimester of human brain development. The alcohol

exposure regime that was the focus of the present study delivered pulses of very high concentrations of dietary alcohol to artificially-reared rat pups postnatal days 5 and 6. Previous studies in this lab have shown this exposure produced mean peak BACs of 392 mg/dl (Phillips et al.,'96).

Animals were from a Sprague-Dawley colony maintained at the MSU Animal Resource Center, and maintained under the conditions described for the previous exposure. 3-4 month old nulliparous females (200-300g) were staged for the estrous cycle, mated individually with a male overnight, and checked for vaginal plugs the following morning. Pregnant dams were housed in individual nesting cages under controlled light and temperature conditions, with ad libitum access to standard rat chow and water.

The day newborn pups were first found in the cages was designated postnatal day 0. Litters were culled to 8 pups on postnatal day 0 by choosing animals closest to the mean pup weight, and allowed to nurse from mothers on 0-4 days of age Pups were artificially reared via gastrostomy on postnatal days 4-11. The artificial rearing and gastrostomy exposure procedures used in this experiment were similar to other postnatal exposures done in this lab (Phillips,'94), and are similar to the exposure paradigms developed by West, et al. (West et al.,'84; West,'93). 4 day old male pups from 8 litters were culled and divided into two experimental groups composed of at least one pup from each litter to produce similar mean litter weights for both alcohol-exposed and control artificially reared groups.

On postnatal day 4 cannulation was done on pups anesthetized with methoxyflurane. A silastic-covered wire was threaded through the esophagus to the stomach. The wire was bared and pushed through the gastric and abdominal walls. A polyethylene cannula was attached to the wire at the oral end and the wire pulled through the gastric and abdominal walls to seat the cannula. The flared end of the cannula was positioned against the gastric wall and fixed externally with a plastic washer. This created a direct passage for diet to be infused into the pups' stomachs. Infusion was

done with computerized syringe pumps that controlled the timing and amount of diet dispensed. The diet was artificial milk, supplemented with vitamins, minerals, and proteins (West et al.,'84). Each day pups were fed 33% of the average daily body weight of the entire artificially-reared group. The calculated amount was split over twelve feeding cycles of 20 minutes each. Alcohol-exposed pups received diet containing 15% (v/v) absolute ethanol in artificial diet on the 12:00 PM and 2:00 PM cycles on postnatal days 5 and 6. For these same cycles control pups received isocaloric diets with ethanol calories substituted with maltose-dextrin in the same diet. For the remaining ten 2-hour cycles, alcohol-exposed and control pups received the regular diet. On postnatal day 11, animals were fostered to surrogate chow-fed females until either sacrifice on day 15 or weaning on day 20. Surrogate chow-fed females gave birth at approximately the same time as those dams whose litters were artificially reared and were allowed to suckle their own litters until receiving artificially reared pups on postnatal day 11.

Body weights were obtained at the time of sacrifice on 15 and 90 days of age. Animals were perfused with 4% paraformaldehyde/ 2% glutaraldehyde in 0.1M cacodylate buffer (pH=7.4). Immediately after perfusion, skulls and vertebral columns were opened and the brains and spinal cords were exposed to primary fixative in situ for three hours. Brains were removed from the skull, trimmed, and weighed, and midbrain blocks were removed as previously described for the chronic prenatal exposure, using the same anatomical landmarks. As in the other experiment, two consecutive 200 μm slabs were cut with a vibratome from the SC and prepared as described for plastic embedded chronic prenatal exposure tissues.

Quantitative Stereological Analysis

All cell counts and tissue analysis were performed by one investigator and were done blind with respect to alcohol-exposed and control groups. The quantitative histological analysis used the

same methods for analysis of plastic-embedded tissues from both gestational exposure and postnatal binge experiments. For the gestationally-exposed animals the first 200 μm tissue slab collected from the left SC hemisphere of each animal was analyzed. For the postnatally-exposed animals one 200 μm slab from the left SC was analyzed but because the two 200 μm tissue slabs were not labeled, the relative rostrocaudal placement over the combined 400 μm of SC tissue collected was not known. Each tissue slab analyzed was serially sectioned at a thickness of 1 μm using a Reichert-Jung Ultracut microtome and glass knives to produce 80 serial sections. 80 1 μm sections could consistently be produced from each 200 μm tissue slab due to variation in the orientation of each 200 μm SC tissue slab at the block face (i.e. the surface of most of these large tissue slabs was not flat, or flush with the block face), and because of tissue lost both at the initial facing of each block and after each knife change. Thus, 80 serial sections (numbered 1 through 80) were mounted on gelatin-coated glass slides in sequence, and stained with basic toluidine blue.

Section thickness of semi-thin plastic sections cut at 1 μm was verified using two separate methods, Small's minimal fold method and the step method (De Groot,'88; Evans and Howard,'89). Small's minimal fold method involved measuring the width of the narrowest randomly occurring folds observed on semi-thin sections used in the physical disector analysis (De Groot,'88). Folds were viewed at 1000X under oil immersion, drawn using a drawing tube, and the width of folds was measured on the bit pad then divided by two. The theory of Small's fold method is that the width of the smallest fold will equal twice the section thickness. The mean of the individual measurements for the section thickness was 1.2 ± 0.2 μm (n=15).

The step method involved measuring the height of a step cut into a plastic bullet on the microtome set to advance a known distance (1 μm), and then dividing the height of the step by the number of sections cut in forming the step (Evans and Howard,'89). The face of a blank plastic bullet was trimmed to form a trapezoid, then faced with a glass knife. The knife was replaced with a

fresh glass knife and the microtome set to advance 1 μm. One complete section was cut from the block face to ensure that the fresh knife and block face were aligned. The position of the knife was then moved to the right so that the next section cut half of the trapezoid face. Twenty sections were then cut from half the trapezoid, leaving a step in the trapezoid face equal to the height of twenty sections. Twenty sections were used because in collecting tissues for physical disector analysis, each knife was used to cut, on average, twenty sections. The block was then mounted on a glass microscope slide with melted wax so that the step could be viewed from above using a microscope with a 40X objective lens and drawing tube. The step was drawn, then the height of the step was measured on the bit pad (=0.02mm), and divided by 20 to find the average section thickness. This method, done once, determined that the average section cut was indeed 1 μm.

Five physical disector pairs, described below, were used from each animal. Records were kept on where knife changes occurred during sectioning, and section sequences spanning a knife change (which occurred on average every twenty sections due to declining knife quality) were not used as a physical disector pair. Each physical disector pair consisted of two sections, the reference section and the look-up section, separated by a known distance, h. Since the two 1 μm sections of each physical disector pair were separated by one section (considered a place-keeper), h = 2 μm.

The placement of the physical disectors over the 80 serial sections followed a systematic random sampling design (Gundersen,'86; Gundersen and Jensen,'87) so that the five physical disectors for each animal were spaced equally, or systematically, over the eighty serial sections. Therefore, the physical disectors were spaced 16 sections apart (80/5=16). The aggregate of the five physical disectors were at the same time randomly applied to the eighty serial sections. The first physical disector pair had a random start within the first 16 serial sections, with the following four physical disectors being systematically applied. Any instance where either or both sections of the physical disector pair were deemed unusable (due to wrinkles, knife change, etc.), the next acceptable

physical disector pair was used. The predetermined systematic placement of each following physical disector remained as predetermined. For example, Table 3 shows the actual physical disector pairs used for one individual animal. In this case, the random number between 1 and 16 that determined the placement of the first physical disector pair was 4.

Table 3. Physical Disector Pairs¶ for Animal D, 35d, Gestational Exposure

Theoretical Disector Pairs	Actual Physical Disector Pairs Used
4,6	4,6
20,22	22,24*
36,38	36,38
52,54	52,54
68,70	68,70

* 20,22 was not used due to a knife change. 21,23 was not used because section 23 was too wrinkled. 22,24 was the first acceptable disector pair.

Each reference section was traced on a bit pad at 34X or 86X using an Olympus BH-2 microscope with a drawing tube and either a 4X or 10X objective lens, respectively (Figure 2). Each drawing included the pial surface of the SC, the border between the SGS and SO, the deep border of the SO, and major blood vessels, all of which were used as landmarks. The medial and lateral edges of approximately 150 μm were marked on each drawing and were excluded to avoid boundary problems associated with the narrowing and indistinct borders of the laminae at the medial and lateral egdes (Albers et al.,'88). A transparency was made of a printed grid with dimensions designed such that the absolute area of each grid square corresponded to the absolute area of the 10 x 10 grid in a 10X eyepiece at the respective magnifications (5 x 5mm for 34X drawings, or 15 x 15mm for 86X drawings). The grid was then randomly placed over the drawing and each square overlaying the SGS was numbered sequentially from left to right on the grid. A random number was generated, and the grid square with that number defined the target sampling area for the disector (Figure 2).

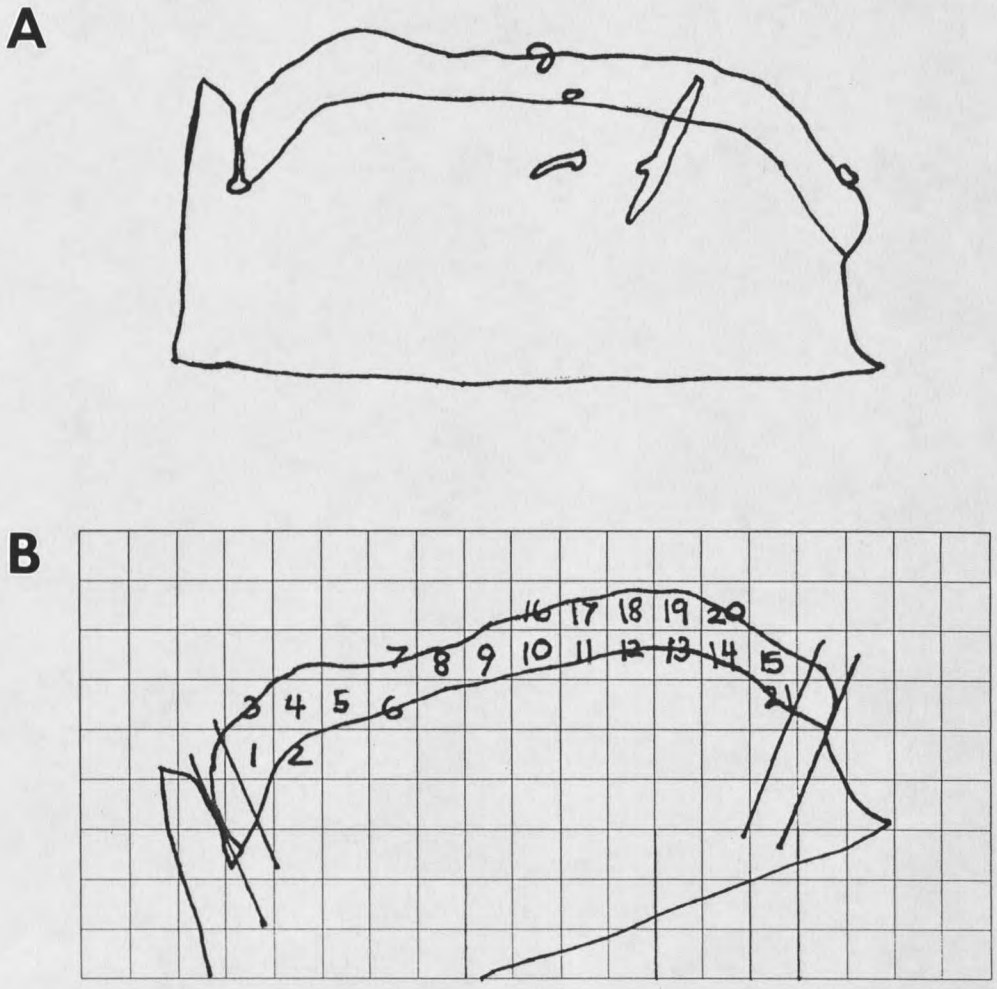

Figure 2. Illustration of the procedure used to randomly define a location for the counting frame. A: Camera lucida drawing of a reference section of a 15d animal (34X). B: A transparency grid was randomly placed over the camera lucida drawing and squares overlaying at least approximately half the height of the SGS from superficial to deep (excluding the medial and lateral edges of approx. 150 μm) were numbered from left to right. A random number was generated and the corresponding grid square determined the location of the counting frame.

The 10 x 10 eyepiece grid was centered over this target location and the sampling area was viewed using the 40X objective lens. The eyepiece grid defined the unbiased counting frame (0.032 mm^2) with two adjacent lines considered the inclusion lines (top and right) and the other two adjacent lines considered the forbidden lines (bottom and left). Because the orientation of each 1 μm section on the slide varied, the "top" of the counting frame was not necessarily equivalent to the superficial border of the SGS, and thus the inclusion and exclusion lines were random with respect to the superficial and deep borders of the SGS. The area both within the grid and within the SGS defined the area to be sampled for all 15 and 35d animals. Because the average height of the SGS for 90 day old animals was so much larger than the dimension of the eyepiece grid and because the density of cells dramatically increased from superficial to deep in the SGS, the transparency grid was used to randomly assign a medial to lateral location for the counting frame. The width of the counting frame was then defined by the width of the eyepiece grid, but the height of the counting frame extended from the deep border of the SGS to the superficial border of the SGS. Thus the area of the counting frame for each 90 day old animal varied slightly (0.039±0.007 mm^2). A camera lucida drawing was made of this sampled region of the reference section (the first of the two sections of the pair) and included the borders of the unbiased counting frame, blood vessels, and other physical structures which could be used as landmarks (Figure 3). The nuclear profiles of both neurons and glial cells were used as the counting units and were counted at the same time. Nuclear profiles totally inside the frame were marked with an "x" on the drawing. Nuclear profiles touching an inclusion line, whether mostly inside or mostly outside the frame, were also marked with an "x" on the drawing. Any nuclear profile touching the forbidden lines, even if mostly inside the counting frame, was not counted. Next, the look-up section (the second of the two sections of the pair) was examined at the same magnification. The drawing of the reference section sampling area, as viewed with a drawing tube, was aligned with the corresponding area on the look-up section using physical landmarks. All nuclei

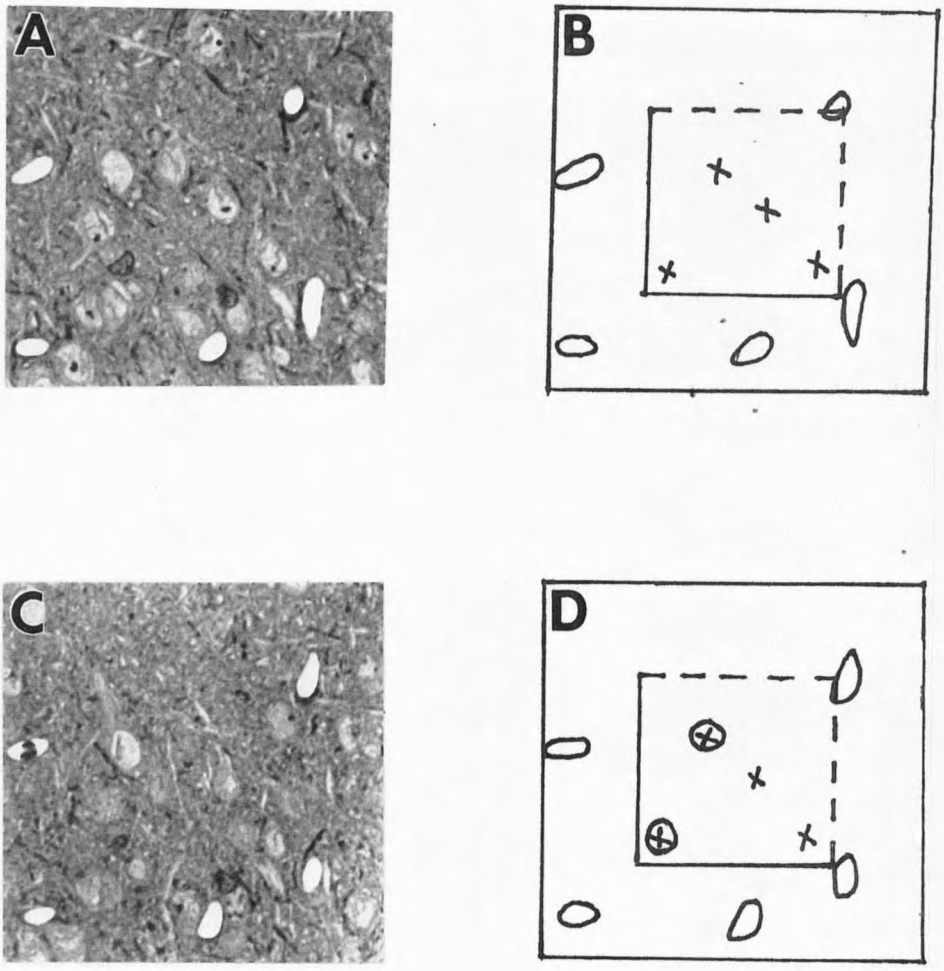

Figure 3. Illustration of the procedure used for the physical disector analysis. Light micrographs of the reference section (A) and look-up section (C) and the corresponding camera lucida drawings (B, D) are shown. On the camera lucida drawings, solid lines denote the exclusion lines and dashed lines denote the inclusion lines of the unbiased counting frame. B: The location of neurons and macroglia are marked with an "x" in the reference section drawing using colored pencils such that in practice the cells of each type are color-coded. D: Neurons and macroglia not found in the look-up section are noted by circling the corresponding "x." These are the cells that are counted for this physical disector pair.

marked on the reference section drawing were looked for in the look-up section, and those not present in the look-up section were circled on the drawing, thus each physical disector pair was represented by one drawing. The number of cells per disector was determined by counting those nuclei included in the reference section but not in the look-up section (Q-). On each drawing, these nuclei were represented by an "x" and were circled. The volume of each disector (Vdis) was calculated, where Vdis was equal to the area of the counting frame (Afr) multiplied by the distance between the disector pairs (h=2 μm). Afr was measured on a digitizing tablet interfaced with computer software (SigmaScan, Jandel Sci.). The number of cells counted per disector (Q-) divided by the volume of the disector (Vdis) yields the volume density (V_D) of cells (e.g. neurons per mm^3, see Equation 2 below). From each drawing, the volume density of cells was calculated and the values from the five physical disectors were averaged for each animal.

Equation 2: $V_D = Q- / (Afr \times h)$ (Gundersen,'86)

The other parameter calculated from measurements of the reference sections of each physical disector was the reference volume (Vref) of the SGS included in an 80 μm slab of tissue. The reference volume (Vref) was estimated using Cavalieri's method of volume estimation (Equation 3). Drawings of the reference section using the 4X or 10X objective lens were used. The five reference sections for each animal served as a systematic random subset of sections, separated by distance, d = 16 μm. The area of the SGS on each reference section was measured by point-counting. For this method, a X-Y grid transparency was made such that each intersection grid lines defined one point. The area of one grid square was equal to the area associated with each point (Api). The grid was randomly placed over each reference section drawing and the number of points touching the SGS was counted. The area (A) was then estimated by multiplying the number of points touching the SGS by the area associated with each point. Vref is then equal to the sum of the areas of the SGS from the five reference sections multiplied by the distance (d) between the reference sections (16 μm):

Equation 3: $V_{ref} = \Sigma A \times d$ (Gundersen,'86)

The total number of cells (N for neurons or GL for glia) in the reference volume was then estimated by multiplying volume density of cells by the reference volume:

Equation 4: $N \text{ or } GL = V_D \times V_{ref}$ (Gundersen,'86)

Statistical analysis of results was done using standard statistical methods. A Student's t-test was used to compare differences between Et and Ct groups at each age and time point. An ANOVA was used when both differences between groups and ages were compared. The efficiency of the systematic random sampling design utilized was evaluated by calculating the coefficient of error (CE) for each parameter (Gundersen and Jensen,'87; West and Gundersen,'90; Geinisman et al.,'96; Miller et al.,'97). According to current stereological principles, the CE should be ~10% or less. Sample calculations are well-documented in the stereological literature (West and Gundersen,'90; Miller et al.,'97), and actual calculations and equations used in the present study can be found in the Appendix. The mean CEs are calculated by taking the root-mean-square of the individual CEs (Gundersen and Jensen,'87). The mean CE calculated for ΣP is the CE for Vref, where ΣP is the sum of the points counted for each animal in estimating the reference volume using Cavalieri's method of volume estimation. The mean CE calculated for ΣQ is the CE for Nv, where ΣQ is the sum of the neurons counted for each animal in estimating the volume density of neurons using the physical disector analysis.

Morphological Criteria for Classification of Neurons and Glial Cells

Neurons were typically the largest cells, and were identified by their size, characteristic pale-staining nuclei with scattered chromatin, and obvious darker staining surrounding cytoplasm with a relatively distinct cell border. A nucleolus was often present. Astrocytes were usually smaller than neurons and were identified by their pale-staining nuclei with a band of heterochromatin lining the

nuclear membrane and pale-staining cytoplasm lacking a distinct cell border. Oligodendrocytes were smaller than the neurons, and were identified by their darkly stained nuclei containing heterochromatin and darkly stained soma with a distinct cell border. Oligodendrocytes were typically found in the SO and in the SGS near the border of the SO. Astrocytes and oligodendrocytes were grouped together as macroglia due to the low numbers of oligodendrocytes. Every cell with the exception of endothelial cells was counted and therefore some cells at 15 days of age did not fall into the neuron or macroglia classification. These cells were most often characterized by a small, pale-staining nucleus with no obvious heterochromatin and no distinct cytoplasm. These cells were classified as "unidentified" and were presumed to be immature neuronal or glial cells. Cells were grouped into three classes for analysis (neurons, glia, and unidentified) and each class was given an abbreviation to be consistently referred to in the results (N,GL, and UNID, respectively).

Analysis of Immunocytochemically Stained Tissues

The previously prepared tissues from chronic prenatal exposure animals stained for either S-100 (for astrocyte cell bodies) or GFAP (for astrocyte cell bodies or processes) were compared. A morphometric volume density estimation (Weibel,'69) of positively stained structures for each stain was done, similar to methods used by Al-Rabiai and Miller ('89) to quantify the effects of gestational alcohol exposure on the development of the CNS.

All counts were done blind to the Et and Ct groups. Four to six sections were analyzed from each animal and values averaged for each animal. After each section was drawn using a 4X objective lens and medial and lateral edges of approximately 150 μm were excluded, a transparency grid was randomly placed over the drawing to select a random area to analyze. Boxes included in the SGS were numbered, then a random number was generated to determine which box to use as a sample. An X-Y grid, where each intersection of the grid lines defined a point, was generated using

SigmaPlot (Jandel Scientific) for use in point counting in a drawing. The area to be sampled was centered in the viewing field using a 40X objective lens, and the grid aligned with this target area using a drawing tube. Each point on the grid corresponding to a positively stained structure was circled on the grid drawing (Figure 4). The volume density of positively stained structures, the percentage of volume occupied by positively stained structures, was determined by dividing the number of positive points by the total number of grid points:

Equation 5: Vv% = (number of positive points*100)/total number of grid points (Weibel,'69)

Uniform grids were used to examine all animals for a particular stain, but the grids were modified for each stain, such that the appropriate number of positive points would be counted (approximately 100 positive stained points) (Gundersen,'86).

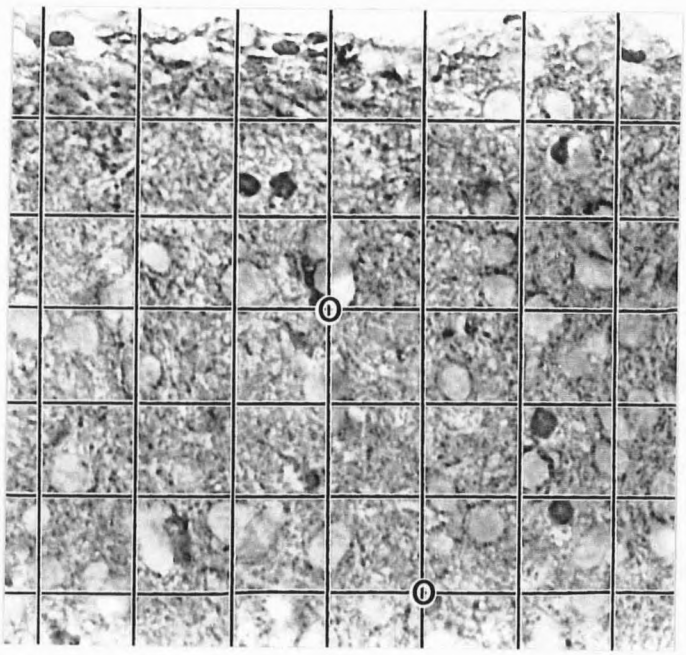

Figure 4. Light micrograph of the SGS of a 40 μm thick coronal section through the left superior colliculus, immunocytochemically stained for S-100 calcium binding protein. S-100 staining is primarily localized to astrocyte cell bodies. A grid was placed over a randomly selected area in the SGS with each intersection of grid lines defining one point. Each point overlying an S-100+ structure was circled and the fractional volume percent determined by dividing the number of positive points by the total number of grid points overlying the section.

RESULTS

Gestational Exposure

Weight Gain, Blood Alcohol Concentrations, General Appearance of Tissues

Alcohol-exposed dams gained less weight during gestation (G0-G20) (64.6±34.0g) than control dams (126.4±13.2g), (p=0.0053). The mean BAC of the alcohol-exposed dams was 140±44 mg/dl (n=6) when measured at 10PM on G16 (Shetty et al.,'93; Burrows et al.,'95). Alcohol did not cause a significant effect on body weights of offspring at either sacrifice age, but did cause a slight decrease in brain weight at 15 days of age (-4%) (Table 4). A similar decrease in means at 35 days of age (-6%) was not statistically significant. General observation of the toluidine blue plastic sections revealed little apparent differences between animals. Alcohol had no effect on either the volume density of unidentified cells (E/C=1.03; p=0.86) or the total number (E/C=0.77; p=0.17) of unidentified cells at 15 days of age. At 35 days of age (d) there were no unidentified cells counted.

Table 4. Body and Brain Weights of Offspring in the Gestational Exposure Experiment

Age	N	Body Weight (g)	E/C	P	Brain Weight (g)	E/C	P
15d-Control	6	35.0±1.5			1.16±0.03		
15d-EtOH	6	33.7±1.2	0.96	0.14	1.11±0.03	0.96	0.006
35d-Control	6	128.6±3.9			1.57±0.08		
35d-EtOH	6	127.5±4.5	0.99	0.66	1.48±0.14	0.94	0.22

Body and brain weights reported are the group mean ± standard deviation.

Neuronal Number

At 15d (Figure 5), alcohol caused a dramatic reduction in the estimated total number of neurons (-30%) that accompanied a decrease in the reference volume (-25%), while the volume density of neurons was unaffected (Figure 6). At 35d (Figure 7), there were no statistically significant alcohol-induced effects on neuronal density, reference volume, or total number of neurons, although there was a nonsignificant trend towards an alcohol-induced decrease in both the volume density of neurons (-9%) and the estimated total number of neurons (-11%) (Figure 6).

Glial Number

All glial cell nuclei were counted but it was apparent that in the SGS the vast majority of glial cells were astrocytes (Figures 5 and 7). At 15d (Figure 5), although alcohol caused a significant reduction in the reference volume (-25%), there was no effect on the volume density of glia and there was a statistically nonsignificant trend towards an alcohol-induced decrease in estimated total number of glia (-23%) (Figure 8). In contrast, at 35d (Figure 7) alcohol caused a dramatic increase in both the volume density of glia (+83%) and in the estimated total number of glia (+85%), but had no effect on the reference volume (Figure 8).

Coefficients of Error

The mean CEs for the estimated Vref, and the neuronal parameters of Nv (volume density of neurons) and N (estimated total number of neurons) are shown in Table 5 for 15d animals and in Table 6 for 35d animals. Individual CEs for each animal were calculated using equations illustrated in the Appendix, Table 16. The CEs were all near to or less than the targeted value of 0.10. The mean CEs for glial counts for estimated reference volume (Vref), volume density (GLv), and number of glia (GL) are shown in Table 7 for 15d animals and in Table 8 for 35d animals. Individual CEs

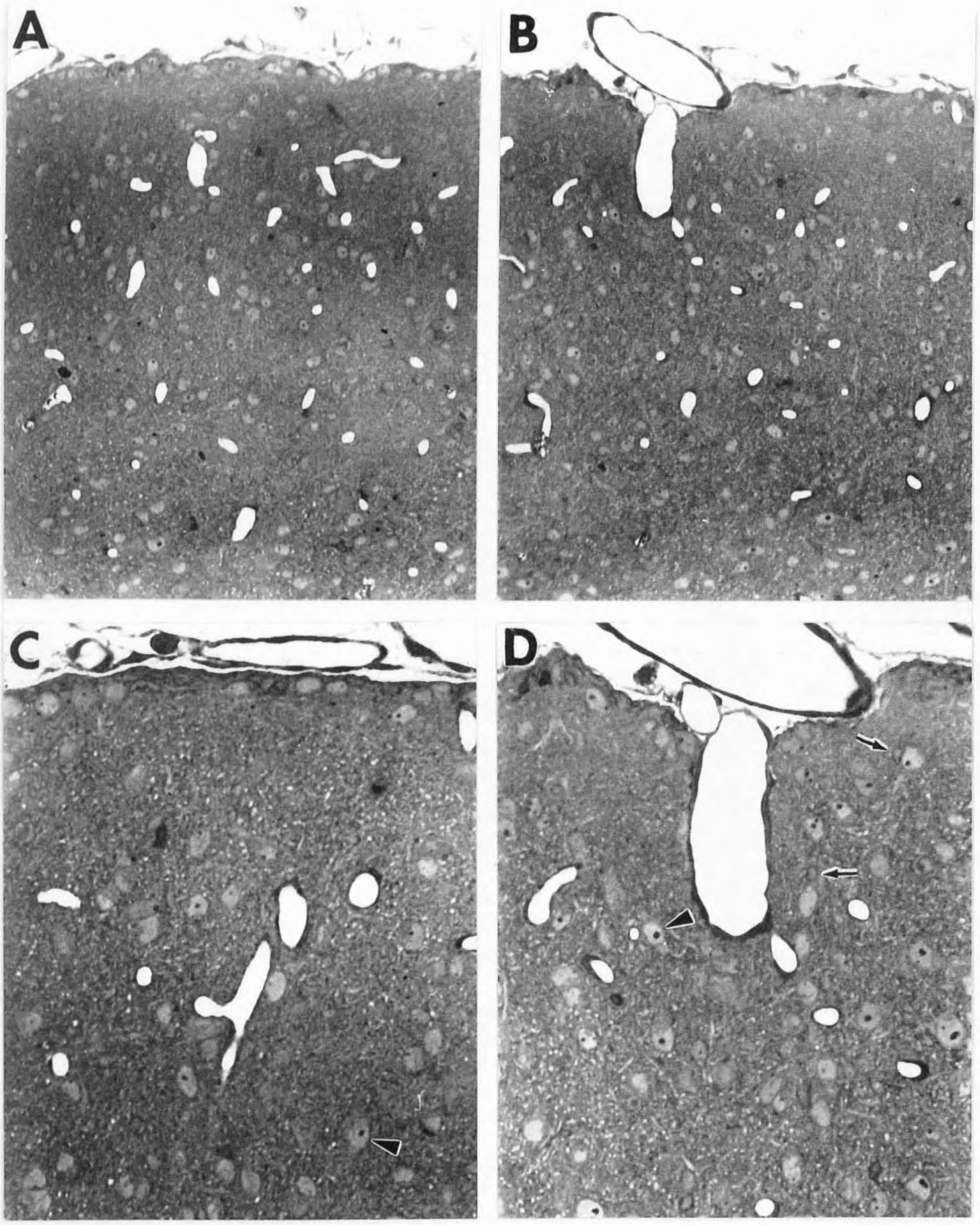

Figure 5. Light micrographs from the left SC of 15d control (A, C) and alcohol exposed (B, D) animals from the gestational alcohol exposure. All micrographs are oriented so that the pial (superficial) surface is up. Neuronal nuclei (arrowheads) and astrocyte nuclei (arrows) are marked for comparison. Magnifications are 150X (A, B) and 300X (C, D).

Figure 6. Effects of Gestational Alcohol Exposure on Neuronal Density, Reference Volume, and Estimated Total Number of Neurons in Sampled Region of the SGS of the Superior Colliculus (Mean and Standard Deviation)

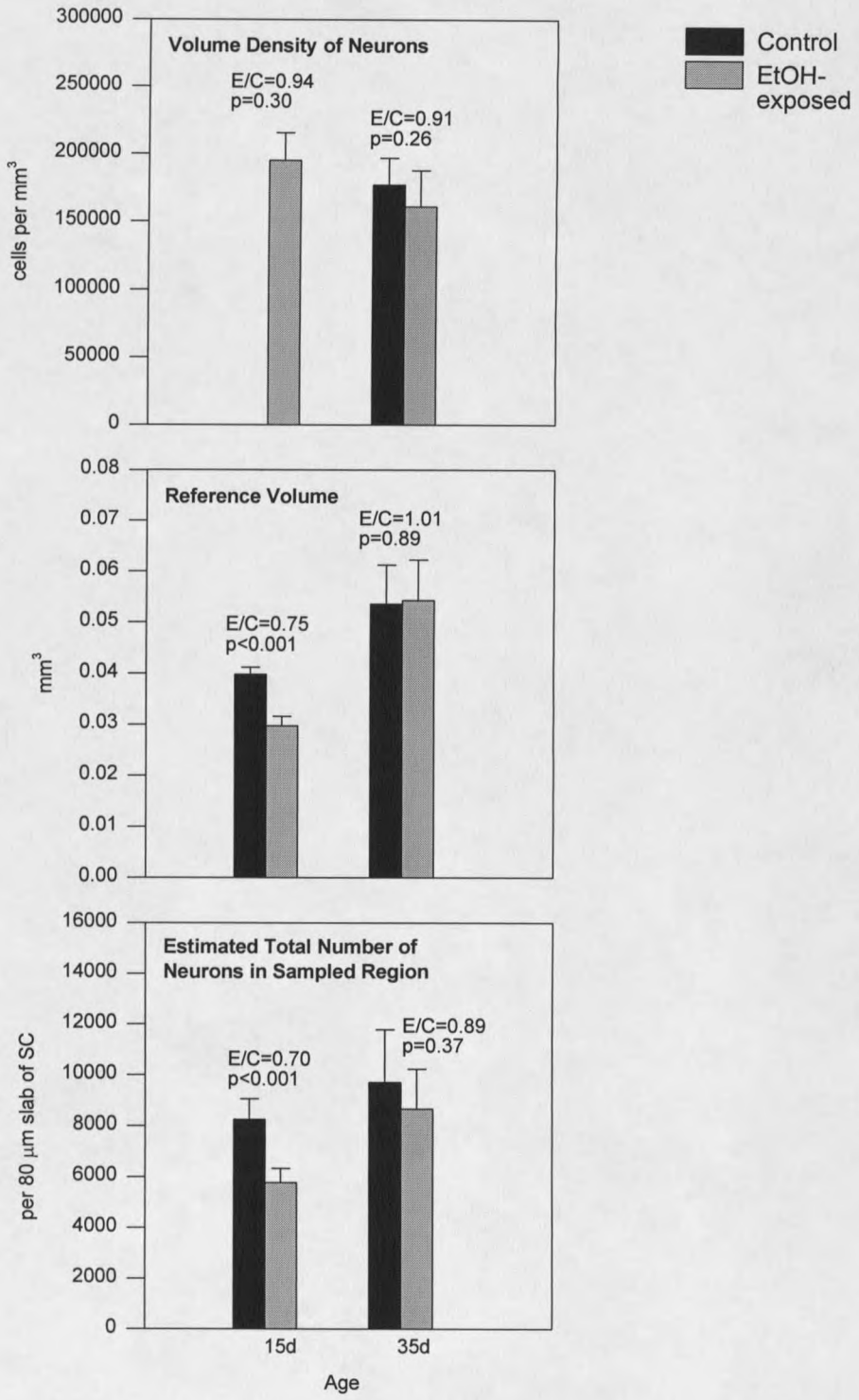

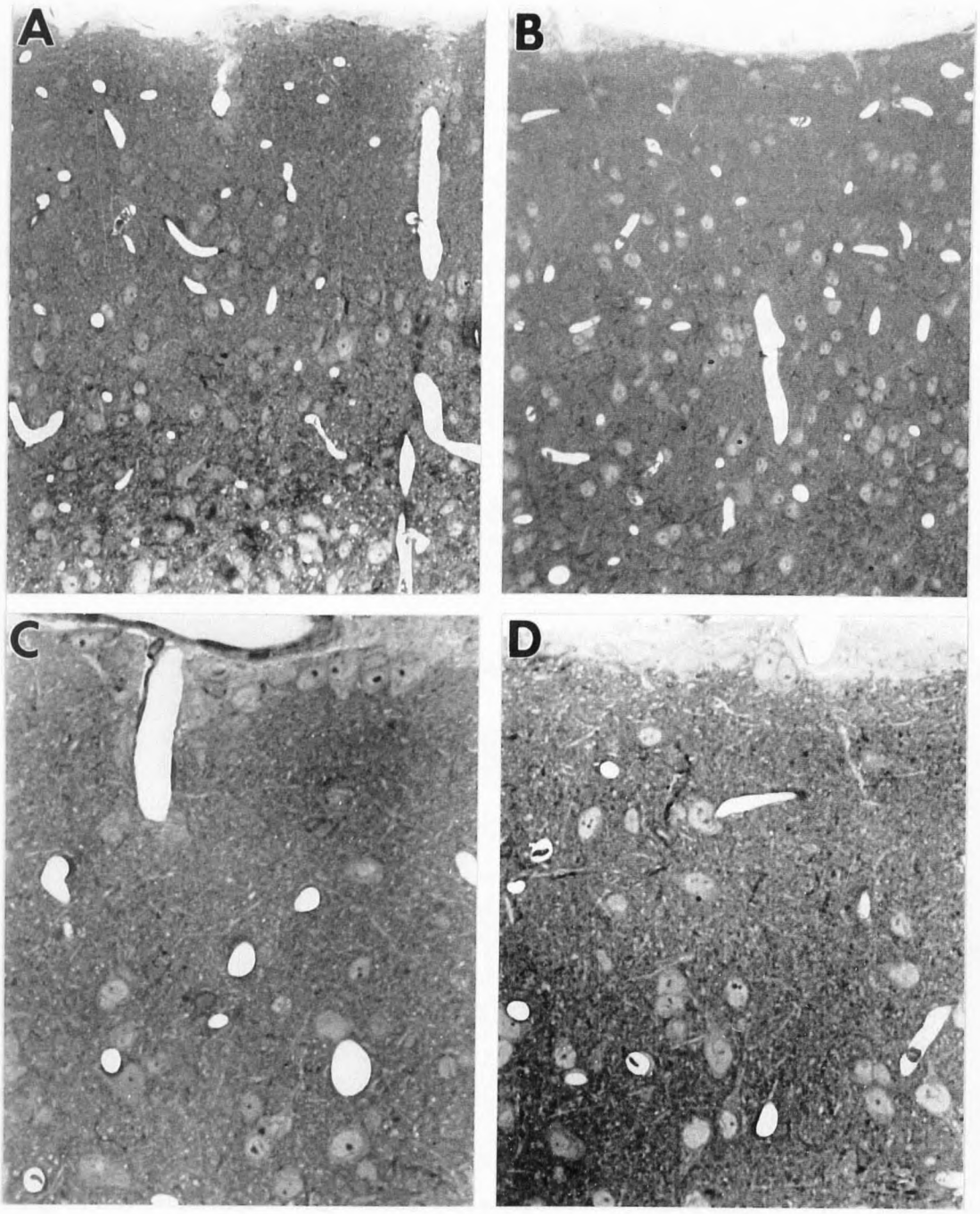

Figure 7. Light micrographs from the left SC of 35d control (A, C) and alcohol exposed (B, D) animals from the gestational alcohol exposure. Magnifications are 175X (A, B) and 375X (C, D).

Figure 8. Effects of Gestational Alcohol Exposure on Glial Density, Reference Volume, and Estimated Total Number of Glia in Sampled Region of the SGS of the Superior Colliculus (Mean and Standard Deviation)

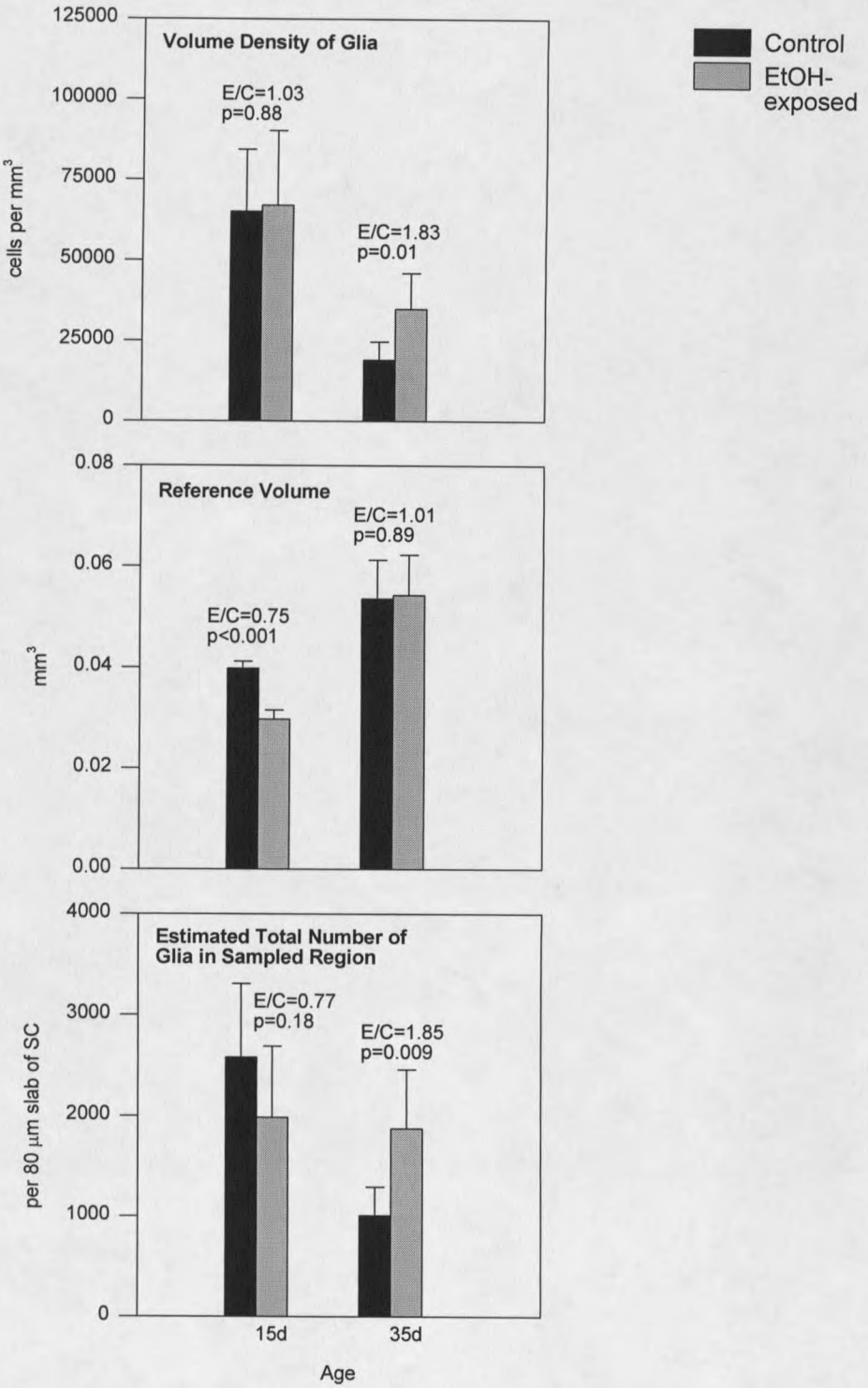

for each animal were calculated using equations illustrated in the Appendix, Table 16. The CEs ranged between 0.09 and 0.21, and were generally slightly higher than the targeted value of 0.10.

Table 5. Data from Individual 15d Animals Showing Coefficients of Error for Neuronal Parameters Measured in the Gestational Exposure Animals

Animal	No. of disectors	ΣP	CE(ΣP)	ΣQ	CE(ΣQ)	Vref (mm^3)	Nv	N	CE(N)
1C	5	191	0.12	66	0.11	0.041	205631.61	8444.7	0.07
2C	5	183	0.08	70	0.12	0.039	229002.45	9010.57	0.06
3C	5	185	0.09	65	0.11	0.040	206768.08	8224.63	0.09
4C	5	192	0.09	70	0.07	0.041	222436.18	9182.64	0.06
5C	5	186	0.08	57	0.12	0.040	179785.98	7190.02	0.05
6C	5	174	0.09	60	0.12	0.037	198767.09	7436.26	0.07
MEAN		185	0.09	64.7	0.11	0.040	207065.23	8248.14	0.07
SD		6.5		5.3		0.0015	17508	809.02	
CV		0.03		0.082		0.038	0.085	0.098	
1E	5	143	0.08	59	0.13	0.031	201128.93	6184.03	0.08
2E	5	136	0.08	74	0.06	0.029	228858.06	6692.16	0.03
3E	5	133	0.07	60	0.12	0.029	189601.46	5421.94	0.06
4E	5	124	0.08	57	0.09	0.027	202146.16	5389.50	0.08
5E	5	143	0.08	55	0.12	0.031	172114.87	5291.95	0.09
6E	5	149	0.09	52	0.06	0.032	176590.28	5657.36	0.05
MEAN		138	0.08	59.5	0.10	0.030	195073.29	5772.82	0.07
SD		8.9		7.662		0.0018	20624	552.97	
CV		0.06		0.129		0.06	0.106	0.096	

SD- standard deviation; CV- coefficient of variation (SD/mean); ΣP = the total number of points counted using the Cavalieri method of volume estimation; ΣQ = the total number of neurons counted; CE- coefficient of error calculated as in Table 15; Mean CE- root-mean-square.

Table 6. Data from Individual 35d Animals Showing Coefficients of Error for Neuronal Parameters Measured in the Gestational Exposure Animals

Animal	No. of disectors	ΣP	CE(ΣP)	ΣQ	CE(ΣQ)	Vref (mm^3)	Nv	N	CE(N)
1C	5	159	0.07	63	0.13	0.054	163019.82	8727.34	0.06
2C	5	153	0.08	62	0.09	0.052	181608.72	9355.61	0.03
3C	5	164	0.09	55	0.07	0.055	171421.72	9465.72	0.11
4C	5	195	0.09	68	0.11	0.066	191168.70	12551.5	0.08
5C	5	150	0.09	67	0.08	0.051	205046.56	10355.9	0.04
6C	5	134	0.10	45	0.12	0.045	150523.13	6791.29	0.09
MEAN		159	0.09	60	0.10	0.054	177131.44	9541.23	0.07
SD		20.3		8.7		0.0069	19678	1896.8	
CV		0.12		0.145		0.128	0.111	0.200	
1E	5	147	0.09	64	0.09	0.050	147716.51	7311.23	0.07
2E	5	164	0.07	64	0.11	0.055	188625.24	10415.6	0.07
3E	5	127	0.08	56	0.08	0.043	184508.15	7889.75	0.05
4E	5	161	0.08	42	0.11	0.054	125660.85	6811.93	0.05
5E	5	170	0.10	64	0.09	0.057	180710.61	10343.7	0.05
6E	5	198	0.09	49	0.05	0.067	138524 20	9234.96	0.07
MEAN		161	0.09	56.5	0.09	0.054	165457.59	8667.88	0.06
SD		23.7		9.3		0.0079	21616	1554.1	
CV		0.14		0.165		0.146	0.131	0.179	

SD- standard deviation; CV- coefficient of variation (SD/mean); ΣP = the total number of points counted using the Cavalieri method of volume estimation; ΣQ = the total number of neurons counted; CE- coefficient of error calculated as in Table 15; Mean CE- root-mean-square.

Table 7. Data from Individual 15d Animals Showing Coefficients of Error for Glial Parameters Measured in the Gestational Exposure Animals

Animal	No. of disectors	ΣP	CE(ΣP)	ΣGL	CE(ΣGL)	Vref (mm^3)	GLv	GL	CE(GL)
1C	5	159	0.07	18	0.11	0.054	56378.20	2315.29	0.18
2C	5	153	0.08	23	0.19	0.052	75518.07	2971.41	0.15
3C	5	164	0.09	14	0.09	0.055	45252.68	1800.02	0.12
4C	5	195	0.09	14	0.15	0.066	44526.63	1838.16	0.13
5C	5	150	0.09	29	0.14	0.051	91559.56	3661.66	0.15
6C	5	134	0.10	22	0.13	0.045	77514.15	2899.96	0.08
MEAN		159	0.09	20	0.14	0.054	65124.88	2581.08	0.14
SD		20.3		5.8		0.0069	19267	728.60	
CV		0.12		0.29		0.128	0.30	0.28	
1E	5	147	0.09	31	0.15	0.050	105966.86	3258.12	0.08
2E	5	164	0.07	16	0.14	0.055	49331.34	1442.52	0.14
3E	5	127	0.08	20	0.13	0.043	62980.18	1801.01	0.09
4E	5	161	0.08	21	0.19	0.054	75748.45	2019.56	0.21
5E	5	170	0.10	22	0.11	0.057	68740.82	2113.55	0.07
6E	5	198	0.09	11	0.15	0.067	39322 43	1259.76	0.11
MEAN		161	0.09	20.2	0.15	0.054	67015.01	1982.42	0.13
SD		23.7		6.7		0.0079	23205	706.06	
CV		0.14		0.33		0.146	0.35	0.36	

SD- standard deviation; CV- coefficient of variation (SD/mean); ΣP = the total number of points counted using the Cavalieri method of volume estimation; ΣGL = the total number of glia counted; CE- coefficient of error calculated as in Table 15; Mean CE- root-mean-square.

Table 8. Data from Individual 35d Animals Showing Coefficients of Error for Glial Parameters Measured in the Gestational Exposure Animals

Animal	No. of disectors	ΣP	CE(ΣP)	ΣGL	CE(ΣGL)	Vref (mm^3)	GLv	GL	CE(GL)
1C	5	191	0.12	8	0.18	0.041	20628.93	1104.38	0.13
2C	5	183	0.08	5	0.23	0.039	14672.68	755.87	0.18
3C	5	185	0.09	3	0.25	0.040	10310.89	569.36	0.28
4C	5	192	0.09	7	0.29	0.041	19603.57	1287.10	0.25
5C	5	186	0.08	8	0.09	0.040	24138 93	1219.14	0.05
6C	5	174	0.09	7	0.15	0.037	25035.17	1129.53	0.11
MEAN		185	0.09	6.3	0.21	0.040	19065.03	1010.90	0.18
SD		6.5		2.0		0.0015	5657.7	283.71	
CV		0.03		0.32		0.038	0.30	0.28	
1E	5	143	0.08	15	0.18	0.031	42939.85	2125.31	0.15
2E	5	136	0.08	9	0.18	0.029	25562.86	1411.55	0.18
3E	5	133	0.07	13	0.24	0.029	44135.15	1887.26	0.19
4E	5	124	0.08	6	0.18	0.027	18230.72	988.27	0.17
5E	5	143	0.08	16	0.07	0.031	45113.93	2582.28	0.09
6E	5	149	0.09	12	0.11	0.032	33846.36	2256 43	0.08
MEAN		138	0.08	11.8	0.17	0.030	34971.48	1875.18	0.15
SD		8.9		3.8		0.0018	11139	584.74	
CV		0.06		0.32		0.06	0.32	0.31	

SD- standard deviation; CV- coefficient of variation (SD/mean); ΣP = the total number of points counted using the Cavalieri method of volume estimation; ΣGL = the total number of glia counted; CE- coefficient of error calculated as in Table 15; Mean CE- root-mean-square.

Immunocytochemistry Analysis: Effects of Alcohol on Astrocytes

There was a large alcohol-induced decrease in the mean volume percent of SGS occupied by GFAP-positive stained structures at 15d (-23%), although the difference was not statistically significant (Figures 9 and 10), and there was no apparent effect at 35d. There were no statistically significant alcohol-induced effects on the volume percent of the SGS occupied by S-100-positive astrocyte cell bodies at either 15 or 35d (Figures 9 and 11).

Figure 9. Effects of Gestational Alcohol Exposure on Astrocytes of the SGS of the Superior Colliculus
(Mean and Standard Deviation)

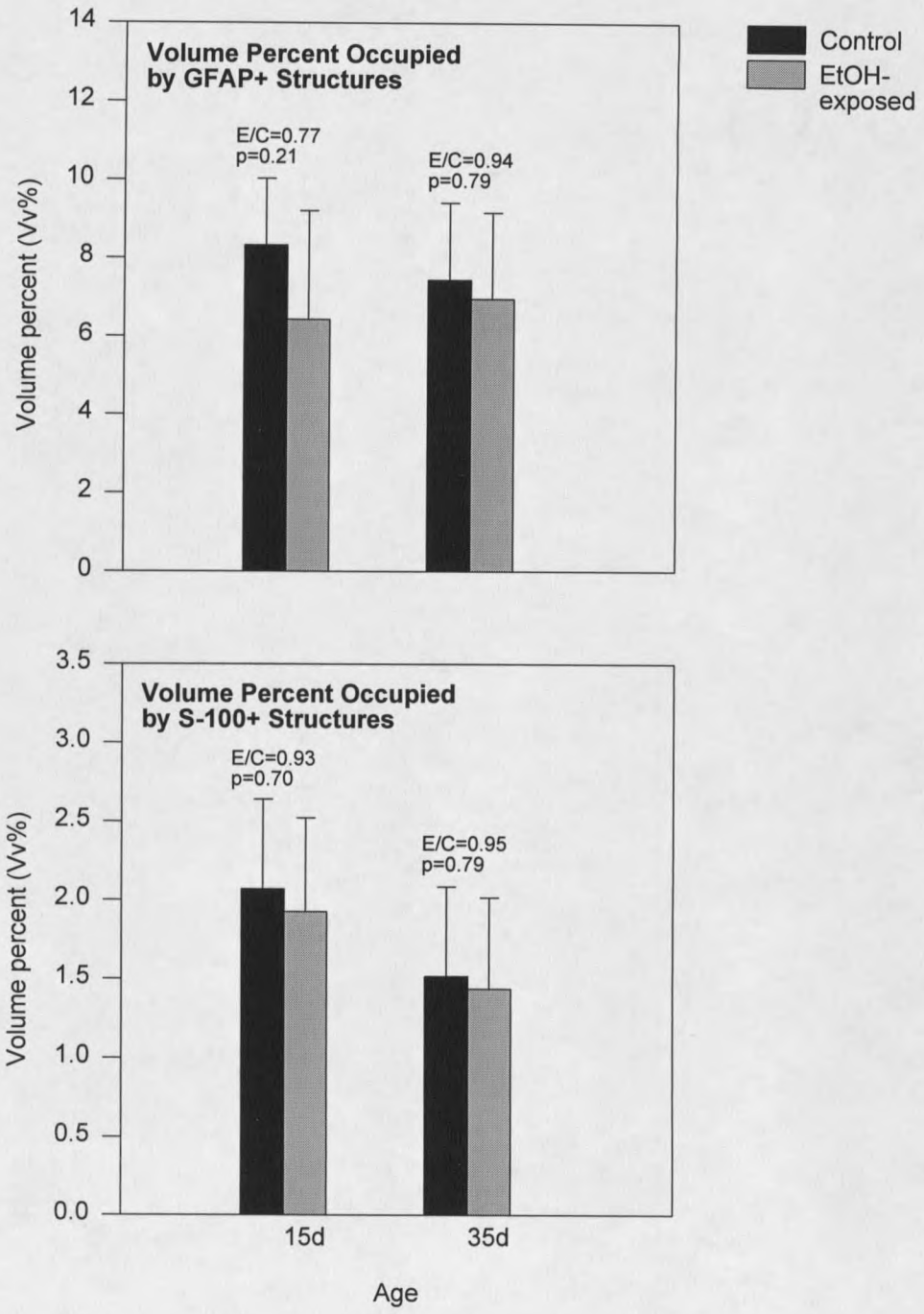

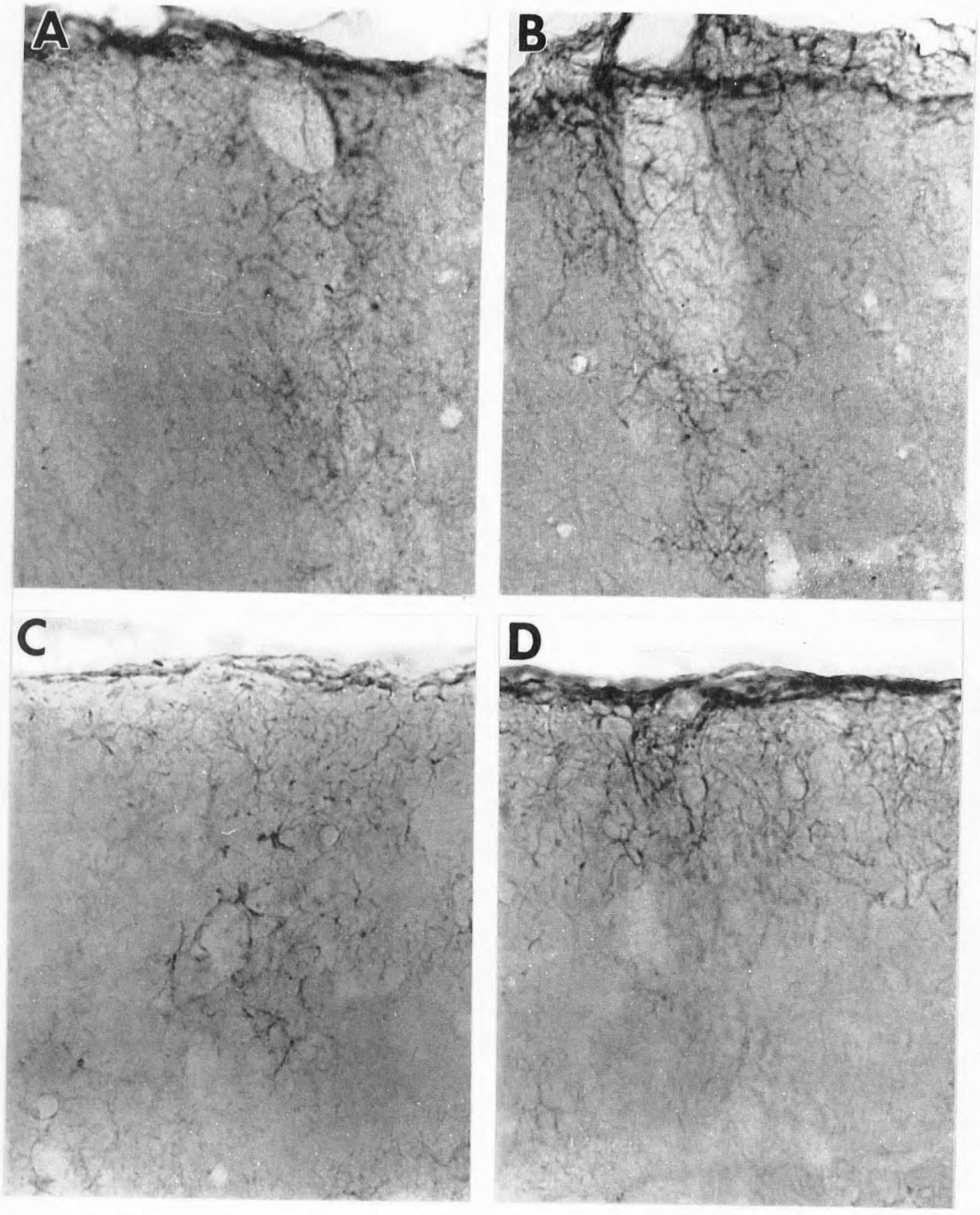

Figure 10. Light micrographs of GFAP stained tissues from the left SC of 15d control (A), 15d alcohol-exposed (B), 35d control (C), and 35d alcohol-exposed (D) animals from the gestational alcohol exposure. Note the intense staining surrounding blood vessels and at the glia limitans. Magnifications are 325X.

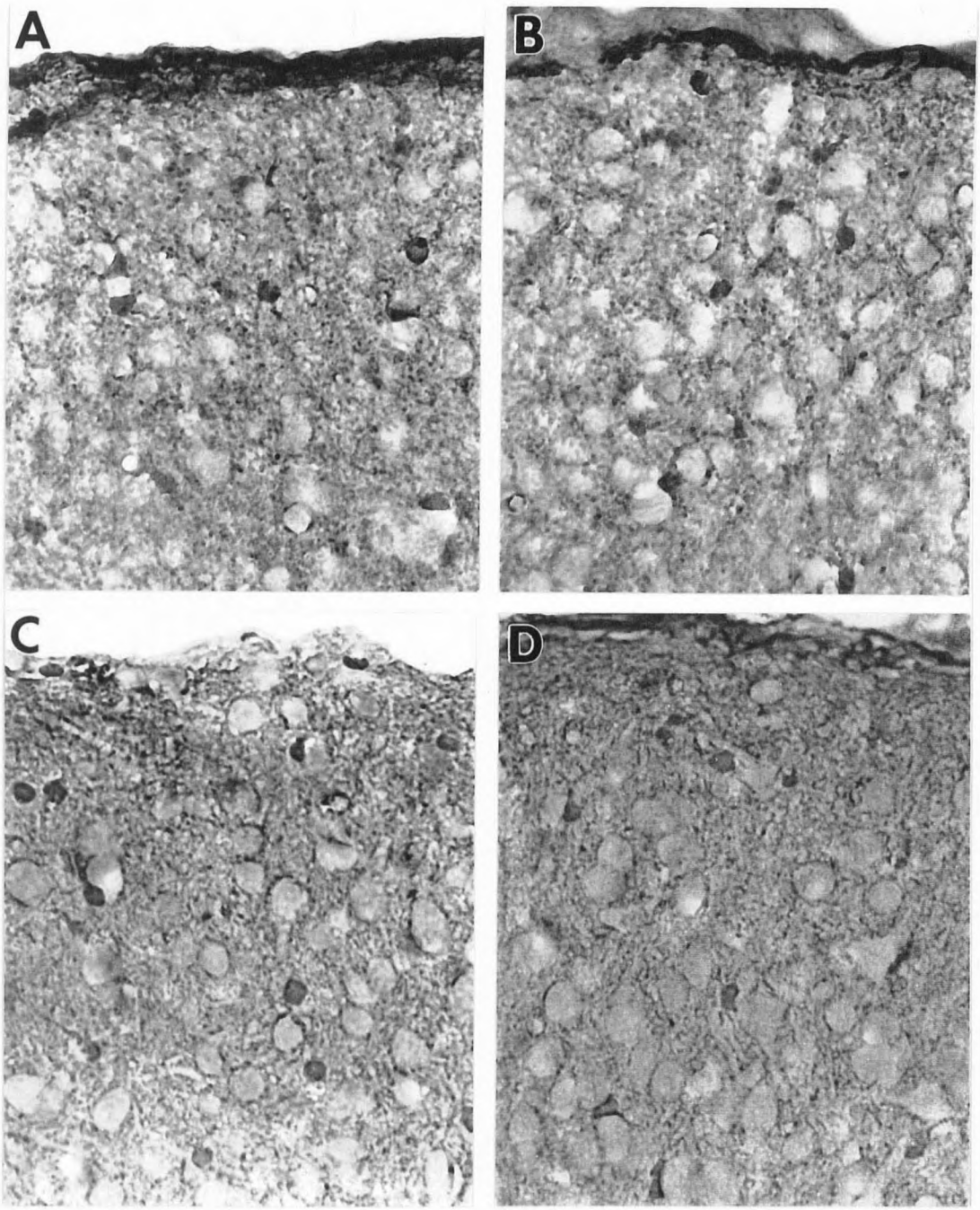

Figure 11. Light micrographs of S-100 stained tissues from the left SC of 15d control (A), 15d alcohol-exposed (B), 35d control (C), and 35d alcohol-exposed (D) animals from the gestational alcohol exposure. Magnifications are 325X (A, B) and 350X (C, D).

5-6d Postnatal Binge Exposure

Weight Gain and General Appearance of Tissues

Alcohol did not affect the body weight of animals at either 15 or 90d, but brain weights were dramatically decreased at both ages (Table 9). General observation of the toluidine blue plastic sections revealed little apparent differences between animals. Alcohol had no effect on either the volume density of unidentified cells (E/C=0.98; p=0.86) or the total number (E/C=0.81; p=0.17) of unidentified cells at 15d. At 90d few unidentified cells were counted and there were animals in both groups in which none were counted, and therefore no comparison could be made.

Table 9. Body and Brain Weights of Animals in the 5-6 Binge Exposure

Sacrifice Age	N	Body Weight (g)	E/C	P	Brain Weight (g)	E/C	P
15d-Ct-ar	9	30.7±2.8			1.07±0.04		
15d-Et-ar	7	30.2±2.9	0.98	0.77	0.87±0.08	0.81	<0.001
90d-Ct-ar	8	361.8±15.6			1.75±0.09		
90d-Et-ar	9	352.7±32.4	0.98	0.49	1.48±0.16	0.85	<0.001

Body and brain weights reported are the group mean ± standard deviation.

Neuronal Number

At 15d (Figure 12), alcohol caused a significant reduction (-16%) in the reference volume of the SGS, but did not cause any effect in the volume density of neurons or the estimated total number of neurons (Figure 13). At 90d (Figure 14), there was still an alcohol-induced decrease in the reference volume of the SGS (-16%) and a marginally statistically significant increase (p=0.06) in the density of neurons (+17%), but there was no effect on the estimated total number of neurons (Figure 13).

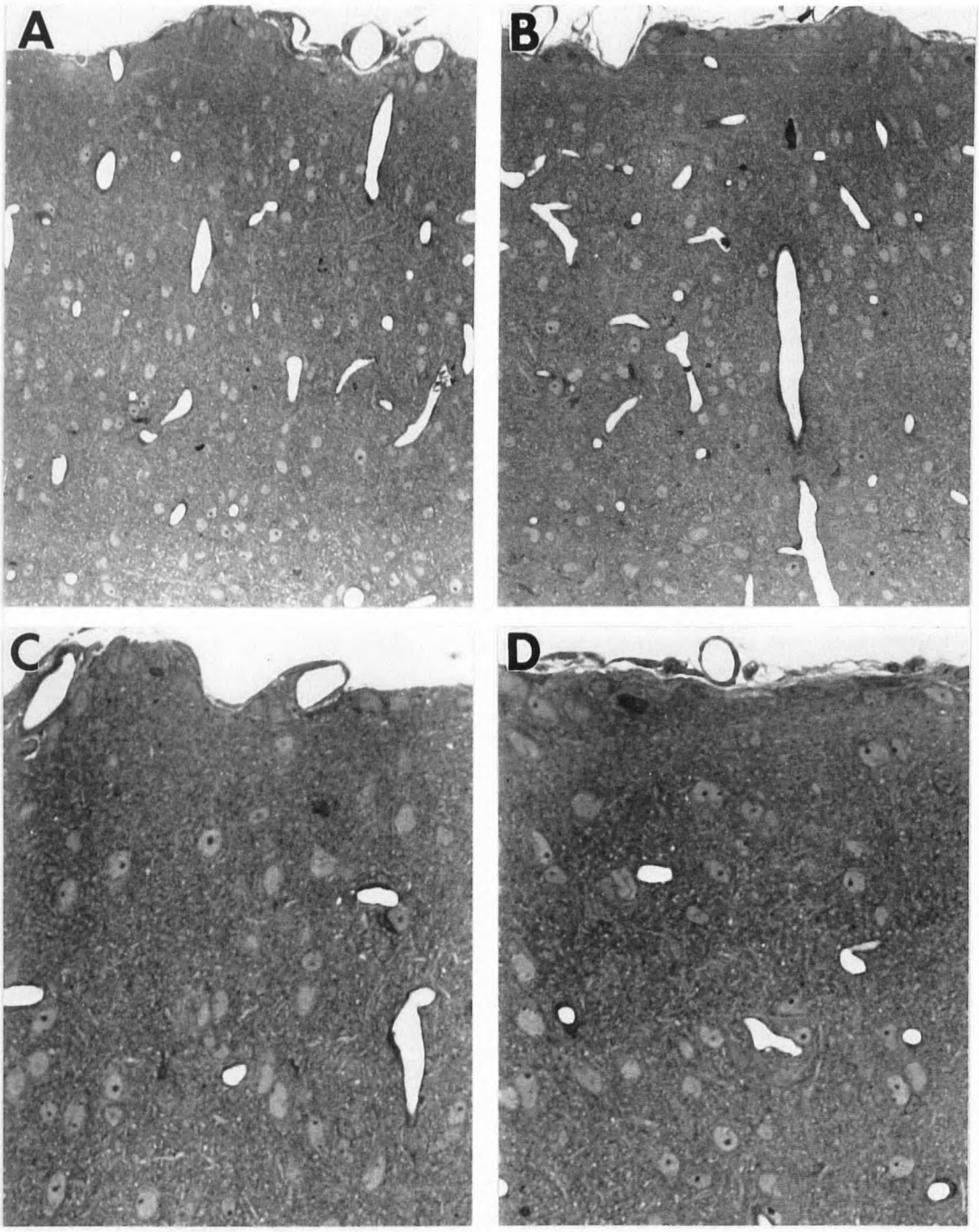

Figure 12. Light micrographs from the left SC of 15d control (A, C) and alcohol exposed (B, D) animals from the postnatal binge alcohol exposure. Magnifications are 175X (A, B) and 350X (C, D).

Figure 13. Effects of 5-6d Postnatal Binge Alcohol Exposure on Neuronal Density, Reference Volume, and Estimated Total Number of Neurons in the Sampled Region of the SGS of the Superior Colliculus (Mean and Standard Deviation)

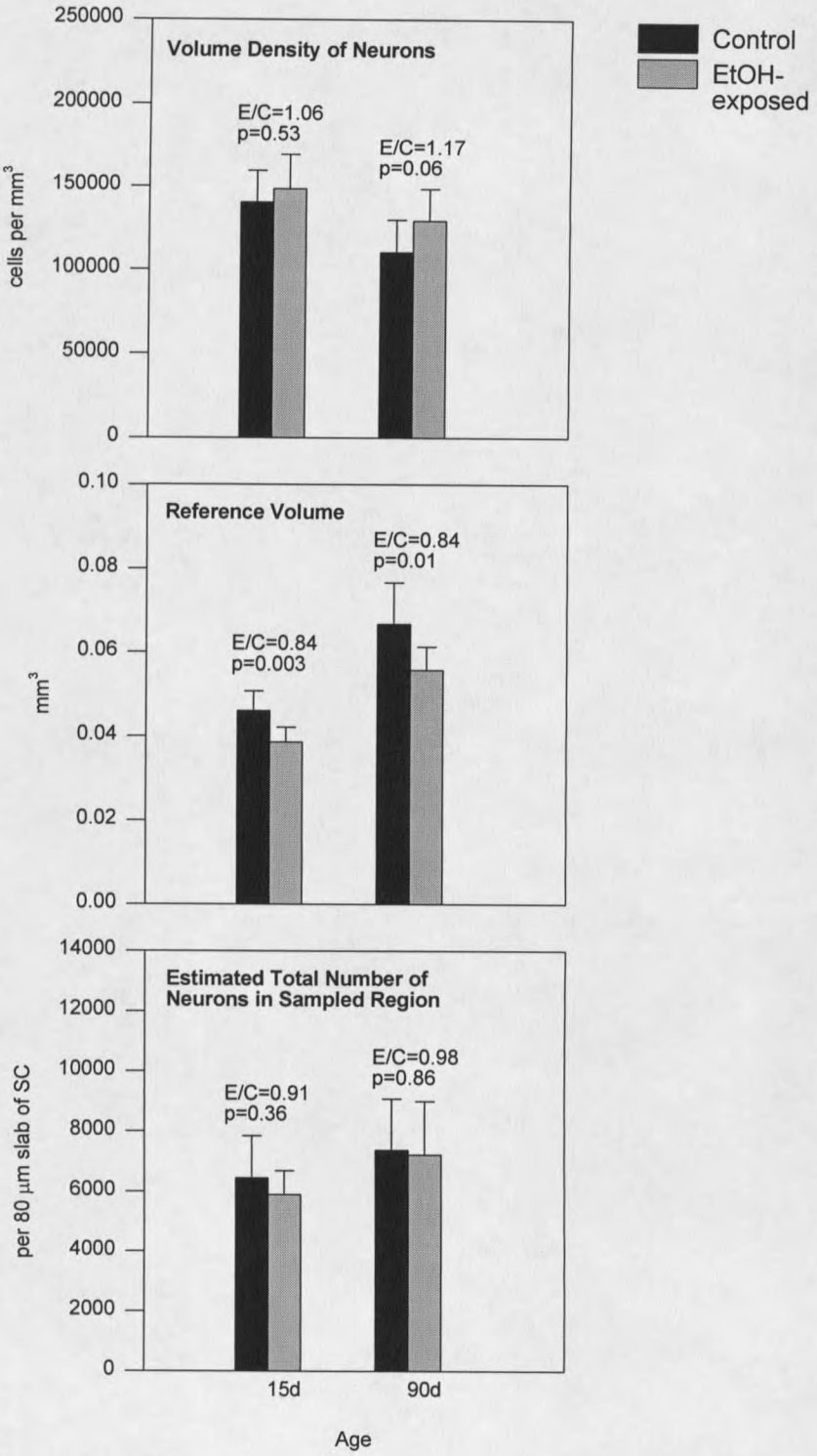

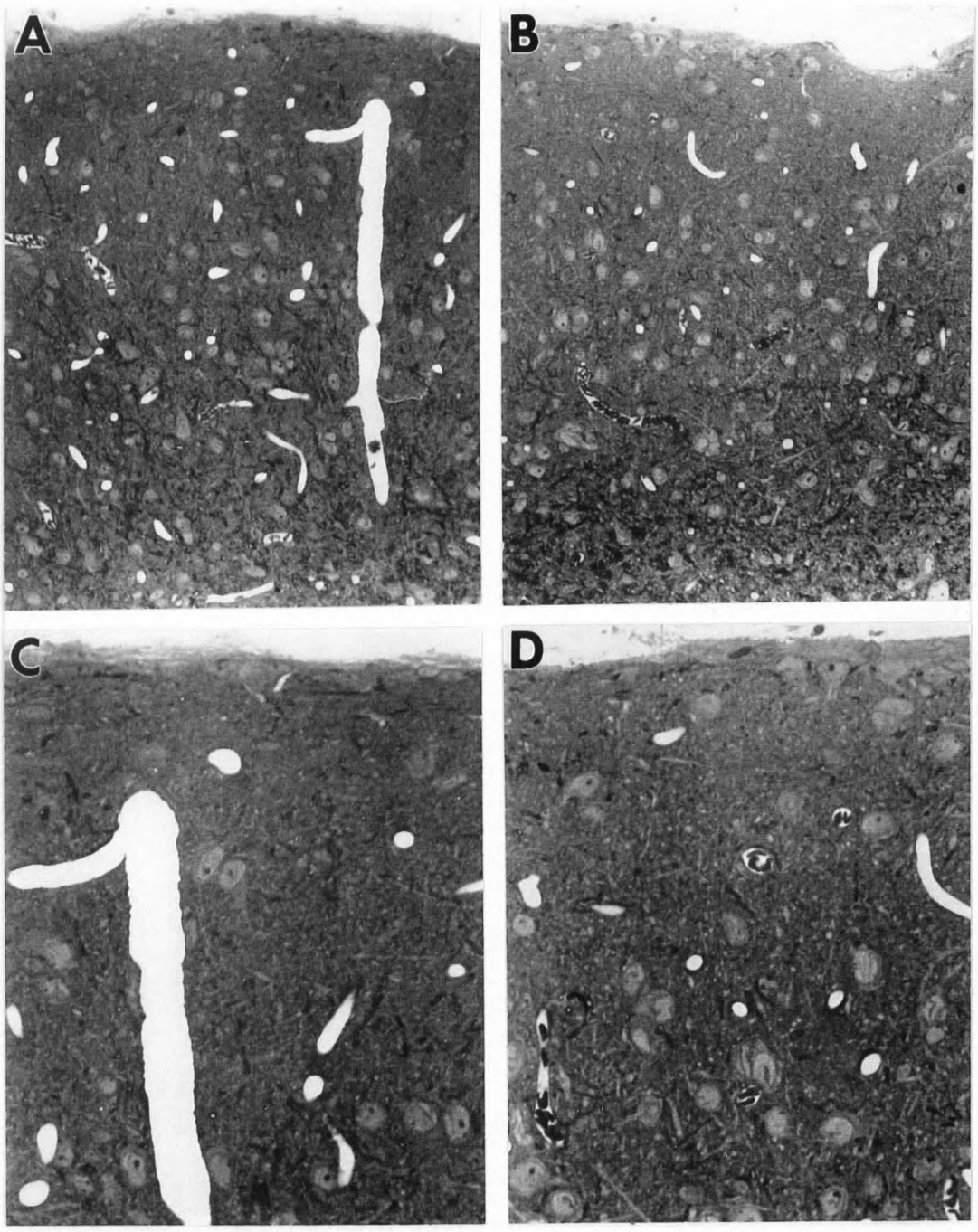

Figure 14. Light micrographs from the left SC of 90d control (A, C) and alcohol exposed (B, D) animals from the postnatal binge alcohol exposure. Magnifications are 175X (A, B) and 350X (C, D).

Glial Number

At 15d (Figure 12), the alcohol-induced reduction in the reference volume (-16%) was accompanied by a marginally significant decrease in the estimated total number of glia (-18%, p=0.06), although there was no effect on the volume density of glia (Figure 15). At 90d (Figure 14), the alcohol-induced reduction in the reference volume (-16%) was not accompanied by statistically significant changes in volume density or number, although there were dramatic decreases in means in both cases (volume density of glia = -21%; estimated total number of glia = -30%) (Figure 15).

Coefficients of Error

The mean CEs for the neuronal parameters of Nv (volume density of neurons), estimated Vref, and N (estimated total number of neurons) are shown in Table 10 for 15d animals and in Table 11 for 90d animals. Individual CEs for each animal were calculated using equations illustrated in the Appendix, Table 16. The CEs were all near to or less than the targeted value of 0.10. The mean CEs for the glial cell parameters of GLv (volume density of glial cells), estimated Vref, and GL (estimated total number of glial cells) are shown in Table 12 for 15d animals and in Table 13 for 90d animals. Individual CEs for each animal were calculated using equations illustrated in the Appendix, Table 16. The CEs ranged from 0.07 to 0.21 with many of the values slightly over the targeted value of 0.10.

Figure 15. Effects of 5-6 Postnatal Binge Developmental Alcohol Exposure on the Glial Density, Reference Volume, and Estimated Total Number of Glia in the Sampled Region of the SGS of the Superior Colliculus (Mean and Standard Deviation)

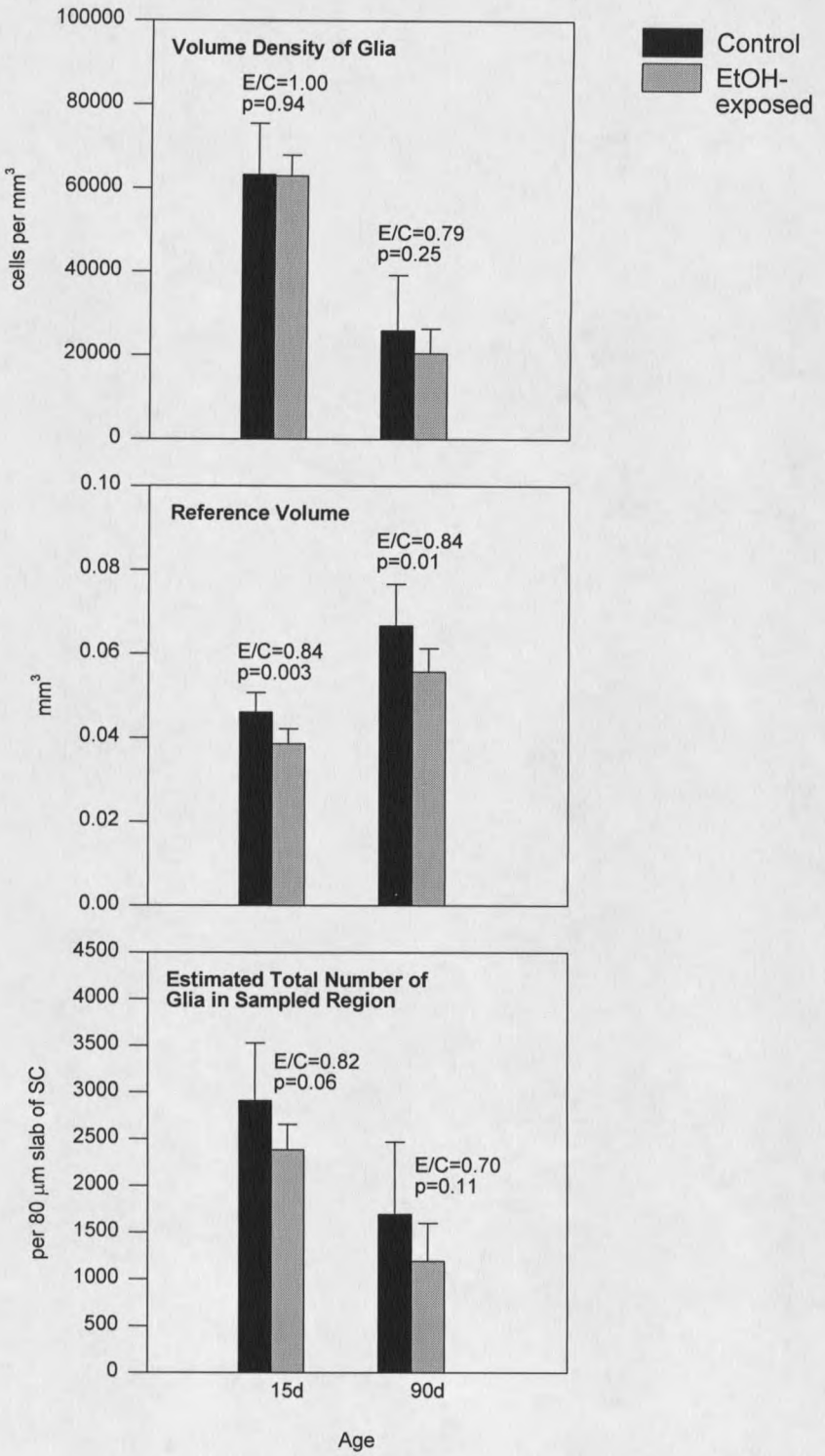

Table 10. Data from Individual 15d Animals Showing Coefficients of Error for Neuronal Parameters Measured in the 5-6d Postnatal Binge Exposure

Animal	No. of disectors	ΣP	CE(ΣP)	ΣQ	CE(ΣQ)	Vref (mm^3)	Nv	N	CE(N)
17C	5	212	0.08	48	0.05	0.046	148058.64	6748.87	0.06
15C	5	224	0.08	60	0.13	0.048	185641.49	8940.96	0.12
24C	5	228	0.08	44	0.12	0.049	136137.09	6673.79	0.09
32C	5	226	0.09	53	0.11	0.049	163983.31	7968.36	0.03
40C	5	206	0.09	45	0.08	0.044	139231.11	6166.87	0.03
11C	5	193	0.08	32	0.08	0.042	99008.79	4108.59	0.09
26C	5	247	0.09	34	0.12	0.053	105196.84	5586.77	0.08
43C	5	173	0.08	48	0.09	0.037	162708.11	6052.24	0.07
31C	5	219	0.10	40	0.07	0.047	123760.99	5827.60	0.08
MEAN		214.	0.09	44.89	0.10	0.046	140414.04	6452.67	0.08
SD		21.6		8.824		0.0047	28302	1392.10	
CV		0.10		0.20		0.10	0.20	0.22	
25E	5	170	0.08	46	0.12	0.037	144942.92	5297.94	0.04
38E	5	168	0.08	50	0.08	0.036	157152.30	5676.64	0.06
5E	5	173	0.09	54	0.14	0.037	174207.40	6479.98	0.12
28E	5	194	0.10	53	0.10	0.042	163983.31	6840.11	0.06
16E	5	159	0.09	47	0.09	0.034	150371.58	5140.72	0.06
19E	5	207	0.08	47	0.10	0.045	153022.69	6810.63	0.08
30E	5	184	0.10	41	0.12	0.040	126855.02	5018.65	0.13
MEAN		179.	0.09	48.29	0.11	0.039	152933.60	5894.95	0.09
SD		16.6		4.461		0.0038	14961	797.38	
CV		0.09		0.09		0.10	0.10	0.14	

SD- standard deviation; CV- coefficient of variation (SD/mean); ΣP = the total number of points counted using the Cavalieri method of volume estimation; ΣQ = the total number of neurons counted; CE- coefficient of error calculated as in Table 15; Mean CE- root-mean-square.

Table 11. Data from Individual 90d Animals Showing Coefficients of Error for Neuronal Parameters Measured in the 5-6d Postnatal Binge Exposure

Animal	No. of disectors	ΣP	CE(ΣP)	ΣQ	CE(ΣQ)	Vref (mm^3)	Nv	N	CE(N)
5C	5	198	0.08	60	0.07	0.067	146835.25	9789.04	0.03
36C	5	230	0.08	49	0.08	0.077	102157.76	7911.22	0.04
13C	5	241	0.08	46	0.09	0.081	103597.26	8406.39	0.03
20C	5	201	0.09	43	0.13	0.068	105063.50	7110.37	0.06
35C	5	165	0.09	41	0.14	0.056	95094.29	5283.02	0.13
1C	5	212	0.09	45	0.06	0.071	113193.17	8079.80	0.05
7C	5	180	0.07	50	0.06	0.061	129790.07	7866.07	0.04
26C	5	200	0.08	33	0.08	0.053	85555.15	4551.42	0.06
MEAN		203.	0.08	45.89	0.09	0.067	110160.81	7374.67	0.06
SD		24.6		7.791		0 0098	19658	1704.40	
CV		0.12		0.17		0.15	0.18	0.23	
2E	5	147	0.08	34	0.11	0.050	122055.64	6041.14	0.10
11E	5	179	0.10	52	0.09	0.060	165641.79	9983.13	0.08
39E	5	195	0.08	61	0.08	0.066	153052.77	10048.9	0.03
15E	5	155	0.09	52	0.12	0.052	125164.72	6532.17	0.06
8E	5	155	0.08	47	0.11	0.052	120232.87	6274.79	0.09
6E	5	174	0.08	56	0.09	0.056	128920.81	7552.94	0.03
4E	5	159	0.08	49	0.11	0.054	119539.49	6399.59	0.04
19E	5	177	0.08	49	0.09	0.060	124465.53	7417.65	0.05
3E	5	185	0.07	38	0.14	0.050	96144.08	4791.02	0.09
MEAN		169.	0.08	48.67	0.11	0.056	128357.52	7226.82	0.07
SD		16.1		8.367		0.0055	20146	1771.90	
CV		0.10		0.17		0.10	0.16	0.25	

SD- standard deviation; CV- coefficient of variation (SD/mean); ΣP = the total number of points counted using the Cavalieri method of volume estimation; ΣQ = the total number of neurons counted; CE- coefficient of error calculated as in Table 15; Mean CE- root-mean-square.

Table 12. Data from Individual 15d Animals Showing Coefficients of Error for Glial Parameters Measured in the 5-6d Postnatal Binge Exposure

Animal	No. of disectors	ΣP	CE(ΣP)	ΣGL	CE(ΣGL)	Vref (mm^3)	GLv	GL	CE(GL)
17C	5	212	0.08	18	0.14	0.046	55351.53	2523.06	0.08
15C	5	224	0.08	24	0.10	0.048	74256.59	3576.38	0.09
24C	5	228	0.08	19	0.08	0.049	58786.47	2881.87	0.10
32C	5	226	0.09	18	0.20	0.049	55692.45	2706.24	0.14
40C	5	206	0.09	21	0.08	0.044	64974.52	2877.87	0.08
11C	5	193	0.08	19	0.11	0.042	58786.47	2439.47	0.05
26C	5	247	0.09	25	0.09	0.053	77350.62	4107.92	0.08
43C	5	173	0.08	24	0.07	0.037	80940.57	3010.74	0.07
31C	5	219	0.10	14	0.13	0.047	43316.35	2039.66	0.11
MEAN		214.	0.09	20.2	0.12	0.046	63272.84	2907.02	0.09
SD		21.6		3.6		0.0047	12210	618.58	
CV		0.10		0.18		0.10	0.19	0.21	
25E	5	170	0 08	18	0.12	0.037	56725.23	2073.42	0.09
38E	5	168	0.08	19	0.09	0.036	60012.00	2167.75	0.04
5E	5	173	0.09	20	0.08	0.037	66193.65	2462.20	0.08
28E	5	194	0.10	18	0.09	0.042	55692.45	2323.06	0.09
16E	5	159	0.09	21	0.08	0.034	66775.40	2282.84	0.03
19E	5	207	0.08	19	0.12	0.045	65303.78	2906.50	0.08
30E	5	184	0.10	20	0.09	0.040	61880.50	2448.12	0.06
MEAN		179.	0.09	19.3	0.10	0.039	61797.57	2380.56	0.07
SD		16.6		1.1		0.0038	4520.2	270.90	
CV		0.09		0.06		0.10	0.07	0.11	

SD- standard deviation; CV- coefficient of variation (SD/mean); ΣP = the total number of points counted using the Cavalieri method of volume estimation; ΣGL = the total number of glia counted; CE- coefficient of error calculated as in Table 15; Mean CE- root-mean-square.

Table 13. Data from Individual 90d Animals Showing Coefficients of Error for Glial Parameters Measured in the 5-6d Postnatal Binge Exposure

Animal	No. of disectors	ΣP	CE(ΣP)	ΣGL	CE(ΣGL)	Vref (mm^3)	GLv	GL	CE(GL)
5C	5	198	0.08	12	0.21	0.067	31275.31	2085.03	0.17
36C	5	230	0 08	7	0.11	0.077	14675.39	1136.48	0.17
13C	5	241	0.08	9	0.11	0.081	21132.63	1714.81	0.12
20C	5	201	0.09	10	0.13	0.068	23940.73	1620.23	0.07
35C	5	165	0.09	7	0.18	0.056	17769.91	987.22	0.22
1C	5	212	0.09	7	0.14	0.071	17427.93	1244.02	0.15
7C	5	180	0.07	21	0.12	0.061	56044.08	3396.61	0.09
26C	5	200	0.08	9	0.12	0.053	25687.12	1366.52	0.08
MEAN		203.	0.08	10.3	0.14	0.067	25994.14	1693.87	0.14
SD		24.6		4.7		0.0098	13245	772.54	
CV		0.12		0.46		0.15	0.51	0.46	
2E	5	147	0.08	7	0.20	0.050	25738.27	1273.92	0.18
11E	5	179	0:10	7	0.24	0.060	21608.82	1302.35	0.22
39E	5	195	0.08	11	0.25	0.066	27620.59	1813.48	0.25
15E	5	155	0.09	5	0.22	0.052	12886.03	672.50	0.20
8E	5	155	0.08	5	0.28	0.052	13775.71	718.94	0.26
6E	5	174	0.08	12	0.21	0.056	28706.42	1681.79	0.18
4E	5	159	0.08	6	0.14	0.054	15171.38	812.21	0.08
19E	5	177	0.08	10	0.24	0.060	23075.94	1375.23	0.25
3E	5	185	0.07	8	0.08	0.050	21060.70	1049.49	0.11
MEAN		169.	0.08	7.9	0.21	0.056	21071.54	1188.88	0.20
SD		16.1		2.6		0.0055	5940.4	408.77	
CV		0.10		0.33		0.10	0.28	0.34	

SD- standard deviation; CV- coefficient of variation (SD/mean); ΣP = the total number of points counted using the Cavalieri method of volume estimation; ΣGL = the total number of glia counted; CE- coefficient of error calculated as in Table 15; Mean CE- root-mean-square.

DISCUSSION

The present study showed that developmental alcohol exposure, whether via gestational exposure or postnatal binge exposure, affected the developing neuronal and glial populations of the SGS, though the exposure times produced different effects (Table 14). In the gestational exposure alcohol produced a 25% reduction in the 80 μm sampled volume of the SGS and a 30% reduction in the number of neurons at 15 days of age, but these effects were compensated for by 35 days of age. Macroglial cells identified on toluidine blue-stained sections were not affected by alcohol at 15 days of age, but by 35 days of age alcohol caused an 80-85% increase in both volume density and total number. Immunocytochemical analysis of the astroglial population in the SGS did not reveal any effects of alcohol. In the postnatal binge exposure alcohol had no effect on the total number of neuronal or glial cells at 15 days of age, but at 90 days of age alcohol caused a permanent 16% decrease in the sampled volume and a probable ($p=0.06$) 17% increase in volume density of neurons, with no effect on the total number of neurons.

Table 14. Summary of Effects of Developmental Alcohol Exposure on the Development of the SC

Gestational Exposure:	15d	35d	90d
Volume of Visual Layers	25% ↓ in Vref	no effect	N/A
Neurons	30% ↓ in N	no effect	N/A
Glia	no effect	80-85% ↑ in vol. density and total number	N/A
Postnatal Exposure:			
Volume of Visual Layers	16% ↓ in Vref	N/A	16% ↓ in Vref
Neurons	no effect	N/A	17% ↑ in vol. density
Glia	no effect	N/A	no effect

Developmental events that occur at distinct times in the formation of the SC are expected to be affected differently by exposures to alcohol that occur at different times (Figure 16). The normal prenatal development of the rat SC includes: genesis of all of the neurons (Altman and Bayer,'81), radial glia (Wu et al.,'95), and most astrocytes (Harvey et al.,'93); neuron migration from the ventricular zone to the tectum of the midbrain (Mustari et al.,'79; Raedler et al.,'81); and ingrowth of optic nerve afferents (Raedler and Sievers,'75), all of which could be susceptible to alcohol-induced alterations. Postnatal development includes the maturation of neurons in terms of cell and dendritic growth and dendritic branching (Labriola and Laemle,'77; Warton and Jones,'85), naturally occurring (apoptotic) cell death of neurons (Arees and Astrom,'77; Cunningham et al.,'82; Giordano and Cunningham,'82) and concomitant loss of ON afferents (Perry et al.,'83), synaptogenesis and synaptic pruning (Warton and McCart,'89), the development of the definitive layers of the SC (Warton and Jones,'85), gliogenesis (particularly of oligodendroglia) (Raedler and Sievers,'75; Mares and Bruckner,'78; Harvey et al.,'93), maturation of oligodendrocytes, initiation of myelination, myelin maturation (Mares and Bruckner,'78; Warton and Jones,'85), and astrocytic maturation (Mares and Bruckner,'78). This postnatal period of development of the SC, particularly for the SGS, is dependent on the functional activity and further development of the ON and retina (Cunningham et al.,'82; Giordano and Cunningham,'82). If alcohol affects the development of the ON input at any stage, whether during gestational or postnatal alcohol exposure, then there could be repercussions manifested in the further development of the SC.

Alcohol-induced reduction in neuron number in the SGS was only found after the gestational alcohol exposure and only at 15d. Gestational alcohol-induced neuron loss in the SGS could be due to a reduction in the proliferation of neurons, to a reduction or delay of migration of neurons, to an increase in the number of dying neurons, or to some combination of these three effects.

Figure 16. Development of the Superficial Laminae of the Superior Colliculus and Temporal Windows of Alcohol Exposure

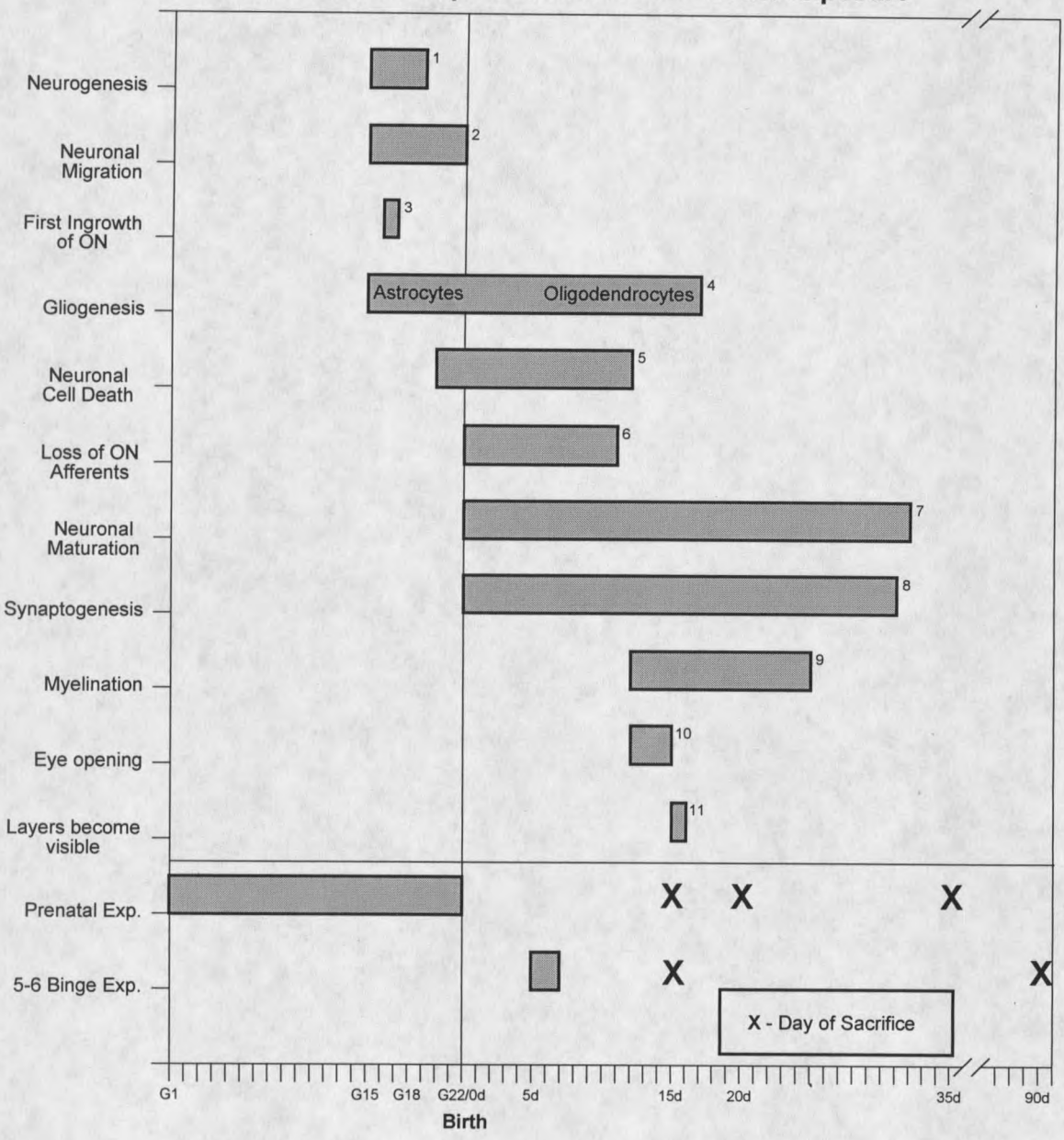

Summary diagram of developmental events from:

[1] Altman and Bayer, 1981; Mustari et al., 1979

[2] Mustari et al., 1979

[3] Bunt et al., 1983

[4] Harvey et al., 1993; Mares and Bruckner, 1978

[5] Arees and Astrom, 1977; Cunningham et al., 1982

[6] Perry et al., 1983

[7] Warton and Jones, 1985

[8] Warton and McCart, 1989

[9] Warton and Jones, 1985

[10] Lund and Lund, 1972

[11] Warton and Jones, 1985

Neurogenesis

Neurogenesis occurs prenatally in the SC (Mustari et al.,'79; Altman and Bayer,'81) and involves an initial overproduction of neurons with subsequent postnatal cell death (Arees and Astrom,'77). The gestational alcohol exposure in the present study caused a reduction in neurons at 15 days of age in the SGS, and so the possibility exists that neuronal proliferation is affected. Gestational alcohol exposure is known to reduce the proliferation of neuronal precursors in certain brain regions including the cerebral cortex and hippocampal formation (Miller,'95b; Miller,'96b). Of particular significance to the present study is that alcohol has been shown to reduce or delay neuron proliferation in the brain stem in the principal sensory nucleus (PSN) of the trigeminal nerve (Miller,'95a).

Miller ('95a) investigated the effects of alcohol on neuronal proliferation versus neuronal cell death in the PSN using three groups of alcohol-exposed rats that were each exposed to alcohol during a different time point in development: either gestational days 11-19 to target neuronal proliferation; postnatal days 4-12 to target naturally occurring neuronal death; or postnatal days 31-39 at which time the PSN is considered mature. Miller analyzed the total number of neurons in the PSN in mature animals and was able to show a significant permanent cell loss (27%) that was caused by reduced neuronal proliferation and not by increases in cell death from the limited gestational alcohol exposures. However, the present study did not find a reduction in neuron numbers at 35 days of age in the SGS, indicating the loss at 15 days of age was not permanent, and actually found an increase in neurons between 15 and 35 days of age in the Et group (+33%, $p \leq 0.01$, ANOVA). These data argue that cell loss was not due to reduced neuronal proliferation alone since reduced neuronal proliferation would be expected to be permanent, but rather is more likely due to delays in neuronal proliferation or to delays in neuronal migration.

Neuronal Migration

Neuronal migration, the movement of neurons from their place of birth in the wall of the neural tube to their final location, is thought to involve a process whereby radial glia serve as guides for migration (Rakic,'72). Radial glia in the developing midbrain extend from the ventricle to the pial surface and are present throughout the period of neuronal migration that occurs on gestational days 15-22 to form the superficial SC (Mustari et al.,'79; Raedler et al.,'81; Wu et al.,'95). The reduction in neuronal number at 15 days of age in the gestational alcohol exposure could have been caused by an alcohol-induced delay in neuronal migration, especially since neuronal loss was transient and the number of neurons in the SGS of the alcohol-exposed group increased by 33% between 15 and 35 days of age such that by 35 days of age there was no difference in neuron number in the SGS. Previous studies have shown that gestational alcohol exposures can decrease the migration rate of neurons in the rat cerebral cortex, and that neurons often stop migrating before reaching the proper location (Miller,'86; Miller,'93). Studies in this lab have shown that gestational alcohol can delay the maturation of radial glia in the cerebellum with the implication that such changes could cause delays in neuronal migration (Shetty and Phillips,'92). Delayed neuronal migration could affect the appropriate development of proper connections of these neurons, permanently altering their functional state in the adult brain.

It is likely that in the present study both delayed neuronal proliferation and delayed neuronal migration were related, and together produced the reduction in neurons shown at 15 days of age in the gestational alcohol exposure. To characterize both processes as "delayed," rather than "reduced" or "suppressed," seems most appropriate in this interpretation because at 35 days of age, the neuronal number in the alcohol-exposed group was no longer affected.

In the postnatal exposure animals, there was no evidence that either neuronal proliferation or migration was affected by alcohol because total numbers of neurons in the SGS at both 15 and 90

days of age were unaffected. This seems intuitive because neuronal proliferation and migration were complete by the time alcohol exposure occurred (Figure 16).

Neuronal Cell Death

Naturally occurring neuronal cell death in the SC is primarily a postnatal event, occurring in the normal development of the rat SC from gestational day 20 to postnatal day 11, with the peak rate occurring at birth (Arees and Astrom,'77; Cunningham et al.,'82). Thus, cell death is occurring in some cells while other neurons are growing and differentiating. The timing of the postnatal alcohol exposure occurs for a limited time during the period of neuronal cell death.

In the present study the postnatal alcohol exposure did not cause increased cell loss at either 15 or 90 days of age, so it appears unlikely that the 5-6d binge exposure affected the rate of cell death. This is surprising because in the study by Miller ('95a) (discussed above in relation to neurogenesis in the brainstem), early postnatal alcohol exposure (4-12 days of age) caused increases in cell death during the period of growth and maturation of neurons in the PSN of the brainstem. It is possible that the differences between Miller's ('95a) work and the present study relate to the more temporally limited exposure used in the present study. It is possible that increased cell death was responsible for some of the cell loss shown at 15 days of age following the gestational exposure of the present study, but it seems unlikely since the effect was not permanent.

From the parameters measured in this study, it is difficult to interpret what mechanism or combination of mechanisms are responsible for the neuron loss at 15 days of age following the gestational exposure. An experiment that could possibly narrow the possibilities would be parallel autoradiographic studies in which the nuclei of dividing cells are labeled with H^3-thymidine on gestational days 15-18 and quantified at various times throughout development, including on or before gestational day 20, when the period of cell death begins, through maturation. The additional

parallel labeling of cell nuclei undergoing apoptosis may help tease apart the contributions of neuronal proliferation, migration, and cell death to the final number of neurons in the SC. Another possible approach would be to label the nuclei of dividing cells with the thymidine analog bromodeoxyuridine (BrdU) and to label the nuclei of dying cells with a stain for apoptotic cells. It may be possible to double label dying neurons that were born at a specific time due to immunofluorescent staining and thus to compare the rate of neuronal proliferation to the rate of cell death.

There are several cell populations in the rat CNS that are extremely vulnerable to alcohol-induced cell death after limited postnatal exposures. These include the mitral cells of the olfactory bulb and the projection neurons of the cerebellum (Purkinje cells) and hippocampus (pyramidal cells) (West et al.,'90; Bonthius et al.,'92; Pantazis et al.,'93; Maier et al.,'99). However, the projection neurons in the SGS do not appear to be significantly affected by a similar postnatal binge exposure. These vulnerable neuronal populations are born during mid to late gestation (mitral cells of the olfactory bulb are born on gestational days 14-16, Purkinje cells of the cerebellum are born on gestational days 14-15, and pyramidal cells of the hippocampus proper are born on gestational days 17-19) (Altman and Bayer,'95) and thus are all in the maturation phase of development when most vulnerable. Perhaps the maturing neurons of the SGS are not susceptible to postnatal binge exposures because as they mature their axons project to the deep layers of the SC and do not have as far to travel as other susceptible projection neuron populations, which is less taxing on the cellular machinery for growth (protein synthesis, cell metabolism, etc).

Neuronal Maturation and Synaptogenesis

The processes of neuronal maturation (Labriola and Laemle,'77) and synaptogenesis (Warton and McCart,'89) in the SGS occur primarily postnatally, and are dependent on ON afferents

(Giordano and Cunningham,'82). There is a postnatal age-induced decrease in volume density of neurons in the SGS that occurs in development found both in the present study and others (Warton and Jones,'85). This is likely due to neuronal maturation (Warton and Jones,'85), with the assumption that the increase in volume is due to the development of dendrites and synapses. Although there were no data collected in the present study that directly investigate alcohol-induced effects on synaptic development in the SGS, synaptogenesis would likely be affected as part of any effect on neuronal maturation. Postnatal alcohol exposures have been shown to decrease the synaptic efficacy in the CA1 region of the rat hippocampal formation (Bellinger et al.,'99), and to delay synaptogenesis in the cerebellum (Volk,'84; Klintsova et al.,'97). The maturation of neurons in the SGS could be affected by either alcohol exposure in the present study because the ON has been shown to be affected by both gestational (Ashwell and Zhang,'94) and postnatal (Phillips et al.,'98) alcohol exposures. Based on the parameters measured in the current study, delayed neuronal maturation would be expected to be reflected by a reduction in reference volume with a subsequent increase in the volume density of neurons.

In the present study, there was an alcohol-induced reduction in both reference volume and total neuron number at 15 days of age after gestational alcohol exposure, but the volume density of neurons was not affected. The reduction in reference volume was likely due to the cell loss, but could also have been due, in part, to delayed neuronal maturation and thus to delayed synaptogenesis. At 35 days of age there was no effect on either parameter; however, at this age the density and total number of glia in the SGS were both significantly increased and presumably took up volume replacing part of the normal neuropil containing dendrites, axons, and synapses. Therefore, the findings suggest that dendritic complexity and thus synaptic connectivity in the SGS was permanently decreased by the gestational alcohol exposure. This correlates with previous studies in this lab showing that gestational alcohol exposures cause a reduction of dendritic complexity in

Golgi-stained type II ganglion cells in the superficial SC (Wall and Phillips,'93), as well as in the substantia nigra (Shetty et al.,'93), and in the oculomotor nucleus (Burrows et al.,'95). Additionally, another study has shown that the density of NOS+ cells was decreased by gestational alcohol exposure at both 15 days of age (-24%) and 35 days of age (-20%) in the SGS (Phillips et al.,'99). The NMDA-NO system may be an important feedback mechanism for stabilizing synapses and synaptic refinement in the developing retinocollicular projection (Hofer and Constantine-Paton,'94), thus contributing to neuronal maturation; however, the exact role of NO is still being defined. When the NMDA-NO system is inhibited, the retinocollicular projection does not mature properly and aberrant connections persist (Wu et al.,'94; Ernst et al.,'99). The findings of Phillips et al. ('99) indicate that neuronal maturation could be affected due to an altered NMDA-NO feedback mechanism. This correlates with the findings of the present study that suggest neuronal maturation has been affected and neuropil complexity has been reduced at 35 days of age by gestational alcohol exposure.

The main effect of alcohol on neurons in the 5-6d binge exposure at 90 days of age was to decrease the reference volume and to increase the volume density of neurons, with no subsequent cell loss. The 40% reduction in rat optic nerve fibers produced by this same exposure at both 15 and 90 days (Phillips et al.,'98) may be sufficient to explain a large proportion of the reduction in reference volume because most of the optic nerve fibers in the rat project to the superficial laminae of the SC (Sefton and Dreher,'95). The 40% reduction in optic nerve fibers was already present in 15 day old animals when neuronal growth and maturation are occurring in the SGS. These developmental processes could also have been affected, producing smaller dendrites with fewer synaptic contacts, which would further contribute to a reduction in reference volume. Therefore postnatal alcohol exposure may also have caused a permanent alcohol-induced reduction in the complexity of the neuronal dendritic tree and synapses of the SGS secondary to the loss of optic nerve fibers.

Additionally, it is known that postnatal "binge-like" methods of alcohol exposure of the type used in the present study can alter the metabolism of neurons, including the inhibition of protein synthesis, and disrupt the cytoskeleton (West et al.,'90). These effects of alcohol could contribute to the reduced dendritic growth and complexity.

Correlation of Alcohol-induced Neuronal Effects with Previous Studies in the SC

The total number of neurons in the sampled volume was reduced by gestational alcohol exposure at 15 days of age in the present study. Results of two previous gestational alcohol exposure studies done in mice contrast somewhat with the results of the present gestational exposure in rats (Zajac et al.,'88; Ashwell and Zhang,'94). Ashwell and Zhang ('94) exposed fetal mice to alcohol through maternal intraperitoneal (IP) injection on G8 and examined offspring on 15 days of age. They showed an alcohol-induced increase in neuronal areal density (neurons per mm^2) in the SGS and decreased volume of the SGS, and predicted there should be no change in the total number of neurons. Several factors that may account for differences in the results of Ashwell and Zhang (1994) and those of the present study include the species used (rat vs. mouse), and the method, dosage, and timing of alcohol exposure (IP injection on one day vs. maternal ingestion of liquid diet throughout gestation). These studies would be expected to differ somewhat in that the methods of alcohol exposure utilized were quite different, and more dramatic changes would be expected to occur in the full gestational exposure of the present study. Both the volume of the entire SGS in the study by Ashwell and Zhang (1994) and the reference volume of the SGS through 80 μm of the SGS in the present study were determined by the Cavalieri method. It is significant that Ashwell and Zhang (1994) found a 40% reduction in volume for the entire SGS, though the present study found a 25% reduction in the reference volume for 80 μm through the SGS. If the reduction in volume of the SGS in the present study, which was fixed at 80 μm, was projected for the entire rostrocaudal extent

of the SGS, the effect on volume may actually be much more dramatic because the rostrocaudal dimension could have also been reduced. It is also significant that Ashwell and Zhang (1994) did not find a loss of neurons whereas the present study found a 30% reduction. The most likely explanation for that difference is that alcohol given as a pulse early in development may not have been sufficient to induce a neuronal loss. Another possibility is that their simple areal densities, rather than disector analysis of volume density, overestimated cell numbers.

In the study by Zajac et al. ('88), fetal mice were exposed to alcohol through maternal consumption of liquid diet during gestation, and then offspring were removed by C-section from the mothers and examined on gestational day 18. The authors found an alcohol-induced increase in areal density of neurons in the superficial SC (layers were not yet apparent), and a decreased cross-sectional area of the SC, implying no change in total number. Several factors that may account for differences between this study and the present study, including the species used (rat vs. mouse); method, dosage, and timing of alcohol exposure; and age of offspring at analysis. This study is hard to interpret because only G18 fetal mice were analyzed and interpretation would have been facilitated had older animals been included in the study. Although the experimental dams were fed alcohol-inclusive liquid diet, a pair-fed paradigm was not used, so it is possible that the control group does not represent a proper control for nutrition. Additionally, the alcohol exposure ended on gestational day 18 with animal sacrifice at a crucial time in neuronal migration, so the same animals examined a few days later may have shown neuron loss.

Correlation of Alcohol-induced Effects on the Development of the SC with the ON

The development of the ON and the SC are interdependent in terms of numbers of neurons, maturation of neurons, and proper development of the retinotopic map in the SC (Cunningham et al.,'79; Cunningham et al.,'82; Galli-Resta et al.,'93). Prenatal (Ashwell and Zhang,'94), postnatal

(Phillips,'89; Phillips et al.,'98), and combined pre- and postnatal (Phillips et al.,'91) exposures to alcohol have been shown to cause delays in myelin development, thinner myelin, and decreases in ON fiber numbers. Thus, it is expected that the number of neurons and connectivity of the developing SC should be affected by these same exposures.

It is surprising that the total number of neurons in the sampled volume of the SGS was not affected in the 5-6d binge alcohol-exposed animals since there was a 40% reduction in the number of ON fibers in these same animals (Phillips et al.,'98), and because studies have shown that cell death in the rat SC is increased if either ON activity is blocked (Galli-Resta et al.,'93) or if the eyes are removed at birth (Giordano and Cunningham,'82). It is possible that the amount of ON input lost is a crucial factor in determining cell death, in that following treatment with TTX or enucleation total activity was lost, while in the 5-6d binge alcohol-exposed animals 60% of the ON fibers remained. It could be that the remaining 60% of the ON fibers had a sufficient trophic effect to sustain the normal number of SGS neurons. It is also possible that timing of ON loss could be a factor, in that the study in which ON activity was blocked with TTX, did so at 2d (Galli-Resta et al.,'93), and that in the enucleation experiment, the eyes were removed at birth (Giordano and Cunningham,'82). In these studies, the ON was altered at the beginning of the postnatal period, several days earlier than in the 5-6d binge exposure. It is possible that by the time the ON fiber numbers are reduced in the 5-6d binge exposure, the neurons of the SGS have already made efferent axonal contacts which act as sustaining collaterals, or that other afferent fibers, such as those from the visual cortex, have already established contact with dendrites of neurons of the SGS, exerting a sustaining trophic effect. It is also possible that there was a loss of neurons for the entire SGS that was not detected in the present study because the total volume of the entire rostrocaudal extent of the SGS was not measured.

In the present study, gestational alcohol exposure caused a reduction in the total number of neurons in the SGS at 15d. Since ON fiber loss has been shown in the mouse model of gestational

alcohol exposure (Ashwell and Zhang,'94), it is likely that ON fiber loss is also a factor in the rat animal model. Cell loss at 15d then could be explained in part by the presumed loss of ON afferents.

It is likely that any effects of alcohol on cell death during the development of the SC and the ON are subtle. No attempt was made to quantify the neurons of each classification in the SGS. While it is assumed that all SGS neurons receive ON input, most of the larger (projection) neurons project to the deeper laminae of the SC, while many of the smaller, more superficially located neurons are local interneurons (Warton and Jones,'85; Boyes and Veronesi,'88). It would be interesting to see how alcohol may affect the cytoarchitecture of the SC, in terms of proliferation and cell death of each class of neuron.

Development of Macroglia

Glial cells are formed in the SC both prenatally (dominated by the development of astrocytes) and postnatally (dominated by the development of oligodendrocytes) (Raedler and Sievers,'75). It would be expected that the gestational alcohol exposure would affect astrocyte development while the postnatal alcohol exposure would be more likely to affect oligodendrocyte development. Gestational alcohol exposure did not appear to affect glial number at 15d, but dramatically increased the volume density of glia (83%) and total number of glia (85%) in the SGS (likely astrocytes) at 35d, implying gliosis. It is possible that at 15d, immature astrocytes were present that, due to their immature morphology, were not identified, and therefore were not counted as astrocytes but rather as unidentified cells. The gliosis at 35d could be secondary to alcohol-induced neuronal damage (Shetty and Phillips,'92; Guerri and Renau-Piqueras,'97; Guerri,'98) or to changes in the activity of neurons and related synaptogenesis. Because the blood-brain barrier and related astrocytes have been shown to be intact in prenatally exposed animals (Phillips et al.,'97), gliosis associated with vascular damage appears unlikely. There were no alcohol-induced effects on

the reference volume, density, or total number of neurons in the SGS at 35d, so by these measures alone, neuronal damage was not indicated. However, because the number of astrocytes was dramatically increased, it would appear possible that they replaced a significant portion of the volume of neuropil in the 35d alcohol-exposed animals. The most probable explanation for this is in response to some type of alcohol-induced damage to neuronal growth and maturation.

Another possible explanation for gliosis in the 35d animals from the gestational exposure is that changes in neuronal activity somehow increased the proliferation of astrocytes. Recently, astrocytes cultured from the SGS have been implicated in enhancing the efficacy of synapses of cultured rat retinal ganglion cells by increasing the frequency and amplitude of the excitatory postsynaptic currents (EPSCs) of retinal ganglion cells (Pfrieger and Barres,'97). A possible hypothesis is that prenatal alcohol exposure affects the proliferation of astrocytes by first affecting myelination and the activity of afferent neurons, then as synaptogenesis occurs with altered afferent activity, the proliferation of astrocytes is upregulated in response to reduced activity to enhance synaptic function and compensate for losses secondary to ON damage.

The ICC analysis of astrocyte bodies and processes following prenatal alcohol exposure did not support the findings of the physical disector analysis. The ICC analyses did not reveal significant differences in the fractional volume of tissue labeled by either GFAP or S-100, although most of the measurements were highly variable and for the GFAP studies n was small (3). Stereological analysis of these ICC tissues, as prepared, was not possible because the thick sections (30-40 μm) had variable stain penetration. The most appropriate method to quantify the staining was to measure the fractional volume percent by point-counting, which determined the volume density of positively stained structures (Weibel,'69; Mendis-Handagama et al.,'88; Al-Rabiai and Miller,'89). Briefly, the image of a sampled region in the SGS was superimposed on a grid of points and the total number of points over positively stained structures was divided by the total number of points on the grid. The

disadvantage to this method of analysis is that the actual numbers of glial cells in these tissues cannot be estimated. However, one would expect that dramatic changes in total numbers of cells, density of cells, or density of cellular processes (i.e., cellular hypertrophy), would be detected by this method of analysis (Mendis-Handagama et al.,'88). One possible explanation for the discrepancy is that the respective ICC stains may not have stained all GFAP- or S-100-positive cells due to technical problems with the antibodies used or the staining technique. It may be possible to further investigate this matter by taking serial semithin plastic sections, and staining alternate sections with either toluidine blue or either of the antibodies used as astrocyte markers by plastic section ICC. Comparisons could then be made directly between individual cells with the morphology of astrocytes in the toluidine blue-stained sections, and then determine whether each cell stains positive for either GFAP or S-100. The disadvantage to this experiment would be that plastic section ICC is very difficult because the plastic must be etched, and because glutaraldehyde-fixed plastic-embedded tissues used in the present study show a lot a variation in ICC staining.

Postnatal alcohol exposure caused a marginally significant decrease in the total number of glia (-18%, p=0.06) at 15 days of age, although there was no effect on the total number of glia at 90 days of age. In the ON of these 15 day old animals the number of glial cells was also reduced and correlated with alcohol-induced delays in both oligodendrocyte and myelin acquisition (Phillips et al.,'96). Since oligodendrocytes are acquired primarily postnatally (Mares and Bruckner,'78), the decreased total numbers of glia in the SGS was also likely due to an alcohol-induced delay in oligodendrocyte acquisition.

Validity of Stereological Methods

Any use of unbiased stereological methods must address the issue of whether the methods used are the most appropriate for the tissues that were available. In a preliminary study of tissues

collected from the gestational alcohol exposure experiment, a single 2 μm plastic section from each SC was stained with toluidine blue and analyzed by comparing the areal densities of nuclear profiles at a uniform location in the SGS (Selong and Phillips,'98). Results obtained from that preliminary study indicated a significant alcohol-induced increase in neuronal areal density at 15 days of age (compared with cell loss in the present study), with no change at 35 days of age and no changes in glial cell areal densities at either age. The areal density method of cell counts used in that preliminary analysis, although widely reported in the literature for similar studies (Zajac et al.,'88; Bonthius and West,'90; Coggeshall and Lekan,'96), is now generally not considered the most appropriate method to compare cell numbers unless it can be shown that cell size and shape are unaffected (Coggeshall and Lekan,'96) and that the reference volume is constant (Coggeshall et al.,'94). The areal density results differed dramatically from those obtained in the present stereological analysis and demonstrate why stereological methods are necessary in many studies. Recent advances made in stereology have led to more frequent acknowledgement of these methods as being the most appropriate methods for determining experimentally-induced changes in cell numbers (Sterio,'84; Guntinas-Lichius et al.,'93; Coggeshall et al.,'94; Mayhew and Gundersen,'96).

The preliminary study in the gestational alcohol exposure experiment may not have detected "real" changes in the cell populations of the SGS using nuclear profile counts (areal densities) due to changes in volume of the SGS that may have occurred. It stands to reason that if total volume of the SGS was decreased by developmental alcohol exposure at a particular age, but the actual number of neurons was unchanged, then it is expected that the density of neurons in the alcohol-exposed SGS would increase. An increased density could errantly be interpreted in the preliminary study as an increase in the number of neurons where no change occurred. In the absence of information regarding changes in volume that may or may not be occurring, cell densities alone are difficult to interpret (Oorschot,'94).

Another possible reason that the preliminary profile count for the gestational alcohol exposure was not sufficient to detect "real" changes in cell numbers in the SGS is that the amount of sampling per animal was not sufficient to produce "real" averages. A single area on one section was analyzed per animal and so the assumption would have to be that the areal density of nuclear profiles calculated from one sampled area for each animal represented the average areal density for each animal. This seems to be a rather large assumption as the standard deviations for preliminary profile counts were calculated and ranged from 30-40% of the means, and no further studies were completed including more sampling per animal to see how close the initial areal densities were to the average for each animal. Further appreciation of the variation possible looking at single sections can be gained by examination of Table 16 in the Appendix that shows that the number of neurons counted per disector pair for one animal ranges from 28-36 cells.

The physical disector for the unbiased stereological methods used in the present study was adapted from Sterio ('84). Two consecutive 200 μm thick slabs of SC had been previously cut from the SC in a uniform manner using visual landmarks and section thicknesses to insure a uniform depth within the nucleus. The entire SC was thus not available for random stereological sampling, but instead one slab from each animal was analyzed. Eighty consecutive 1 μm sections were cut from this block and mounted in order on glass microscope slides and stained with toluidine blue. Since the SC is considered homogeneous in terms of neuronal distribution (Albers et al.,'88), it would follow that a loss or gain of cells in a uniform slab of the SC should translate to a loss or gain for the entire nucleus. However, it is possible that the alcohol exposure could have changed the rostrocaudal dimensions of the SC (which were not measured), and therefore the actual changes may be more dramatic than estimated by the method presented here.

The efficiency and the appropriateness of the physical disector analysis was evaluated by calculating both the coefficient of error (CE) of individual estimates for each parameter measured

(Gundersen and Jensen,'87) and the coefficient of variation (CV) of the means as measures of biological variability (see Appendix). Briefly, in evaluating the stereological sampling design, the contribution of the OCE^2 should be roughly half or less than half of the OCV^2, where "O" refers to "observed" or computable values (Gundersen and Jensen,'87). The calculation of CE allows the investigator to ask: to what extent is the observed variance for the group (for N) due to the true biological variability in cell numbers among animals, and to what extent is it due to the intra-animal variation of cells counted in each physical disector?

It can be concluded that for neuronal estimates, the sampling design used in the present study was sufficient (Tables 5,6,10, and 11). For instance, in the gestational exposure at 35 days of age, Vref, Nv, and N were estimated for the Ct group with a precision of 9, 10, and 7%, respectively, and the CVs (as an indicator of biological variability) were 13, 11, and 20%, respectively. Therefore, most of the variation is due to true biological variation among animals (Appendix). Applying the general guidelines from the literature, one can conclude that the sampling design for neurons was appropriate, and that the differences obtained in the neuronal populations in the present study, are indeed real for the region of the SC sampled. It is further expected that these differences are representative of changes in the entire SC, but additional studies are needed for confirmation of that.

In terms of glial cells, far fewer cells were counted, and therefore the CEs of the glial estimates, although generally close to acceptable values, were not all in the acceptable range (Tables 7,8,12, and 13). This is because too few cells were counted per disector. This could be corrected by using a different sampling strategy that includes a larger counting frame.

This study could have benefited from a more proper stereological design. The major disadvantage to the present study, in which stereological methods were applied "after-the-fact," was that the entire SC was not available for sampling, so all parameters measured represented only a limited region of the length of the SC. Though care was taken in collecting the region of the SC

analyzed such that the regions should be uniform for all animals, there is no absolute control to insure that this was the case, or that the differences in the 80 μm slab are actually representative of total differences. In fact, the dramatic changes in reference volume were determined by measuring dimensions in only two planes (mediolateral and superficial-deep), because the sampled length of the SC was fixed at 80 μm. The SC, as a 3-D structure, was also likely affected in the rostrocaudal (length) dimension, which one would expect would lead to similar but even more dramatic alcohol-induced effects. For example, at 15 days of age following gestational alcohol exposure, the reference volume over 80 μm of SGS was reduced by 25% while the volume density of neurons was unchanged, thus indicating a 30% reduction in the total number of neurons. If the entire rostrocaudal dimension of the control SGS is estimated at 2 mm and if this dimension is also reduced by 25% in the alcohol-exposed group, then the predicted neuronal loss for the entire SGS can be calculated as actually 45%.

If this experiment were to be repeated for similarly exposed animals, several major changes would be advantageous for the best stereological analysis. Starting with the embedding of the SC the entire SC would need to be available for sampling. When harvesting the brain, the midbrain would be blocked and the tectum separated from the tegmentum. Then the two hemispheres of the SC could be separated with a cut down the midline of the midbrain. One hemisphere could be used primarily for an optical disector analysis, and the other for immunocytochemical studies. Each entire hemisphere would then be available for systematic random sampling. The benefits obtained therein would be that the total number of neurons could be estimated accurately for the entire volume of the SC hemisphere.

For efficiency, the optical disector method of analysis is a better choice than the physical disector. The optical disector requires a standard light microscope modified with a z-axis microcator to accurately measure vertical movement of the microscope stage, and with high magnification

objective lenses having shallow depths of focus. The optical disector is similar in principle to the physical disector, the major difference being that the reference section and the look-up section of the optical disector are optical planes, rather than physical sections. The entire length of the SC could be exhaustively sectioned into thick sections (~50μm), and viewed at high magnification (1000x oil immersion). To make the optical disector even more efficient, there are computerized systems equipped with stereological software and interfaced with motorized microscopes, which can digitize the microscopic image, supplementing the need to make drawings, counting frames, grids, etc.

For maximum efficiency, neurons could be counted with this analysis, and glial cells could be investigated separately using ICC. The main reason for this is that neurons are more easily recognized based on their morphology, whereas the identification of glial cells based on morphology, especially in neonatal animals where gliogenesis is ongoing and many immature cells are present, can be a difficult and time-consuming task.

Conclusions

Gestational exposure to alcohol caused a loss of neurons in the SGS in the SC at 15 days of age. This cell loss was likely due to a combination of effects causing decreases or delays in neuronal proliferation and migration, and increases in cell death. Gestational exposure to alcohol caused a dramatic increase in the number and volume density of glial cells (likely astrocytes) in the SGS at 35 days of age. Since the reference volume and the number and density of neurons were unaltered, gliosis was probably secondary to effects on neuronal maturation. Postnatal binge exposure to alcohol caused a marginally significant loss of glia at 15 days of age. This cell loss was likely due to a delay in oligodendrocyte maturation. Postnatal binge exposure to alcohol increased the volume density of neurons at 90 days of age. This increase was likely due to the 40% reduction of optic nerve fibers produced by this same exposure. Further studies are needed to examine the complexity

of the neuropil and the development of synapses in an ultrastructural analysis of the effects of alcohol on the development of the SC.

LITERATURE CITED

Abbott, N.J. (1987) Neurobiology. Glia and the blood-brain barrier. Nature *325*:195

Abel, E.L. and Sokol, R.J. (1987) Incidence of fetal alcohol syndrome and economic impact of FAS-related anomalies. Drug Alcohol Depend. *19*:51-70.

Abel, E.L. and Sokol, R.J. (1991) A revised conservative estimate of the incidence of FAS and its economic impact. Alcoholism: Clin.Exp.Res. *15*:514-524.

Abercrombie, M. (1946) Estimation of nuclear population from microtome sections. Anat.Rec. *94*:239-247.

Al-Rabiai, S. and Miller, M.W. (1989) Effect of prenatal exposure to ethanol on the ultrastructure of layer V of mature rat somatosensory cortex. J.Neurocytol. *18*:711-729.

Albers, F.J., Meek, J., and Nieuwenhuys, R. (1988) Morphometric parameters of the superior colliculus of albino and pigmented rats. J.Comp.Neurol. *274*:357-370.

Altman, J. and Bayer, S.A. (1981) Time of origin of neurons of the rat superior colliculus in relation to other components of the visual and visuomotor pathways. Exp.Brain Res. *42*:424-434.

Altman, J. and Bayer, S.A. (1995) Neurogenesis and Neuronal Migration. In: Paxinos, G. (ed): The Rat Nervous System. San Diego: Academic Press, pp. 1041-1078.

Angevine, J.B. and Sidman, R.L. (1961) Autoradiographic study of cell migration during histogenesis of cerebral cortex in the mouse. Nature *192*:766-768.

Arees, E.A. and Astrom, K.E. (1977) Cell death in the optic tectum of the developing rat. Anat.Embryol. *151*:29-34.

Aronson, M., Hagberg, B., and Gillberg, C. (1997) Attention deficits and autisitic spectrum problems in children exposed to alcohol during gestation: a follow up study. Dev.Med.Child Neurol. *39*:583-587.

Aronson, M., Kyllerman, M., Sabel, K.-G., Sandin, B., and Olegard, R. (1985) Children of alcoholic mothers: Developmental, perceptual and behavioural characteristics as compared to matched controls. Acta Paediatr.Scand. *74*:27-35.

Ashwell, K.W.S. and Zhang, L.-L. (1994) Optic nerve hypoplasia in an acute exposure model of the fetal alcohol syndrome. Neurotoxicol.Teratol. *16*:161-167.

Becker, H.C., Randall, C.L., Salo, A.L., Saulnier, J.L., and Weathersby, R.T. (1994) Animal research: Charting the course for FAS. Alcohol Health Res.World *18*:10-16.

Bellinger, F.P., Bedi, K.S., Wilson, P., and Wilce, P.A. (1999) Ethanol exposure during the third trimester equivalent results in long-lasting decreased synaptic efficacy but not plasticity in the CA1 region of the rat hippocampus. Synapse *31*:51-58.

Bonthius, D.J., Bonthius, N.E., Napper, R.M.A., and West, J.R. (1992) Early postnatal alcohol exposure acutely and permanently reduces the number of granule cells and mitral cells in the rat olfactory bulb: A stereological study. J.Comp.Neurol. *324*:557-566.

Bonthius, D.J. and West, J.R. (1990) Alcohol-induced neuronal loss in developing rats: Increased brain damage with binge exposure. Alcoholism: Clin.Exp.Res. *14*:107-118.

Bosco, A., Carri, N.G., and Linden, R. (1993) Neuritogenesis of retinal ganglion cells is differentially promoted by target extract. Brain Res. *632*:303-307.

Boulder Committee, (1970) Embryonic vertebrate central nervous system: revised terminology. Anat.Rec. *166*:257-262.

Boyes, W.K. and Veronesi, B. (1988) Electrophysiological and morphological evidence for a diameter-based innervation pattern of the superior colliculus. Exp.Neurol. *101*:190-207.

Bruckner, G., Mares, V., and Biesold, D. (1976) Neurogenesis in the visual system of the rat. An autoradiographic investigation. J.Comp.Neurol. 245-256.

Bunt, S.M., Lund, R.D., and Land, P.W. (1983) Prenatal development of the optic projection in albino and hooded rats. Dev.Brain Res. *6*:149-168.

Burrows, R.C., Shetty, A.K., and Phillips, D.E. (1995) Effects of prenatal alcohol exposure on the postnatal morphology of the rat oculomotor nucleus. Teratol. *51*:318-328.

Chamak, B., Fellous, A., Glowinski, J., and Prochiantz, A. (1987) MAP2 expression and neuritic outgrowth and branching are coregulated through region-specific neuro-astroglial interactions. J.Neurosci. *7*:3163-3170.

Chan, T., Bowell, R., O'Keefe, M., and Lanigan, B. (1991) Ocular manifestations in fetal alcohol syndrome. Br.J.Ophthalmol. *75*:524-526.

Chen, C. and Tonegawa, S. (1997) Molecular genetic analysis of synaptic plasticity, activity-dependent neural development, learning, and memory in the mammalian brain. Ann.Rev.Neurosci. *20*:157-184.

Chen, W.-J.A., Parnell, S.E., and West, J.R. (1999) Effects of alcohol and nicotine on developing olfactory bulb: loss of mitral cells and alterations in neurotransmitter levels. Alcoholism: Clin.Exp.Res. *23*:18-25.

Clarren, S.K. (1981) Recognition of fetal alcohol syndrome. JAMA *245*:2436-2439.

Clarren, S.K. (1986) Neuropathology in fetal alcohol syndrome. In: West, J.R. (ed): Alcohol and Brain Development. New York, Oxford: Oxford University Press, pp. 158-166.

Clarren, S.K., Alvord, E.C., Jr., Sumi, S.M., Streissguth, A.P., and Smith, D.W. (1978) Brain malformations related to prenatal exposure to ethanol. J.Pediatr. *92*:64-67.

Coggeshall, R.E. and Lekan, H.A. (1996) Methods for determining numbers of cells and synapses: A case for more uniform standards of review. J.Comp.Neurol. *364*:6-15.

Coggeshall, R.E., Pover, C.M., and Fitzgerald, M. (1994) Dorsal root ganglion cell death and surviving cell numbers in relation to the development of sensory innervation in the rat hindlimb. Dev.Brain Res. *82*:193-212.

Coles, C.D. (1994) Critical periods for prenatal alcohol exposure. Alcohol Health Res.World *18*:22-29.

Compston, A., Zajicek, J., Sussman, J., Webb, A., Hall, G., Muir, D. et al., (1997) Glial lineages and myelination in the central nervous system. J.Anat. *190*:161-200.

Cook, C.S., Nowotny, A.Z., and Sulik, K.K. (1987) Fetal alcohol syndrome: Eye malformations in a mouse model. Arch.Opthalmol. *105*:1576-1581.

Cowan, W.M., Fawcett, J.W., O'Leary, D.D.M., and Stanfield, B.B. (1984) Regressive events in neurogenisis. Science *225*:1258-1265.

Cramer, K.S. and Sur, M. (1996) The role of NMDA receptors and nitric oxide in retinogeniculate development. Prog.Brain Res. *108*:235-244.

Cunningham, T.J., Huddelston, C., and Murray, M. (1979) Modification of neuron numbers in the visual system of the rat. J.Comp.Neurol. 423-434.

Cunningham, T.J., Mohler, I.M., and Giordano, D.L. (1982) Naturally ocurring neuron death in the ganglion cell layer of the neonatal rat: Morphology and evidence for regional correspondence with neuron death in superior colliculus. Dev.Brain Res. *2*:203-215.

Davis, E.J., Foster, T.D., and Thomas, W.E. (1994) Cellular forms and functions of brain microglia. Brain Res.Bull. *34(1)*:73-78.

De Groot, D.M.G. (1988) Comparison of methods for the estimation of the thickness of ultrathin tissue sections. Journal of Microsc. *151*:23-42.

Derr, R.F., Draves, K., and Rao, G.A. (1987) Inadequate intake by female rats during gestation and lactation of essential nutrients from liquid diets used for alcohol studies: Implication for the fetal alcohol syndrome. Biochem.Arch. *3*:137-145.

Diao, Y.C., Wang, Y.K., and Xiao, Y.M. (1983) Representation of the binocular visual field in the superior colliculus of the albino rat. Exp.Brain Res. *52*:67-72.

Dobbing, J. (1981) The later development of the brain and its vulnerability. In: Dobbing, J. and Davis, J.A. (eds): Scientific Foundations of Paediatrics. London: Heineman Medical Books, pp. 744-759.

Dobbing, J. and Sands, J. (1979) Comparative aspects of the brain growth spurt. Early Hum.Dev. *3*:79-83.

Driscoll, C.D., Streissguth, A.P., and Riley, E.P. (1990) Prenatal alcohol exposure: Comparability of effects in humans and animal models. Neurotoxicol.Teratol. *12*:231-237.

Ernst, A.F., Wu, H.H., El-Fakahany, E.E., and McLoon, S.C. (1999) NMDA receptor-mediated refinement of a transient retinotectal projection during development requires nitric oxide. J.Neurosci. *19*:229-235.

Evans, S.M. and Howard, V. (1989) A simplification of the 'step' method for estimating mean section thickness. Journal of Microsc. *154*:289-293.

Ferriero, D.M., Sheldon, R.A., and Domingo, J. (1992) Somatostatin is altered in developing retina from ethanol-exposed rats. Neurosci.Lett. *147*:29-32.

Galli-Resta, L., Ensini, M., Fusco, E., Gravina, A., and Margheritti, B. (1993) Afferent spontaneous electrical activity promotes the survival of target cells in the developing retinotectal system of the rat. The Journal of Neuroscience *13*:243-250.

Gally, J.A., Montague, P.R., Reeke, G.N.J., and Edelman, G.M. (1990) The NO hypothesis: Possible effects of a short-lived, rapidly diffusible signal in the development and function of the nervous system. Proc.Natl.Acad.Sci.USA *87*:3547-3551.

Ganzler-Odenthal, S.I. and Redies, C. (1998) Blocking N-cadherin function disrupts the epithelial structure of differentiating neural tissue in the embryonic chicken brain. J.Neurosci. *18*:5415-5425.

Garthwaite, J. (1991) Glutamate, nitric oxide and cell-cell signalling in the nervous system. TINS *14(2)*:60-67.

Geinisman, Y., Gundersen, H.J.G., Van der Zee, E., and West, M.J. (1996) Unbiased stereological estimation of the total number of synapses in a brain region. J.Neurocytol. *25*:805-819.

Geinisman, Y., Gundersen, H.J.G., Van der Zee, E., and West, M.J. (1997) Towards obtaining unbiased estimates of the total number of synapses in a brain region: problems of primary and secondary importance. J.Neurocytol. *26*:711-713.

Ghandour, M.S., Langley, O K., Labourdette, G., Vincendon, G., and Gombos, G. (1981) Specific and artefactual cellular localizations of S100 protein: An astrocyte marker in rat cerebellum. Dev.Neurosci. *4*:66-78.

Giordano, D.L. and Cunningham, T.J. (1982) Optic afferents, neuron maturation, and neuron survival in the rat superior colliculus. Dev.Brain Res. *4*:365-368.

Giulian, D., Allen, R.L., Baker, T.J., and Tomozawa, Y. (1986) Brain peptides and glial growth. I. Glia-promoting factors as regulators of gliogenesis in the developing and injured central nervous system. J.Cell Biol. *3*:803-811.

Golden, J.A., Zitz, J.C., McFadden, K., and Cepko, C.L. (1997) Cell migration in the developing chick diencephalon. Development *124*:3525-3533.

Goodlett, C.R., Leo, J.T., O'Callaghan, J.P., Mahoney, J.C., and West, J R. (1993) Transient cortical astrogliosis induced by alcohol exposure during the neonatal brain growth spurt in rats. Dev.Brain Res. *72*:85-97.

Goodlett, C.R., Peterson, S.D., Lundahl, K.R., and Pearlman, A.D (1997) Binge-like alcohol exposure of neonatal rats via intragastric intubation induces both Purkinje cell loss and cortical astrogliosis. Alcoholism: Clin.Exp.Res. *21*:1010-1017.

Goodlett, C.R. and West, J.R. (1992) Fetal alcohol effects: rat model of alcohol exposure during the brain growth spurt. In: Zagon, I.S. and Slotkin, T. (eds): Maternal Substance Abuse and the Developing Nervous System. New York: Academic Press, pp. 45-75.

Goodman, C.S. and Shatz, C.J. (1993) Developmental mechanisms that generate precise patterns of neuronal connectivity. Cell *72*:77-98.

Gottesfeld, Z., Garcia, C.J., Lingham, R.B., and Chronister, R.B. (1989) Prenatal ethanol exposure impairs lesion-induced plasticity in a dopaminergic synapse after maturity. Neurosci. *29(3)*:715-723.

Guerri, C. (1998) Neuroanatomical and neurophysiological mechanisms involved in central nervous system dysfunctions induced by prenatal alcohol exposure. Alcoholism: Clin.Exp.Res. *22*:304-312.

Guerri, C. and Renau-Piqueras, J. (1997) Alcohol, astroglia, and brain development. Molecular Neurobiology *15*:65-81.

Gundersen, H.J.G. (1986) Stereology of arbitrary particles. J.Microsc. *143*:3-45.

Gundersen, H.J.G. and Jensen, E.B. (1987) The efficiency of systematic sampling in stereology and its prediction. J.Microsc. *147*:229-263.

Guntinas-Lichius, O., Mockenhaupt, E., Stennert, E., and Neiss, W.F. (1993) Simplified nerve cell counting in the rat brainstem with the physical disector using a drawing-microscope. J.Microsc. *172*:177-180.

Hagg, T., Van der Zee, C.E.E.M., Ross, G., and Riopelle, R.J. (1997) Response to: Basal forebrain neuronal loss in mice lacking neurotropin receptor p75; by Peterson, D.A. et al. Science *277*:838-839.

Hankin, M. and Lund, R.D. (1991) How do retinal axons find their targets in the developing brain? TINS *14(6)*:224-228.

Harvey, A.R., Plant, G.W., and Kent, A.P. (1993) The distribution of astrocytes, oligodendroglia and myelin in normal and transplanted rat superior colliculus: An immunohistochemical study. J.Neural Transplant.Plastic. *4*:1-14.

Hawrylak, N. and Greenough, W.T. (1995) Monocular deprivation alters the morphology of glial fibrillary acidic protein-immunoreactive astrocytes in the rat visual cortex. Brain Res. *683*:187-199.

Hemond, S.G. and Glover, J.C. (1993) Clonal patterns of cell proliferation, migration, and dispersal in the brainstem of the chicken embryo. J.Neurosci. *13*:1387-1402.

Hofer, M. and Constantine-Paton, M. (1994) Regulation of N-methyl-D-aspartate(NMDA) receptor function during the rearrangement of developing neuronal connections. Prog.Brain Res. *102*:277-285.

Holzman, A.E., Chrousos, G.A., Kozma, C., and Traboulsi, E.I. (1990) Duane's retraction syndrome in the fetal alcohol syndrome. Am.J.Ophthal. *110*:565-566.

Huxlin, K.R., Carr, R., Schulz, M., Sefton, A.J., and Bennett, M.R. (1995) Trophic effect of collicular proteoglycan on neonatal rat retinal ganglion cells in situ. Dev.Brain Res. 77-88.

Janzer, R.C. (1993) The blood-brain barrier: Cellular basis. J.Inher.Metab.Dis. *16*:639-647.

Janzer, R.C. and Raff, M.C. (1987) Astrocytes induce blood-brain barrier properties in endothelial cells. Nature *325*:253-257.

Jeffery, G. (1984) Retinal ganglion cell death and terminal field retraction in the developing rodent visual system. Dev.Brain Res. *13*:81-96.

Jhaveri, S., Erzurumlu, R.S., Friedman, B., and Schneider, G.E (1992) Oligodendrocytes and myelin formation along the optic tract of the developing hamster: An immunohistochemical study using the Rip antibody. Glia *6*:138-148.

Jones, K.L. and Smith, D.W. (1973) Recognition of the fetal alcohol syndrome in early infancy. Lancet *Nov.*999-1003.

Jones, K.L. and Smith, D.W. (1975) The fetal alcohol syndrome. Teratol. *12*:1-10.

Katz, L.M. and Fox, D.A. (1991) Prenatal ethanol exposure alters scotopic and photopic components of adult rat electroretinograms. Invest.Ophthalmol.Vis.Sci. *32*:2861-2872.

Kennedy, L.A. and Elliot, M.J. (1986) Ocular changes in the mouse embryo following acute maternal ethanol intoxication. Int.J.Dev.Neurosci. *4(4)*:311-317.

Klintsova, A.Y., Matthews, J.T., Goodlett, C.R., Napper, R.M., and Greenough, W.T. (1997) Therapeutic motor training increases parallel fiber synapse number per Purkinje neuron in cerebellar cortex of rats given postnatal binge alcohol exposure: Preliminary report. Alcoholism: Clin.Exp.Res. *21*:1257-1263.

Kosaka, T., Nagatsu, I., Wu, J.-Y., and Hama, K. (1986) Use of high concentrations of glutaraldehyde for immunocytochemistry of transmitter-synthesizing enzymes in the central nervous system. Neurosci. *18*:975-990.

Labriola, A.R. and Laemle, L.K. (1977) Cellular morphology in the visual layer of the developing rat superior colliculus. Exp.Neurol. *55*:247-268.

Laemle, L.K. and Labriola, A.R. (1982) Retinocollicular projections in the neonatal rat: An anatomical basis for plasticity. Dev.Brain Res. *3*:317-322.

Langer, T.P. and Lund, R.D. (1974) The upper layers of the superior colliculus of the rat: a Golgi study. J.Comp.Neurol. *158*:405-436.

Lieber, C.S. and Decarli, L.M. (1994) Animal models of chronic ethanol toxicity. Methods Enzymol. *233*:585-595.

Linden, R. and Perry, V.H. (1983) Massive retinotectal projection in rats. Brain Res. *272*:145-149.

Lund, J.S. and Lund, R.D. (1972) The effects of varying periods of visual deprivation on synaptogenesis in the superior colliculus of the rat. Brain Res. 21-32.

Lund, R.D. (1972) Anatomic studies of the superior colliculus. Invest.Ophthalmol. *11*:434-441.

Lund, R.D. and Lund, J.S. (1972) Development of synaptic patterns in the superior colliculus of the rat. Brain Res. *42*:1-20.

Magloczky, Z., Martos, J., and Tombol, T. (1990) Effect of prenatal exposure to ethanol on brains of kittens:I. Changes of neurons in lateral geniculate nucleus. J.Hirnforsch. *31(6)*:761-771.

Maier, S.E., Miller, J.A., Blackwell, J.M., and West, J.R. (1999) Fetal alcohol exposure and temporal vulnerability: regional differences in cell loss as a function of the timing of binge-like alcohol exposure during brain development. Alcoholism: Clin.Exp.Res. *23*:726-734.

Mares, V. and Bruckner, G. (1978) Postnatal formation of non-neuronal cells in the rat occipital cerebrum: an autoradiographic study of the time and space pattern of cell division. J.Comp.Neurol. *177*:519-528.

Martin, D.L. (1992) Synthesis and release of neuroactive substances by glial cells. Glia *5*:81-94.

Mattson, S.N., Jernigan, T.L., and Riley, E.P. (1994) MRI and prenatal alcohol exposure: Images provide insight into FAS. Alcohol Health Res.World *18*:49-52.

Mayhew, T.M. and Gundersen, H.J.G. (1996) "If you assume, you can make an ass out of u and me": A decade of the disector for stereological counting of particles in 3D space. J.Anat. *188*:1-15.

Mendis-Handagama, S.M.L.C., Zirkin, B.R., and Ewing, L.L. (1988) Comparison of components of the testis interstitium with testosterone secretion in hamster, rat, and guinea pig testes perfused in vitro. Am.J.Anat. *181*:12-22.

Miller, M.W. (1986) Effects of alcohol on the generation and migration of cerebral cortical neurons. Science *233*:1308-1311.

Miller, M.W. (1988) Effect of prenatal exposure to ethanol on the development of cerebral cortex: I. Neuronal generation. Alcoholism: Clin.Exp.Res. *12*:440-449.

Miller, M.W. (1993) Migration of cortical neurons is altered by gestational exposure to ethanol. Alcoholism: Clin.Exp.Res. *17(2)*:304-314.

Miller, M.W. (1995a) Generation of neurons in the rat dentate gyrus and hippocampus: Effects of prenatal and postnatal treatment with ethanol. Alcoholism: Clin.Exp.Res. *19*:1500-1509.

Miller, M.W. (1995b) Effect of pre- or postnatal exposure to ethanol on the total number of neurons in the principal sensory nucleus of the trigeminal nerve: Cell proliferation and neuronal death. Alcoholism: Clin.Exp.Res. *19*:1359-1363.

Miller, M.W. (1996) Limited ethanol exposure selectively alters the proliferation of precursor cells in the cerebral cortex. Alcoholism: Clin.Exp.Res. *20*:139-143.

Miller, M.W. (1997) Effects of prenatal exposure to ethanol on callosal projection neurons in rat somatosensory cortex. Brain Res. *766*:121-128.

Miller, M.W. and Potempa, G. (1990) Numbers of neurons and glia in mature rat somatosensory cortex: Effects of prenatal exposure to ethanol. J.Comp.Neurol. *293*:92-102.

Miller, P.B., Charleston, J.S., Battaglia, D.E., Klein, N.A., and Soules, M.R. (1997) An accurate, simple method for unbiased determination of primordial follicle number in the primate ovary. Biol.Reprod. *56*:909-915.

Mize, R.R., Banfro, F.T., and Scheiner, C.A. (1996) Pre- and postnatal expression of amino acid neurotransmitters, calcium binding proteins, and nitric oxide synthase in the developing superior colliculus. Prog.Brain Res. *108*:313-332.

Mize, R.R., Scheiner, C.A., Salvatore, M.F., and Cork, R.J. (1997) Inhibition of nitric oxide synthase fails to disrupt the development of cholinergic fiber patches in the rat superior colliculus. Dev.Neurosci. *19*:260-273.

Morrison, J., Hof, P., Coggeshall, R.E., Geinisman, Y., Turner, J.N., West, M.J. et al., (1998) 1998 Short Course Syllabus -- Quantitative Neuroanatomy: A Picture Is Worth A Thousand Words, But A Number Is Worth A Thousand Pictures. Washington, D.C. Society for Neuroscience.

Mustari, M.J., Lund, R.D., and Graubard, K. (1979) Histogenesis of the superior colliculus of the albino rat: A tritiated thymidine study. Brain Res. *164*:39-52.

Nolte, J. (1999) Visual system. In: Nolte, J. (ed): The human brain. Mosby Year Book, Inc. pp. 275-305.

O'Leary, D.D.M., Crespo, D., Fawcett, J.W., and Cowan, W.M. (1986) The effect of introcular tetrodotoxin on the postnatal reduction in the numbers of optic nerve axons in the rat. Dev.Brain Res. *30*:96-103.

O'Malley, E.K., Sieber, B.A., Morrison, R.S., Black, I.B., and Dreyfus, C.F. (1994) Nigral type I astrocytes release a soluble factor that increases dopaminergic neuron survival through mechanisms distinct from basic fibroblast growth factor. Brain Res. *647*:83-90.

Oorschot, D.E. (1994) Are you using neuronal densities, synaptic densities or neurochemical densities as your definitive data? There is a better way to go. Prog.Neurobiol. *44*:233-247.

Pantazis, N.J., Dohrman, D.P., Goodlett, C.R., Cook, R.T., and West, J R (1993) Vulnerability of cerebellar granule cells to alcohol-induced cell death diminishes with time in culture. Alcoholism: Clin.Exp.Res. *17(5)*:1014-1021.

Paxinos, G. and Watson, C. (1982) The Rat Brain in Stereotaxic Coordinates. London: Academic Press.

Peiffer, J., Majewski, F., Fischbach, H., Bierich, J.R., and Volk, B. (1979) Alcohol embryo- and fetopathy. J.Neurol.Sci. *41*:125-137.

Perry, V.H., Henderson, Z., and Linden, R. (1983) Postnatal changes in retinal ganglion cell and optic axon populations in the pigmented rat. J.Comp.Neurol. *219*:356-368.

Peterson, D.A., Leppert, J.T., Lee, K., and Gage, F.H. (1997) Basal forebrain neuronal loss in mice lacking neurotropin receptor p75. Technical Comment. Science *277*:837-838.

Pfrieger, F.W. and Barres, B.A. (1997) Synaptic efficacy enhanced by glial cells in vitro. Science *277*:1684-1687.

Phillips, D.E. (1989) Effects of limited postnatal ethanol exposure on the development of myelin and nerve fibers in rat optic nerve. Exp.Neurol. *103*:90-100.

Phillips, D.E. (1992) Effects of alcohol on the development of glial cells and myelin. In: Watson, R.R. (ed): Alcohol and Neurobiology: Brain Development and Hormone Regulation. Boca Raton, FL: CRC Press, pp. 83-108.

Phillips, D.E. (1994) Effects of alcohol on glial cell development in vivo: Morphological studies. In: Lancaster, F.E. (ed): Alcohol and Glial Cells; NIAAA Research Monograph 27. Bethesda, Maryland: NIH, National Institute on Alcohol Abuse and Alcoholism, pp. 69-92.

Phillips, D.E., Cummings, J.D., and Wall, K.A. (1999) Effects of developmental alcohol exposures on nitric oxide synthase positive cells in the rat superior colliculus and periaqueductal gray. Manuscript in Preparation 3/98

Phillips, D.E. and Krueger, S.K. (1990) Effects of postnatal ethanol exposure on glial cell development in rat optic nerve. Exp.Neurol. *107*:97-105.

Phillips, D.E. and Krueger, S.K. (1992) Effects of combined pre- and postnatal ethanol exposure (three trimester equivalency) on glial cell development in rat optic nerve. Int.J.Dev.Neurosci. *10*:197-206.

Phillips, D.E., Krueger, S.K., and Rydquist, J.E. (1991) Short- and long-term effects of combined pre- and postnatal ethanol exposure (three trimester equivalency) on the development of myelin and axons in rat optic nerve. Int.J.Dev.Neurosci. *9*:631-647.

Phillips, D.E., Krueger, S.K., and Schubloom, L.A. (1996) Effects of binge alcohol exposures at two different times on myelin development in rat optic nerve. Alcoholism: Clin.Exp.Res. *20*:27A(Abstract)

Phillips, D.E., Krueger, S.K., Schubloom, L.A., and Mitchell, C.L. (1998) Postnatal binge alcohol exposures reduce nerve fiber numbers in rat optic nerve. Alcoholism: Clin.Exp.Res. *22*:185A(Abstract)

Phillips, D.E., Krueger, S.K., Wall, K.A., Smoyer-Dearing, L.H., and Sikora, A.K. (1997) The development of the blood-brain barrier in alcohol-exposed rats. Alcohol *14*:333-343.

Raedler, A. and Sievers, J. (1975) The development of the visual system of the albino rat. Adv.Anat.Embryol.Cell Biol. *50*:3-88.

Raedler, E., Raedler, A., and Feldhaus, S. (1981) Prenatal differentiation of colliculus superior in the rat. Biblio.Anat. 174-191.

Rajan, I. and Cline, H.T. (1998) Glutamate receptor activity is required for normal development of tectal cell dendrites *in vivo*. J.Neurosci. *18*:7836-7846.

Rakic, P. (1972) Mode of cell migration to the superficial layers of the fetal monkey neocortex. J.Comp.Neurol. *145*:61-84.

Rakic, P. (1981) Developmental events leading to laminar and areal organization of the neocortex (the organization of the cerebral cortex). Brain Res. 7-28.

Rao, G.A., Larkin, E.C., and Derr, R.F. (1988) Chronic alcohol consumption during pregnancy: Alleviation of untoward effects by adequate nutrition. Nutr.Res. *8*:421-429.

Roebuck, T.M., Mattson, S.N., and Riley, E.P. (1998) A review of the neuroanatomical findings in children with fetal alcohol syndrome or prenatal exposure to alcohol. Alcoholism: Clin.Exp.Res. *22*:339-344.

Rosenberg, A. (1996) Brain damage caused by prenatal alcohol exposure. Science and Medicine 42-51.

Rothstein, J.D., Dykes-Hoberg, M., Pardo, C.A., Bristol, L.A., Jin, L., Kuncl, R.W. et al., (1996) Knockout of glutamate transporters reveals a major role for astroglial transport in excitotoxicity and clearance of glutamate. Neuron *16*:675-686.

Sakurai, T. and Okada, Y. (1992) Selective reduction of glutamate in the rat superior colliculus and dorsal lateral geniculate nucleus after contralateral enucleation. Brain Res. 197-203.

Schmidt-Kastner, R. and Szymas, J. (1990) Immunohistochemistry of glial fibrillary acidic protein, vimentin and S-100 protein for study of astrocytes in hippocampus of rat. J.Chem.Neuroanat. *3*:179-192.

Schmitz, C. (1997) Towards more readily comprehensible procedures in disector stereology. J.Neurocytol. *26*:707-710.

Schwab, M.E. and Caroni, P. (1988) Oligodendrocyte and CNS myelin are nonpermissive substrates for neurite growth and fibroblast spreading in vitro. J.Neurocytol. *8*:2381-2393.

Sefton, A.J. and Dreher, B. (1995) Visual System. In: Paxinos, G. (ed): The Rat Nervous System. San Diego: Academic Press, pp. 833-898.

Selong, T.H. and Phillips, D.E. (1998) Effects of alcohol on the developing rat superior colliculus. Montana Academy of Sciences Program (Abstract)

Shatz, C.J. (1990) Impulse activity and the patterning of connections during CNS development. Neuron *5*:745-756.

Shetty, A.K., Burrows, R.C., and Phillips, D.E. (1993) Alterations in neuronal development in the substantia nigra pars compacta following in utero ethanol exposure: Immunohistochemical and Golgi studies. Neurosci. *52*:311-322.

Shetty, A.K. and Phillips, D.E. (1992) Effects of prenatal ethanol exposure on the development of Bergmann glia and astrocytes in rat cerebellum: An immunohistochemical study. J.Comp.Neurol. *321*:19-32.

Silver, J. and Sidman, R.L. (1980) A mechanism for the guidance and topographic patterning of retinal ganglion cell axons. J.Comp.Neurol. *189*:101-111.

Simon, D.K. and O'Leary, D.D.M. (1991) Relationship of retinotopic ordering of axons in the optic pathway to the formation of visual maps in central targets. J.Comp.Neurol. *307*:393-404.

Simon, D.K., Roskies, A.L., and O'Leary, D.D.M. (1994) Plasticity in the development of topographic order in the mammalian retinocollicular projection. Dev.Biol. *162*:384-393.

Snow, D.M., Steindler, D.A., and Silver, J. (1990) Molecular and cellular characterization of the glial roof plate of the spinal cord and optic tectum: a possible role for a proteoglycan in the development of an axon barrier. Dev.Biol. *138*:359-376.

Sokol, R.J. and Clarren, S.K. (1989) Guidelines for use of terminology describing the impact of prenatal alcohol on the offspring. Alcoholism: Clin.Exp.Res. *13*:597-598.

Sterio, D. (1984) The unbiased estimation of number and sizes of arbitrary particles using the disector. J.Microsc. *134(2)*:127-136.

Streissguth, A.P. (1986) The behavioral teratology of alcohol: Performance, behavioral, and intellectual deficits in prenatally exposed children. In: West, J.R. (ed): Alcohol and Brain Development. New York: Oxford University Press, pp. 3-44.

Streissguth, A.P., Aase, J.M., Clarren, S.K., Randels, S.P., LaDue, R.A., and Smith, D.F. (1991) Fetal alcohol syndrome in adolescents and adults. JAMA *265(15)*:1961-1967.

Stromland, K. (1990) Contribution of ocular examination to the diagnosis of foetal alcohol syndrome in mentally retarded children. J.Mental Def.Res. *34*:429-435.

Stromland, K. and Hellstrom, A. (1996) Fetal alcohol syndrome - An ophthalmological and socioeducational prospective study. Pediatr. *97*:845-850.

Stromland, K., Miller, M., and Cook, C. (1991) Ocular teratology. Sur.Ophthalmol. *35*:429-446.

Stromland, K. and Pinazo-Duran, M.D. (1994) Optic nerve hypoplasia: Comparative effects in children and rats exposed to alcohol during pregnancy. Teratol. *50(2)*:100-111.

Swiatek, K.R., Dombrowski, G.J., and Chao, K.L. (1986) The inefficient transfer of maternally fed alcohol to nursing rats. Alcohol *3*:169-174.

Tennekoon, G.I., Cohen, S.R., Price, D.L., and McKhann, G.M. (1977) Myelinogenesis in optic nerve: A morphological, autoradiographic, and biochemical analysis. J.Cell Biol. *72*:604-616.

Tenorio, F., Giraldi-Guimaraes, A., and Mendez-Otero, R. (1995) Developmental changes of nitric oxide synthase in the rat superior colliculus. J.Neurosci.Res. *42*:633-637.

Testar, X., Llobera, M., and Herrera, E. (1988) Comparative metabolic effects of chronic ethanol intake and undernutrition in pregnant rats and their fetuses. Alcoholism: Clin.Exp.Res. *12(2)*:197-200.

Thomson, A.D., Pratt, O.E., Jeyasingham, M., and Shaw, G.K. (1988) Alcohol and brain damage. Human Toxicol. *7*:455-463.

Virgili, M., Barnabei, O., and Contestabile, A. (1990) Regional maturation of neurotransmitter-related and glial markers during postnatal development in the rat. Int.J.Dev.Neurosci. *8(2)*:159-166.

Volk, B. (1984) Cerebellar histogenesis and synaptic maturation following pre-and postnatal alcohol administration. Acta Neuropathol. *63*:57-65.

Wall, K.A. and Phillips, D.E. (1993) Effect of prenatal alcohol exposure on development in the superficial lamina of the rat superior colliculus. Soc.Neurosci.Abstr. *19*:1731(Abstract)

Warton, S.S. and Jones, D.G. (1985) Postnatal development of the superficial layers in the rat superior colliculus: A study with Golgi-Cox and Kluver-Barrera techniques. Exp.Brain Res. *58*:490-502.

Warton, S.S. and McCart, R. (1989) Synaptogenesis in the stratum griseum superficiale of the rat superior colliculus. Synapse *3*:136-148.

Weibel, E.R. (1969) Stereological principles for morphometry in electron microscopic cytology. Int.Rev.Cytol. *26*:235-302.

Weinberg, J. (1984) Nutritional issues in perinatal alcohol exposure. Neurobehav.Toxicol.Teratol. *6*:261-269.

West, J.R. (1993) Use of pup in a cup model to study brain development. J.Nutr. 382-385.

West, J.R., Goodlett, C.R., Bonthius, D.J., Hamre, K.M., and Marcussen, B.L. (1990) Cell population depletion associated with fetal alcohol brain damage: Mechanisms of BAC-dependant cell loss. Alcoholism: Clin Exp.Res. *14*:813-818.

West, J.R., Goodlett, C.R., and Kelly, S.J. (1987) Alcohol and brain development. 45-60.(Abstract)

West, J.R., Hamre, K.M., and Pierce, D.R. (1984) Delay in brain growth induced by alcohol in artificially reared rat pups. Alcohol *1*:213-222.

West, M.J. and Gundersen, H.J.G. (1990) Unbiased stereological estimation of the number of neurons in the human hippocampus. J.Comp.Neurol. *296*:1-22.

Wiggins, R.C. (1986) Myelination: A critical stage in development. Neurotoxicol. *7*:103-120.

Wijsman, J.A. and Shivers, R.R. (1993) Heat stress affects blood-brain barrier permeability to horseradish peroxidase in mice. Acta Neuropathol. *86*:49-54.

Williams, C.V., Nordquist, D., and McLoon, S.C. (1994) Correlation of nitric oxide synthase expression with changing patterns of axonal projections in the developing visual system. J.Neurosci. *14*:1746-1755.

Wisniewski, K., Dambska, M., Sher, J.H., and Qazi, Q. (1983) A clinical neuropathological study of the fetal alcohol syndrome. Neuropedia. *14*:197-201.

Wu, D.Y., Jhaveri, S., and Schneider, G.E. (1995) Glial environment in the developing superior colliculus of hamsters in relation to the timing of retinal axon ingrowth. J.Comp.Neurol. *358*:206-218.

Wu, D.Y., Schneider, G.E., Silver, J., Poston, M., and Jhaveri, S. (1998) A role for tectal midline glia in the unilateral containment of retinocollicular axons. J.Neurosci. *18*:8344-8355.

Wu, H., Williams, C.V., and McLoon, S.C. (1994) Involvement of nitric oxide in the elimination of a transient retinotectal projection in development. Science *265*:1593-1596.

Zajac, C.S. (1987) Effects of maternal alcohol ingestion on the neurohistological structure of the midbrain of the fetal mouse. Diss.Abst.Intl. *47*:3200

Zajac, C.S., Bunger, P.C., and Moore, J.C. (1988) Neuron development in the superior colliculus of the fetal mouse following maternal alcohol exposure. Teratol. *38*:37-43.

APPENDIX

CALCULATION OF COEFFICIENTS OF ERROR

The standard equation for determining CE for n independent observations is:

$CE = CV/(n)^{1/2}$; where CV = coefficient of variation = standard deviation/mean

(Gundersen,'86)

This equation is not sufficient to estimate the CE when the observations arise from a systematic random sampling design because the n observations are clearly not independent (Miller et al.,'97). The formulae necessary to calculate CE based on observations from a systematic random sampling design are illustrated below (Table 16) (Gundersen and Jensen,'87; Miller et al.,'97). The benefit to the stereological sampling design then is that the estimated CE is proportional to 1/n, rather than $1/(n)^{1/2}$ (Gundersen and Jensen,'87).

CE calculations for an individual animal are demonstrated in this appendix (Table 16). Pi is the actual number of points counted for determining the area of each cross section used in estimating Vref of the SGS. Qi is the actual number of neurons counted from each physical disector pair for determining the volume density of neurons (Nv) of the SGS. Gi is the number of glial cells counted from each physical disector pair for determining the volume density of glial cells (GLv) of the SGS. Equation 1 is the equation for determining the CE of a parameter with one variable, and is used for Pi, Qi, and Gi which determines the CE for the Vref, Nv, and GLv, respectively (Gundersen and Jensen,'87; West and Gundersen,'90; Miller et al.,'97). The CE for N is dependent on the systematic observations of both Pi and Qi, and therefore involves a calculation that takes into account covariance (Gundersen and Jensen,'87). The covariance of the systematically sampled observations is first determined by equation 2. The covariance is then used in equation 3 to determine the CE for N. Ni is the estimated number of neurons in each physical disector of height = 2μm, for determining the N in the SGS in an 80μm slab of tissue. Ti is the estimated number of glia in each physical disector, and is also calculated using equations 2 and 3 for the glial cell parameters.

Table 15. Sample Calculation for Animal #1C, 35d, Gestational Exposure

Section	Pi	Pi(Pi)	Pi(Pi+1)	Pi(Pi+2)	Qi	Gi	Ni=Qi(Pi)	(Qi(Pi+1)+Pi(Qi+1))/2	(Qi(Pi+2)+Pi(Qi+2))/2	Ti=Gi(Pi)
1	32	1024	1152	992	17	0	544	530	407.5	0
2	36	1296	1116	1152	14	3	504	379	368	96
3	31	961	992	868	9	1	279	268	358.5	38
4	32	1024	896		8	2	256	352		62
5	28	784			15	2	420			64
SUM	159	A=5089	B=4156	C=3012	63	8	D=2003	E=1529	F=1134	258
CE	0.1				0.13	0.18	0.06			0.13

Equation 1: $CE(\Sigma P) = SQRT\frac{(3A + C - 4B)/12}{\Sigma P}$

Equation 2: $Cov\ (\Sigma P, \Sigma Q) = (3D + F - 4E)/12$

Equation 3: $CE\ (N) = SQRT\ ((CE^2(\Sigma Q) + CE^2(\Sigma P) - \frac{2 \times Cov\ (\Sigma P, \Sigma Q))}{\Sigma P \times \Sigma Q}$

Pi- total number of points counted per section in determining Vref; Qi- total number of neurons counted per physical disector in determining Nv; Ni- total number of neurons estimated per 2µm slab of SGS; CE- coefficient of error as calculated by either equation 1 or 2; Cov- covariance between Pi and Qi.

In the present study, mean CEs were calculated from data for each Ct and Et group at each age. However, it is not clear in the literature if, when evaluating a treatment, data should be pooled for both groups (Geinisman et al.,'96; Miller et al.,'97). When comparing groups to see if a treatment had an effect, does the sampling design only need to be efficient enough to detect a true biological difference between groups? Logically, the answer to the question is "yes," but the case for evaluating the efficiency of a sampling design when a treatment was involved in the study is not so clear. For instance, in the present study there was a significant decrease in neuron numbers in the SGS from the gestational exposure at 15d, as determined by comparing the means for the Ct and Et groups with a Student's t-test, which were obviously found to be significantly different. The variance (CV= SD/mean) for the Ct or Et group alone is much smaller than the variance for all of the animals combined at 15d (Ct and Et) (Table 15). If the variance (CV) is larger when the values of the Ct and Et group are combined, then the OCV^2 term in equation 6 above increases, which in theory allows the CE of the individual estimates to be much higher (for the Ct group in the present example, the acceptable CE goes from 7% to 15%!). Because of the ambiguity in the literature regarding the handling of these data when a treatment group exists, the present study erred on the conservative side and estimated the CVs and mean CEs for each group (Ct or Et) separately.

Table 16. Means, Standard Deviations, and Coefficients of Variation for Total Neuron Numbers in the SGS at 15d in the Chronic Prenatal Exposure

Data Type	Mean	SD	CV	Max. Acceptable CE
15d Ct	8248.14	809.02	0 10	0.07
15d Et	5772.82	552.97	0.10	0.07
15d Combined Ct + Et	7010.48	1451.7	0.21	0.15